UNIVERSITY OF CENTRAL OKLAHOMA

Edmond, OK

Jackson College of Graduate Studies

Bloodstain Pattern Analysis with Infrared Photography as a Tool to Visualize Impact and

Satellite Spatter on Denim

A THESIS

SUBMITTED TO THE GRADUATE FACULTY

In partial fulfillment of the requirements

For the degree of

MASTER OF SCIENCE IN FORENSIC SCIENCE

By:

Christina Traverso

Edmond, Oklahoma

2019

Bloodstain Pattern Analysis with Infrared Photography as a Tool to Visualize Impact and

Satellite Spatter on Denim
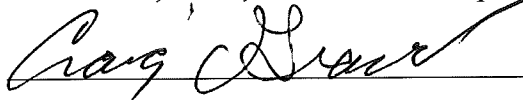
By: Christina Traverso

A THESIS

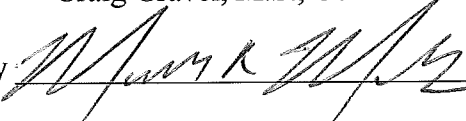APPROVED FOR THE W. ROGER WEBB FORENSIC SCIENCE INSTITUTE

July 2019

By _____

Dwight E. Adams, Ph. D, Committee Chairperson

By _____

Craig Gravel, M.S., Committee Member

By _____

Mark McCoy, Ed.D., Committee Member

Abstract

Correctly classifying bloodstain patterns is a crucial element of providing conclusions in the field of Bloodstain Pattern Analysis, because the type of bloodstain pattern speaks to how the bloodstains were created. Very few studies have compared impact spatter specifically to satellite spatter. The research needs outlined by SWGSTAIN include a better understanding of discriminating between bloodstain patterns containing small stains (present in both impact and satellite spatter), how blood interacts with different types of fabric, and developing new methods of visualizing and enhancing bloodstains (2011). Further, the Organization of Scientific Area Committee (OSAC) on BPA, which absorbed SWGSTAIN, outlines needs to reduce the subjectivity in BPA classification and understanding the interaction between blood and fabrics (OSAC, 2019). The only study to the author's knowledge that specifically compares satellite spatter to impact spatter is Short's 2016 study, which compared the two patterns on several different fabrics. However, Short was not able to visualize spatter on denim, due to dark color of the denim and lack of contrast between the blood and denim surface.

The current study used infrared photography to view simulated satellite spatter and impact spatter on 100% cotton denim and poster board. Both quantitative and qualitative data were collected. Two-way ANOVA, Cochran-Mantel-Haensel, and chi-square tests were performed on the data. Several comparisons found either a significant interaction, difference, or association between independent and dependent variables, depending on the test performed and the type of data analyzed. Overall, by utilizing the methods in this study, it is possible to differentiate between simulated impact and satellite spatter on denim fabric.

Keywords: Impact Spatter, Satellite Spatter, Denim, Infrared Photography

TABLE OF CONTENTS

LIST OF FIGURES

Introduction

Bloodstain Pattern Analysis (BPA)

In the modern age, law enforcement is tasked with the difficult assignment of working with all types of evidence, including fragile evidence, to determine what happened at a crime scene. Bloodstain pattern analysis (BPA) can lead forensic scientists and investigators to several conclusions that can be of aid in finding the truth. Through BPA, analysts can sometimes determine the location of the victim and/or suspect at certain points in the crime scene, establish a general timeline of the crime, estimate when critical individuals were alive, conclude how many blows were struck to a victim (if a weapon was used), if the offender used their right or left hand, what position the victim or offender was in at the time of the crime (standing or sitting), and many other important aspects that give investigators insight into crucial events and details pertinent to a crime (Basu & Bandyopadhyay, 2017; Bevel & Gardner, 2008; DiRienzi, 2009; Raymond, 1997; Robinson, 2009). Not all of these conclusions are able to be determined at every scene, but when the evidence is available, BPA can be a useful tool. Ultimately, BPA can be used to corroborate or refute victim, suspect, and witness statements, as well as investigator theories about an incident (Basu & Bandyopadhyay, 2017). The end goal, however, can usually be summed up in one question: "How was this [blood]stain created?" (Gardner, 2006, p. 551).

Terminology

In order to correctly classify each bloodstain pattern, understanding the terminology of the discipline is crucial. Examples of terms that bloodstain pattern analysts commonly use include, but are not limited to: projected spatter, impact spatter, wipe, swipe, transfer stain, secondary transfer, angle of impact, area of convergence, area of origin, skeleton, spines,

expiratory spatter, mist pattern, parent stain, void, and satellite spatter (SWGSTAIN, 2009).

Many of these terms carried over to the AAFS Standard Board (ASB) terms and definitions

published in 2017. Gardner, a leading expert in the field, specifically notes that in order to

correctly categorize a stain as one of these terms, it is essential that there not only be an

established definition of what the term means, but also an "established taxonomic classification

system", which "articulates physical characteristics" of the stain (Gardner, 2006, p. 554).

According to Gardner, it is the lack of this taxonomic classification system that leads many,

including analysts themselves, "to believe that bloodstain pattern analysis is open to

interpretation"(Gardner, 2006, p. 550).

Proposed Areas of Improvement Regarding BPA

Though BPA has established itself as a discipline in forensic science for over 150 years,

there is a question of its validity in the literature (Gardner, 2006). Bevel and Gardner maintain

that BPA uses inductive and deductive reasoning and the scientific method, while

acknowledging that "subjective analysis in both bloodstain pattern and crime scene analysis is a

fact of life" (Bevel & Gardner, 2008, p. xxviii). However, some worry over this subjectivity. In

2009, the National Academy of Sciences (NAS) published *Strengthening Forensic Science in the*

United States: A Path Forward, which highlighted concerns in the discipline of BPA, including

the difficulty of interpreting overlapping patterns, the tendency of analysts to rely on experience

rather than scientific principles, and more. The Council contested, "the opinions of bloodstain

analysts are more subjective than scientific" (National Research Council, 2009, p. 178). The

more recent 2016 PCAST (President's Council of Advisors on Science and Technology) report,

intended as a follow up to the 2009 NAS assessment, briefly mentioned but did not complete a

partial or full report on bloodstain pattern analysis (Holdren et al., 2007). Instead, the committee

mentioned that the American Association for the Advancement of Sciences (AAAS) would be

pursuing a comprehensive study of BPA.

Several organizations composed of experts in BPA responded to the National Research

Council's report. The Scientific Working Group on Bloodstain Pattern Analysis (SWGSTAIN),

created and sponsored by the Federal Bureau of Investigation, was one of those groups. Though

absorbed into an OSAC in 2015, SWGSTAIN served to stand as a forum for professionals in

BPA and build standard operating guidelines for the education and training of bloodstain pattern

analysts (Holdren et al., 2007; Stanley, 2018; SWGSTAIN, 2009). Much like Bevel and Gardner,

SWGSTAIN recognize that "a limited number of bloodstain pattern analysts have tendered

opinions beyond the scope of the available evidence", and "the opinions of bloodstain pattern

analysts may contain an element of subjectivity" (SWGSTAIN, 2009), and reiterate their

purpose, which is to continue to foster protocols for BPA as a discipline (Bevel & Gardner,

2008). As with any scientific discipline, there is always room for improvement.

In response to the concern of subjectivity by the NAS report, SWGSTAIN published a

document in 2011 detailing several needs for research in BPA. One of these needs acknowledges

that small stains can "appear similar", and that methods need to be developed which can

distinguish between patterns that include very small stains (SWGSTAIN, 2011). For example,

bloodstain patterns such as impact and satellite spatter can both include very small stains, which

can lead to one being misclassified as the other. In this case, however, impact spatter "results

from an object striking liquid blood", while satellite spatter originates "during the formation of a

parent stain as a result of blood impacting a surface" (SWGSTAIN, 2011). Given the disparity

between the origin of these two stains and the implications belonging to BPA analyst's court testimony of said origin, it would be extremely concerning if these stains were assigned to the incorrect category.

A second research need listed by SWGSTAIN was examining how blood behaves when deposited on different fabric surfaces. The absorbency, texture, color, thickness, and state of the fabric the blood was deposited on can all affect if analysts are able to correctly classify or visualize bloodstain patterns (de Castro et al., 2013; Keenan, 2012; Short, 2016). This research need was further published by the BPA OSAC in 2019. Given that blood can be deposited on virtually any surface and still be considered evidence, this need for research with a variety of fabrics will likely be never ending. That being said, the most common fabrics such as denim or cotton should be given special attention, as they are more likely to be submitted into evidence.

The third need called for by SWGSTAIN involves developing new techniques to "locate, enhance, and record bloodstains" (SWGSTAIN, 2011). Many methods have been utilized to view bloodstains on dark, multicolored, or patterned surfaces where the standard traditional photography does not suffice. These methods include various types of photography, image enhancement software, alternate light sources, and microscopy, to name a few (Adair & Shaw, 2005; de Castro et al., 2013; Duncan, 2015; Hill 2012). Chemical reagents are also commonly offered as a remedy in this area. Applying these reagents to evidence is designed to create a contrast between the bloodstain and the substrate (Adair & Shaw, 2005; Duncan, 2015). However, such processing is invasive because it requires physically processing the evidence itself. Noninvasive techniques allow the bloodstains to be processed more than once with greater efficiency, while preserving its original state. One such noninvasive technique is infrared

photography, an adaptation to the already standard traditional photography. Through either a

converted infrared camera and/or an infrared filter on a traditional camera, infrared photography

creates images viewed beyond the visible light spectrum, at approximately 700 nanometers or

above (Duncan, 2015; Farrar, Porter, & Renshaw, 2012; Sterzik, Panzer, Apfelbacher, &

Bohnert, 2016; Xiao, Zhao, Zhuh, & Zhang, 2010). When used on evidence with bloodstains,

infrared photography has been successful in creating an image which provides enough contrast

between the substrate and the bloodstain(s) where the visualization of such bloodstains are

markedly improved, both on fabrics and underneath surfaces such as layers of paint (de Castro et

al., 2013; Farrar et al., 2012).

Literature Review

Impact and Satellite Spatter

In BPA, blood spatter is commonly categorized as low, medium, or high velocity spatter. Low velocity spatter is generally categorized as larger stains, sized at 4 mm or greater in diameter. Medium velocity stains range from 1 to 4 mm in diameter, and high velocity stains are measured at 1 mm and under in diameter (Bevel & Gardner, 2008). That being said, these measurements can overlap into the next category (Bevel & Gardner, 2008). Based on this, Basu clarifies, "bloodstain patterns cannot be particularly classified on the basis of velocity of impact alone", though as a piece of a bigger image, it does provide some insight into classifying patterns (Basu & Bandyopadhyay, 2017, p. 205).

According to ASB's published BPA terminology, impact spatter is "a bloodstain pattern resulting from an object striking liquid blood" (2019). Similarly, Bevel and Gardner define an impact pattern as "a radiating pattern of small individual drops created when a blood source is broken up at a source by some force" (Bevel & Gardner, 2008). In an effort to promote the taxonomic classification Gardner believes is required for an accurate analysis, Bevel and Garner define four criteria that are present in impact patterns. An impact pattern contains "a series of related small spatter stains", with small being defined as typically 5 mm or smaller; the stain has a "radiating distribution" more often than not pointing in one direction; the "individual stain shape" progressively changes "further out in the pattern", and the parent stains range in size, but are "generally consistent throughout the pattern" (Bevel & Gardner, 2008, p. 50-51). Noticeably, a measurement of 5 mm or lower stretches between all ranges of low, medium, and high velocity spatter, which is another reason why it is important to consider these criteria, and not stain size

alone, in classifying a pattern as impact spatter. Examples of impact spatter include blunt force

trauma and gunshot wounds (Bevel & Gardner, 2008). The classic example of impact spatter is

blunt force trauma resulting from a beating. For example, a perpetrator hitting a victim in the

head with a hammer or a baseball bat would generate impact spatter. Figure 1 demonstrates an

example of impact spatter, created by slamming a mousetrap closed on a source of blood:
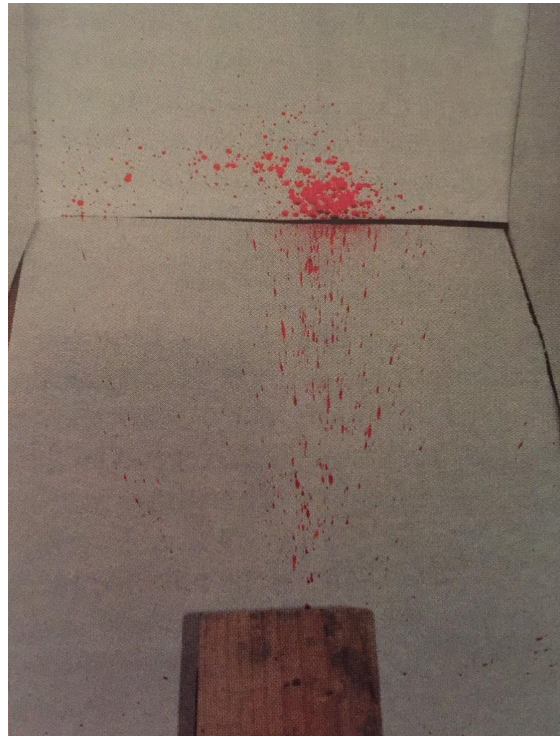
Fig. 1: Impact Spatter

According to the most recent published terminology, satellite spatter is "a smaller

bloodstain that originated during the formation of parent stain as the result of blood impacting a

surface" (2019). Bevel and Gardner further define satellite spatter, or "secondary spatter", as

"small stains created when droplets detach from a large drop as it impacts a target" (Bevel &

Gardner, 2008, p. 41-42). In other words, satellite spatter occurs when blood impacts a surface

and breaks off into smaller stains, all originating from one parent stain. Sometimes, these stains

are connected to the parent stain, and sometimes they are separate (Bevel & Gardner, 2008). A

blood droplet can detach from itself when deposited on a surface, leading to separate parent and secondary spatter, or when blood drips or "splashes" into blood, often creating random distribution and overlapping patterns. Depending on the velocity, height of the source, and the volume of blood being dripped into, the droplets generated from this "splashing" may be "distorted", and do not point in a specific direction (Raymond, 1997, p. 75). The act of blood dripping into blood may be used as a smothering technique in order to distort the original bloodstain. Because of this, satellite spatter can sometimes indicate that a crime scene was staged (Bevel & Gardner, 2008). Sometimes, the parent stain can be distinguished from the secondary spatter, and in others, this may be more difficult to determine (Bevel & Gardner, 2008). Figure 2 represents satellite spatter:
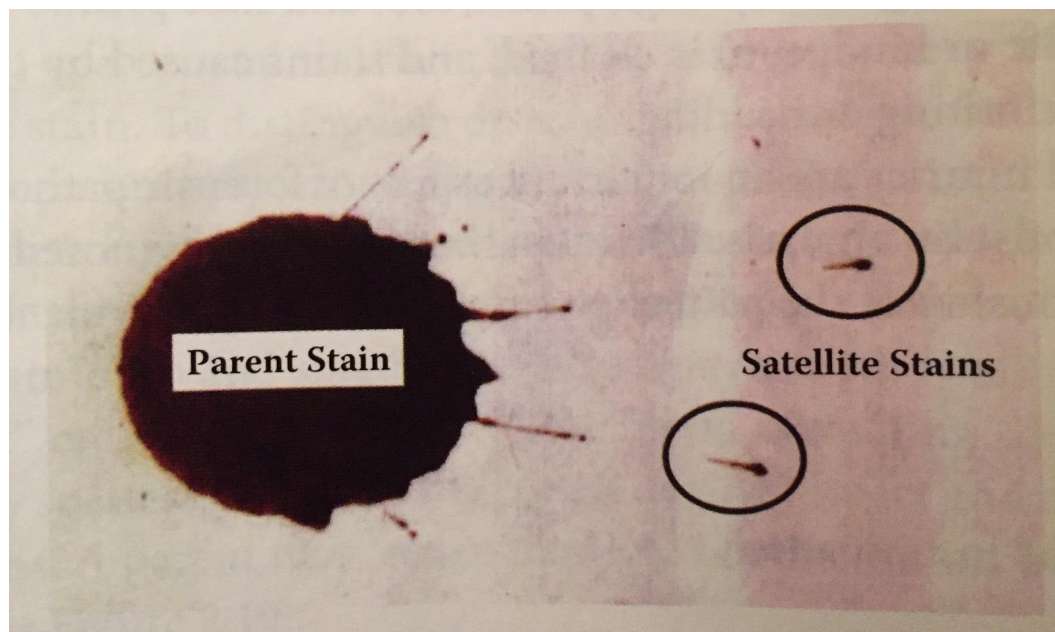
Fig. 2: Satellite Spatter

Distinguishing Between Impact and Satellite Spatter

Because satellite spatter can be attached, partially detached, or fully detached from the parent stain, it presents a challenge for analysts, and can be mistaken for impact spatter in certain

instances (Bevel & Gardner, 2008; Short, 2016). Impact spatter can occur at low, medium, or high velocity, while satellite spatter generally occurs at low velocity. For example, a suspect's shoe may be collected with very small spatter on one side. The suspect may claim that this spatter was created when the victim was already bleeding and they were trying to help them. This may be satellite spatter, generated when blood passively drips into an already existing pool of blood, such as when a wound causes blood to drip down an individual's arm into an already existing volume of blood on the floor created by the same wound. However, when impact spatter is generated by an object being used at medium or high velocity, such as participating in the beating of a victim, the resulting spatter may appear similar in size and distribution. Despite the fact that they occurred at very different velocities, the two scenarios can create spatter share similar characteristics. Small stains can be ambiguous and may make the overall pattern difficult to classify, which is why SWGSTAIN established the need for further research on small stain patterns (2011).

Both impact and satellite spatter require a "radiating" pattern, but satellite spatter occurring when blood drips into blood will radiate in all directions (circular), whereas an impact pattern generally radiates or "point" towards one specific direction. Although the classic impact spatter is usually ejected in a "cone" shape, as seen in figure one, depending on the "avenue of escape", impact spatter may radiate in a circle "all around the point source", in a similar manner to satellite spatter (Bevel & Gardner, 2008, p. 50-51). Depending on how much spatter is present if it is readily visible on based on the background, and the presence of very small spatter, the radiation pattern may be difficult to determine.

Beyond the size of the spatter, impact spatter can be recognized by determining the "directional and impact angles" (Bevel & Gardner, 2008, p. 75). Impact spatter generally points in one direction, though it may also radiate in all directions, and will at least partially generate stains with an elliptical shape, implying a lower angle of impact. By contrast, the satellite spatter created when blood breaks off from a parent stain makes more of a "tadpole" shape, with the tail pointing towards the parent stain, with a rounded head (Short, 2016, p. 56). These differences in shape may be subtle, but they are also crucial.

It is important to distinguish between the two spatters in order to determine the correct source of the bloodletting. Although impact and satellite spatter share many characteristics, limited research has specifically been done to differentiate between these two types of spatter. This determination may be at further risk for inaccuracy if the bloodstains are not readily visible to the naked eye because of the lack of contrast between the evidence and the substrate, or if the interaction between the composition of the substrate and blood as a fluid is not well known.

Bloodstain Pattern Determination on Differing Surfaces

Blood spatter analysis is commonly utilized in beatings, shootings, stabbings, car accidents, or other violent occurrences where bodily harm is issued to a human being. Blood can be present in miniscule or large quantities in a variety of areas and surfaces, from shoes to electronics to upholstery in a car. However, pattern determination can become difficult on certain surfaces, because blood reacts differently depending on the surface. The following images show impact spatter, created from slamming a mousetrap closed on a source of blood onto a control piece of butcher paper and two types of of 100% cotton fabric (Keenan, 2012):
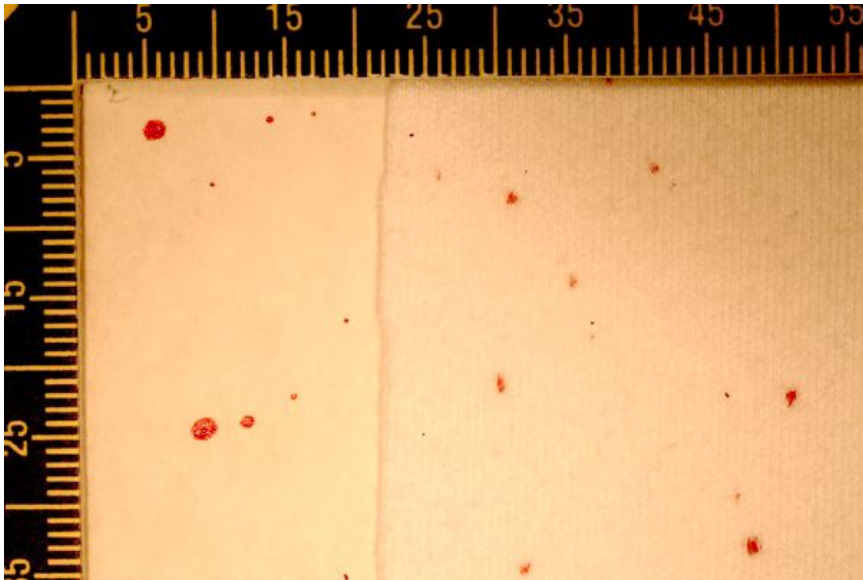
Fig. 3: impact spatter on butcher paper (left) and 100% cotton (right)   Fig. 4: close up of impact spatter on 100% cotton
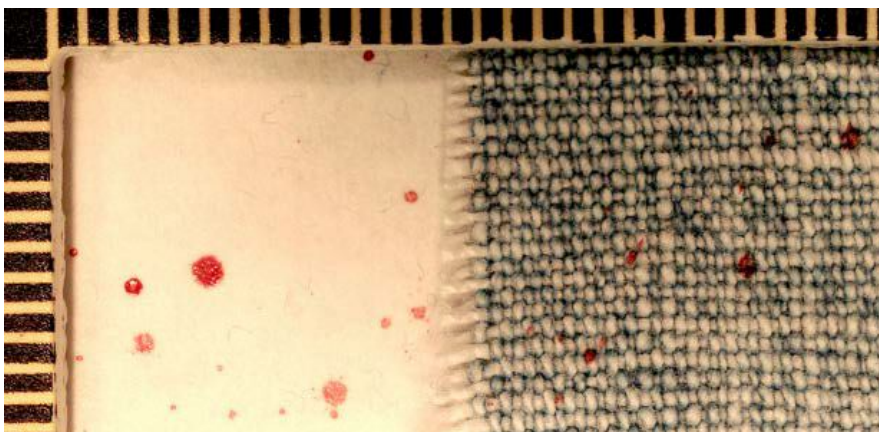
Fig. 5: impact spatter on butcher paper (L) and 100% cotton blue jeans (R) Fig. 6: close up of impact spatter on blue jeans

The blood spatter on the butcher paper in Figures 3 and 5 (left side) creates fairly regular

elliptical or circular drops. The patterns on the cotton on the right side of Figures 3 and 5 and in

Figures 4 and 6 illustrate how the same impact spatter from the same source creates stains which

are more irregular. As seen in Figures 4 and 6, 100% cotton has loose fibers, and is more absorbent

than the butcher paper, which accounts for the differences in droplet size and shape. Thus, different

types of fabrics can distort bloodstain patterns, in contrast with how they would appear on a rigid,

non porous surface. In some instances, this makes pattern conclusions challenging to reach with a

high level of confidence (Keenan, 2012). This effect has been determined to be a compelling factor

in the morphology of bloodstains generated on different surfaces (Basu & Bandyopadhyay, 2017;

Miles, Morgan & Millington, 2014). Blood can become evidence on virtually any surface; from

direct transfer from the offender while they are beating a victim, to secondary transfer wherein an

offender wipes off their bloody hands on a kitchen towel.

Smooth, non-porous surfaces, such as granite countertops, doorknobs, sinks, linoleum

floors, or plastic water bottles have a higher probability of yielding useful evidence for

investigators. Smooth surfaces do not contain the same ability to absorb the blood that

non-porous substances do, and thus non porous substances will create a well-defined shape with

little or no permanent distortion. As seen with Figures 3 and 5 above, the butcher paper yielded

more useful stains, because it did not absorb the blood the way the cotton did. Therefore,

non-porous substances create preferable stains for BPA analysis. However, blood on porous

substances, such as clothing, abound in the world of forensic analysis, and special attention

should be given to the methodology in processing such evidence. Given that blood can be present

on many different substrates, there is arguably a never ending need for research relating to how

blood interacts with specific surfaces of various compositions, specifically with fabrics (AAFS

American Standard Board, 2019; Basu & Bandyopadhyay, 2017; Short, 2016; SWGSTAIN,

2011).

Blood on Denim

Denim is a commonly encountered fabric that may be worn by suspects, victims, and

witnesses alike. Denim is largely composed of cotton, with an occasional minority component

such as elastane (Miles et. al, 2014). However, even a small difference in composition can cause

a difference in texture, affecting bloodstain patterns, and thus bloodstain pattern analysis. Miles

et. al used atomic force microscopy to examine the difference in fabric texture below (2014):
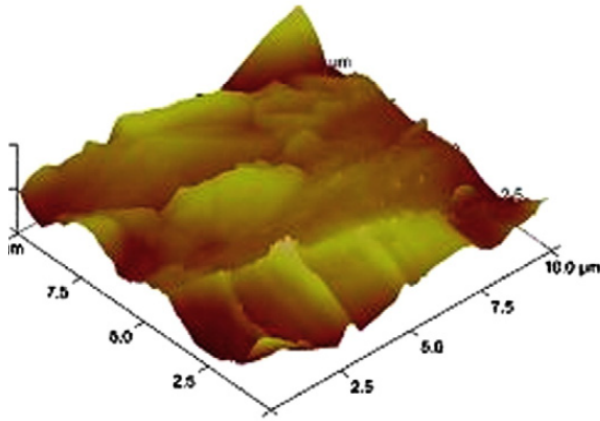
Fig. 7: blue jeans, 98% cotton/2% elastane   **Fig. 8: cotton T shirt, 95% cotton, 5% elastane**
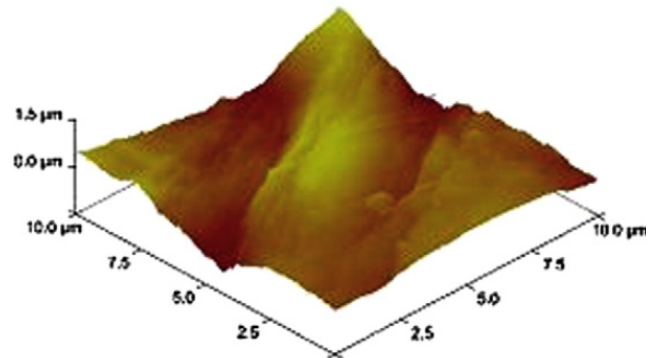
Figures 7 and 8 demonstrate how even a small difference in composition (3% more

elastane and 3% less cotton in Fig 8 than Fig 7) can change the surface texture of the fabric. In

this instance, the cotton jeans had more peaks and valleys, and were determined to be rougher

than the cotton T shirt (Miles et. al, 2014). Including differing angles of impact in their study,

Miles et al. found that this difference was significant enough to create more satellite stains on the

jeans than on the T shirt, because the rougher fabric "disrupted affecting drops more than the

smoother fabric" (2014, p. 265). Speaking in a general sense including all fabrics, Raymond also

came to a similar conclusion, stating, "informed interpretation of bloodstains is not

possible…without considering the target surface texture" (Raymond, 1997, p. 71).

Blood impacting rougher substrates like denim could create more satellite stains, which

means more blood to analyze. As previously discussed, satellite stains are commonly small and

numerous, which can be cause patterns to overlap and become confusing. Taylor et. al found that

"the error rate for classifications on fabric surfaces was higher than that observed on rigid non

absorbent surfaces" (2016, p. 1465). Therefore, it is important to understand how blood behaves

when impacting specific substrates over others.

Visualizing Bloodstain Patterns

Bloodstains, as well as other biological materials, may be difficult to visualize, especially

on dark, multicolored, or porous substances, such as cotton or denim. However, being able to see

bloodstain patterns is of obvious importance in making conclusions. Several techniques have

been utilized to visualize bloodstains on fabrics or surfaces that do not contrast readily to the

naked eye. One common technique involves the use of a chemiluminescent reagent such as

luminol or BlueStar. Such reagents allow investigators to detect latent bloodstains through

fluorescence (Adair & Shaw, 2005; Hill, 2012). When the reagent is applied, if blood is present,

the stain will fluoresce. Figure 9 demonstrates how blood "lights up" using luminol on an article

of clothing (Hill, 2012):

Fig. 9: luminol reacting to blood on a multicolored shirt

It is important to recognize that BlueStar and luminol are presumptive tests, allowing some non-bloodstains to fluoresce as a false positive. Presumptive tests are widely used by investigators and analysts alike, because they are fast, inexpensive, and allow investigators to visualize stains at the scene without heavy lab equipment. Presumptive tests also have a high sensitivity, allowing investigators to detect diluted or small bloodstains (Adair & Shaw, 2005). Webb found that BlueStar is a superior reagent to luminol, in that it was more sensitive, was not affected by a change in temperature, reacted positively independent of the age of bloodstains, was better visualized in light and dark environments, and fluoresced with better visibility on different substrates than luminol (2004). Tobe et al. partially dissented, in that BlueStar had a high sensitivity, but had more false positives than luminol (2007). Both BlueStar and luminol are used by bloodstain pattern analysts today.

Regardless, the use of chemiluminescent reagents is a popular option to visualize blood because it allows analysts to do so on dark, patterned, or multicolored surfaces (Adair & Shaw, 2005; Basu & Bandyopadhyay, 2017, Hill 2012). Suspects, victims, and witnesses do not always wear clothing that presents blood clearly due to a strong contrast, such as a white T shirt. Thus, bloodstains are frequently not as visible as analysts would like in its original condition. In Figures 10-11, Hill demonstrates how luminol, a chemiluminescent reagent, can visualize bloodstain patterns on a dark pair of pants. In Figure 12, Hill expands on his efforts by using Adobe photoshop to create a composite image of the original pair of pants in natural light on top of the darker image, after luminol was applied. The average criminal investigator may not be familiar with photoshop, so Hill includes detailed instructions for how to create this composite image (2011):

Fig. 10: before luminol   **Fig. 11: after luminol**   **Fig. 12: composite image**
                                                                       of Fig. 10 and 11

Infrared Photography in BPA

Though popular, the use of these chemical reagents to visualize bloodstains has some

drawbacks. Some reagents may be a known carcinogen, act to damage DNA evidence, or dilute

the bloodstains when used, preventing further analysis (Tobe, Watson, & Daeid, 2007; Webb,

2004). To avoid this, alternative light sources, ultraviolet, and infrared photography are

nondestructive methods that may be available to crime scene analyst. Of particular interest to this

study is infrared (IR) photography. Lin et al. note that it is "underused" in forensic science

because it is "inconvenient and unable to obtain results quickly", though it is also a "very

powerful tool" (Lin et al., 2007, p. 1148). Within the last decade, improvements have been made

to remedy these limitations, and this heavily implies the need for further research with updated

equipment and techniques.

Infrared photography creates images that are not visible to the naked eye. Light radiates

in wavelengths, which are measured in nanometers along the electromagnetic spectrum, as

illustrated in Figure 13 below. The visible light spectrum, which contains wavelengths the

human eye is able to view, exists between 400-700 nanometers (Duncan, 2015).
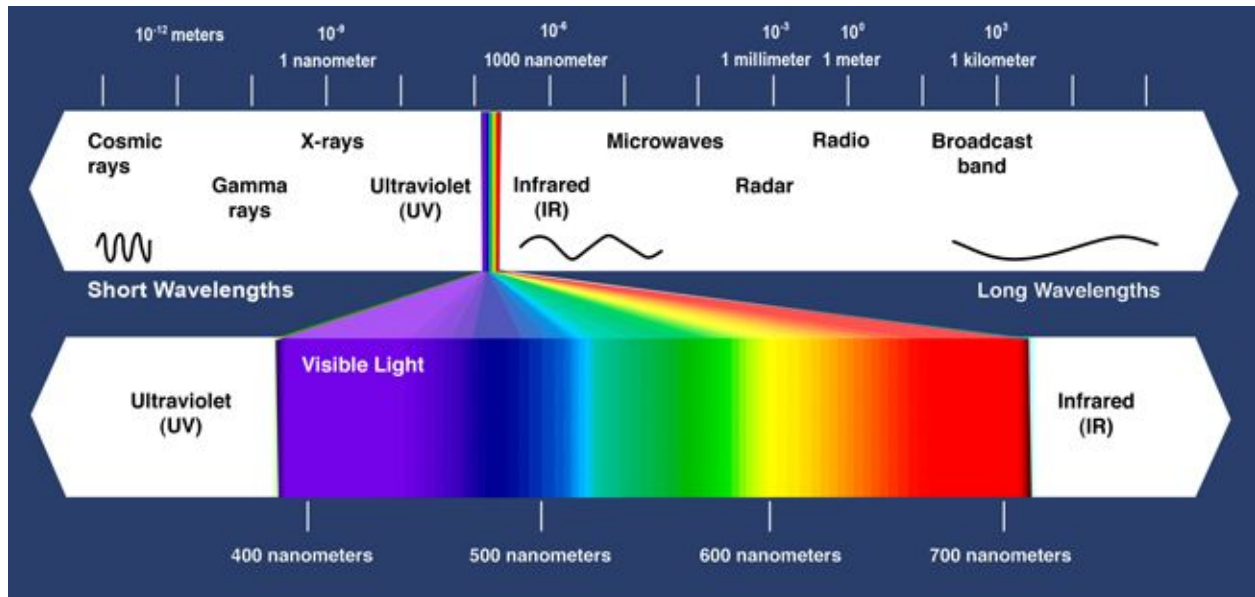
Fig. 13: The Electromagnetic Spectrum

Although infrared and ultraviolet light fall outside of the visible spectrum, infrared cameras can

visualize infrared light below 700 nanometers. This allows the visualization of subjects which

are not visible to the naked eye (Duncan, 2015; Farrar et al., 2012; Lin et al., 2007). This can be

achieved through the use of an IR converted camera, a camera with an IR filter, or both (Duncan,

2015).

Sterzik et. al recognized the forensic importance of being able to identify biological stains

through nondestructive methods such as infrared photography. The authors tested both undiluted

and diluted blood on 29 different materials, with 1:1, 1:10, and 1:100 ratios. In their study, 415

nm was the best overall wavelength to view both diluted and undiluted blood with and without

goggles, which is slightly within the visible spectrum to the naked eye, though blood did not

fluoresce (2016). Blood did appear brighter in infrared images at or equal to 830 nm, especially

on darker fabrics. That being said, only whole blood fluoresced under these images; neither the 1:10 or 1:100 dilutions were visible.

The jeans used in the Sterzik et. al's study were both light wash and dark wash; composed of 99% cotton and 1% elastane. Visibility of whole blood stains on the dark blue jeans was improved with infrared photography (2016). Lin et. al had slightly better results when using IR photography to examine bloodstains on dark fabrics. Their study examined ten types of black fabrics, including black trousers, and found that IR photography increased the visibility of bloodstains up to a 1:8 dilution (2007). One reason for this difference could be that Sterzik et. al examined only whole blood (1:1) and 1:10 dilutions, while Lin et. al utilized 1:1, 1:2, 1:4, 1:8, and 1:16 samples (2007; 2016). Additionally, Schuler et al. was able to visualize undiluted bloodstains on black 100% cotton and 50/50 cotton/polyester denim (2012). One further study concluded that blood could even be detected beneath six layers of white, colored, and black paint using an IR camera (Farrar et al., 2012). Differences may arise in the literature regarding how much blood IR photography can detect, it seems to be a general consensus that at the least, blood can be detected through IR photography and on a variety of contrasting and non-contrasting surfaces, where it would normally be latent.

Problem Statement

Little research has been done specifically distinguishing between impact and satellite blood spatter, which share many characteristics. Impact and satellite spatter can originate from very different sources; potentially indicating that a scene is either the direct result of a blow, or that a scene was staged. In the interest of justice, it is essential that these patterns be classified correctly, but in order to do this both the substrate the blood is deposited on and the ability to

visualize the blood on the substrate become important factors. Denim is a common substrate

submitted as items of evidence, including bloodstain evidence, but the blood may be difficult to

visualize, especially if the denim is dark wash. A common remedy for visualizing bloodstains on

fabrics such as dark wash denim include the use of chemical reagents. These reagents may be

effective at providing an image with a higher contrast between the bloodstain and the substrate,

but it is also invasive. It is in the best interest of all evidence and crime scene processing to start

with non-invasive methods first, in order to preserve evidence for further testing and proper

storage. IR photography is a growing method which may provide a non-invasive alternative to

such chemical processing. Many studies have been done involving infrared photography across

several forensic disciplines, but even so, IR imaging is largely underutilized in the field and the

laboratory (Bevel & Gardner, 2008; Duncan, 2015; Lin et al., 2007).

Purpose of Study

To the author's knowledge, no study has used infrared photography to exclusively

examine satellite and impact blood spatter on denim fabric. Short's study is one of the first to

examine satellite and impact spatter differentiation specifically on different types of cotton

fabric. However, Short was not able to adequately analyze blood on denim (2016). Specifically,

Short stated that the blue denim used as a substrate in her study "could not be reliably analyzed"

because the substrate background was too dark to sufficiently visualize blood with the naked eye

(Short, 2016, p. 31). Additionally, the ImageJ processing software was unable to differentiate

between the background and the bloodstains, and other image software programs were also

unsuccessful. Short recommended the use of an infrared camera to view blood on a dark

substrate such as denim (Short, 2016, p. 31). The current study will utilize the same methods

used by Short with recommended adjustments to examine 100% cotton denim fabric with the

additional visualization technique of infrared photography. The methods and materials used in

this study are purposefully a direct derivative of Short's research, in accordance with adjustments

made by Short for maximum efficiency.

In addition to expanding on the limitations of Short's research, the current study will also

address three research needs listed by SWGSTAIN and the current OSAC group: a better

understanding of discriminating between bloodstain patterns containing small stains, how blood

interacts with different types of fabric, and developing new methods of visualizing and

enhancing bloodstains (2016; 2019; 2011). Given the commonality of denim as an evidentiary

substrate and the significance of correctly classifying bloodstain patterns to indicate their

probable source, the purpose of this study is to fulfill research needs to examine if IR

photography can provide an effective means of visualizing and differentiating between satellite

and impact blood spatter on denim fabric.

Research Hypothesis

Based on the research needs presented by SWGSTAIN, as previously discussed, the author

proposes the following hypotheses:

H_0: It is not possible to differentiate between impact and satellite (blood dripping into

blood) spatter on denim fabric.

H_1: It is possible to visualize and differentiate between impact and satellite (blood

dripping into blood) spatter on denim fabric.

Materials and Methods

Introduction

The current study was conducted at the Forensic Science Institute at the University of Central Oklahoma in Edmond, Oklahoma. The materials and methods utilized by Short were employed by the author, with minor adjustments to accommodate conditions which will be discussed throughout this section. Short analyzed several types of cotton fabric, while the current study examined only 100% cotton denim and poster board as a control. Following simulating impact and satellite spatter on both denim and poster board, ambient lighting images were taken with a Nikon D3500. Infrared images were taken with a Fujifilm X-T1 IR camera. Qualitative and quantitative data were collected by taking ambient and IR images, and statistics were performed on data from both analyses methods.

Materials

Materials were purchased in part both by the researcher and the Forensic Science Institute. While Short obtained her denim fabrics from Testfabrics, Inc., the author elected to procure a 100% cotton denim skirt from an outside source. The denim skirt sample was a size 8 dark wash denim skirt. The tag indicated the brand is the Great Northwest Clothing Company, made in the United Arab Emirates, with AN number listed as 96157. The previous owner of the skirt reported that they purchased it in 2008, about eleven years prior to this study, and they wore the skirt about once every two months on average. The decision to modify the source of the fabric was made in order to provide the realism of analyzing samples which had been worn multiple times by an individual before a bloodletting event occurred on the fabric.

Denim Material Preparation

Prior to cutting the skirt into squares for experimentation, the sample was washed in a

Kenmore Elite front loading washer, with Tide original scent detergent. No other materials were

present in the washer. Six warm temperature cycles with a cold rinse were ran on the "normal"

setting and detergent was poured to the "normal" fill level. Wash cycle times lasted

approximately 30 minutes, based on the load sensing feature. Following each wash, a dryer cycle

was completed, also based on the load sensing feature, for approximately 90-105 minutes.

Because the clothing was washed and dried alone, a dryer sheet was absent during drying cycles.

These methods are consistent with Short's research, backed by the research of Gore et. al and

Slemko, which was "recommended for the testing of stable fabrics" (2016, p. 23; 2006; 2003).

Following washing and drying the denim skirt, the clothing was cut into twelve square

samples. A seam ripper and loop handle rotary cutter was used to remove seams, hems, pockets,

fringe, or other abnormalities which would prevent the fabric from being completely flat. The

squares were cut manually, using a loop handle rotary cutter and a clear fabric ruler measured in

both centimeters and millimeters. Due to the fact that the fabric was cut into squares by hand,

each sample measured between 24 cm x 24 cm to 25 cm x 25 cm. Five samples were needed for

both impact and satellite spatter simulation, adding up to ten samples total. Two samples were

left over as extras and were not used in the rest of the study.

Denim samples mounted on poster board following each simulation, and the poster board

was labeled with black Sharpie. The label indicated orientation as well as the type of spatter, the

fabric, and the number of each sample. Impact spatter denim samples were labeled "ID1"

through "ID5", abbreviated for "impact denim 1" through "impact denim 5". Satellite spatter

denim samples were labeled in the same fashion as "SD1" through "SD5", abbreviated for

"satellite denim 1" through "satellite denim 5".

Control samples of equal sizes to the denim samples were cut from stiff white poster

board. Poster board was chosen as a control because it provided a smooth, non-porous surface on

which blood spatter and its specific features could easily be seen. Control samples were labeled

with a marker in the same fashion as the denim samples, without the type of fabric as "I1"

through "I5", abbreviated for "impact 1" through "impact 5", and "S1" through "S5",

abbreviated for "satellite 1" through "satellite 5".

Simulation Material Preparation

Bovine whole blood with K2 EDTA anticoagulant was obtained from the Forensic

Science Institute and used for both impact and satellite spatter simulations. In order to simulate

the temperature of the human body the blood was warmed to approximately 37 degrees Celcius

in a warm water bath prior to simulation trials. The temperature was measured multiple times

between trials. Though the warm water was consistently refreshed between trials in an effort to

keep the remaining blood at 37 degrees Celsius, some difficulty was encountered in keeping the

temperature high enough. Throughout trials, the temperature was recorded between 34 and 37

degrees Celsius.

<div align="center">**Methods**</div>

Impact Spatter Simulation

Five stiff poster boards were duct taped together to create a box without a ceiling to catch

the blood spatter. A 25 cm by 25 cm square was cut from a separate piece of poster board to

create a "mobile mounting surface". Four velcro fasteners were secured to the back of the

mounting surface and to the furthest wall of the box. One wall of the box was laid flat for the

impact spatter simulation. Before each trial, a denim sample as attached to the mounting surface

with push pins. The mounting surface was placed onto the furthest wall of the box, and the

spatter simulation was conducted. After each trial, the mounting surface was removed from the

box, and the spattered denim sample was unpinned from the mounting surface. The denim

sample was stapled to a separate, equal sized piece of blank poster board and set aside to dry.

The next denim sample was pinned to the mounting surface and fastened back onto the furthest

wall of the box for the next trial.

A mousetrap constructed of two wooden planks hinged together was placed on the flat

poster board wall. The mousetrap was the tool used to simulate impact spatter by closing the two

wooden planks together with blood in the middle. This method is commonly accepted in the field

of bloodstain pattern analysis to simulate impact spatter (Bevel & Gardner, 2008). One milliliter

(mL) of blood was deposited on the front area of the mousetrap using an ErgoOne 100-1000 μL

pipette. After the spatter was created, the blood was wiped off the front of the mousetrap with a

paper towel. Spatter was created on either the denim or control samples when the mousetrap was

closed at an 80 degree angle without any additional force. The angle was measured by mounting

a protractor next to the mousetrap on an equal level. Each denim or control sample was

perpendicular with the floor of the poster board box at a height of zero inches. To create a

sufficient amount of spatter, the mousetrap was mounted on a shoebox with a height of five

inches. Each side of the mousetrap was one inch in height. In total, the surface the blood was

deposited on was raised six inches off the floor and twenty inches away from the mousetrap.

Figures 14 and 15 show the set up for impact spatter simulation:
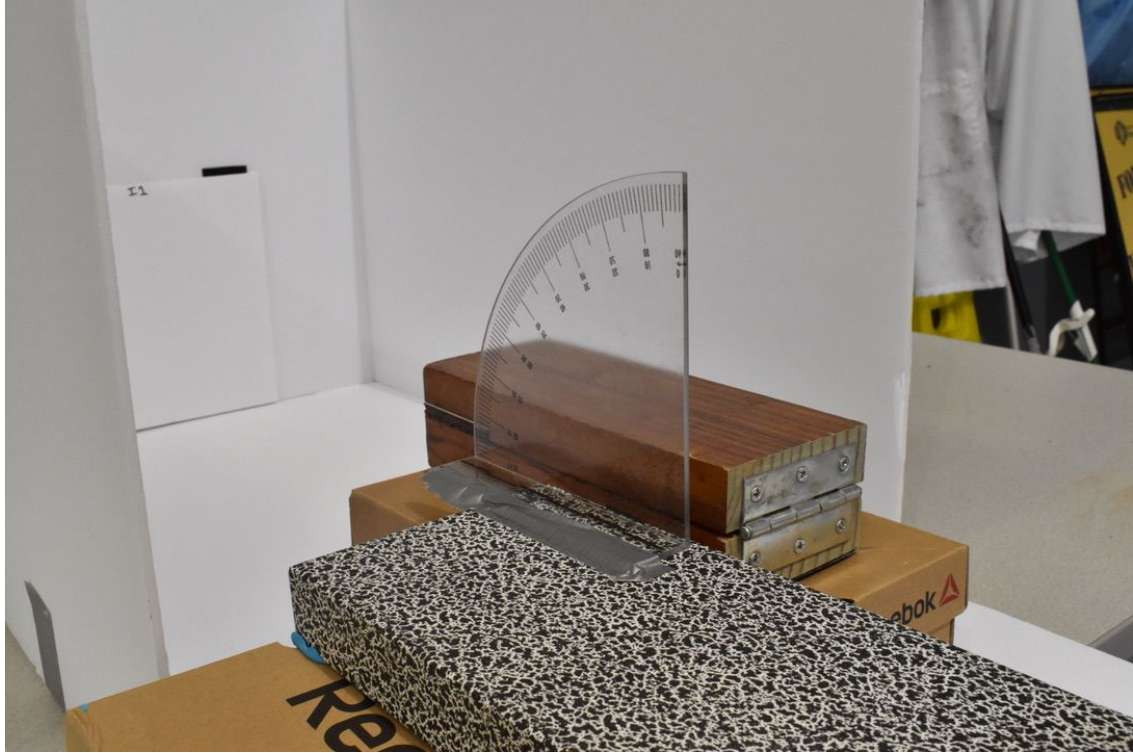
Fig. 14: Impact Spatter Simulation Set Up

Fig. 15: Impact Spatter Simulation (angled)

Ten impact spatter trials were conducted on five denim samples and five control samples. One spatter event was produced on each sample, with the exception of two spatter events produced on denim sample number two (ID2). Two events were produced because insufficient spatter was seen when conducting one spatter event.

After each trial, all samples were set aside to dry. Ambient lighting images were taken with and without scale after a minimum of ten minutes of drying time. images were taken with a Nikon D3500 camera and a Nikon 18.0-55.0 mm f/3.5-5.6 lens.

Satellite Spatter Simulation

The same poster board box was used to conduct the satellite spatter trials. Instead of laying one side of the box flat on the floor, the board was flipped up and duct taped to create a full box without a ceiling. A drip rig obtained from Bevel, Gardner & Associates was used to create the satellite spatter. The drip rig was composed of a tent pole secured to a block of wood. An eye dropper was secured at the top of the tent pole and could be adjusted to remain at different heights. The drip rig was placed inside the poster board box and the eye dropper was suspended at forty inches in height. A flat mirror was placed directly below and adjacent to the drip rig. The drip rig and flat mirror were secured to the poster board floor using Loctite mounting putty on each corner. The outline of the mirror was traced with a pencil so it could be removed, cleaned, and replaced in the same area. The mirror was rinsed off with water and dried with a paper towel between trials. The mirror was placed four inches away from the perpendicular mounting surface where control and denim samples were placed. Two milliliters of blood was deposited on the flat mirror directly below the eye dropper using an ErgoOne

100-1000 µL pipette. In total, the blood was about 6 inches away from the denim and control

samples during trials. Figures 16 and 17 show the set up for satellite spatter simulation:

Fig. 16: Drip Rig Set Up
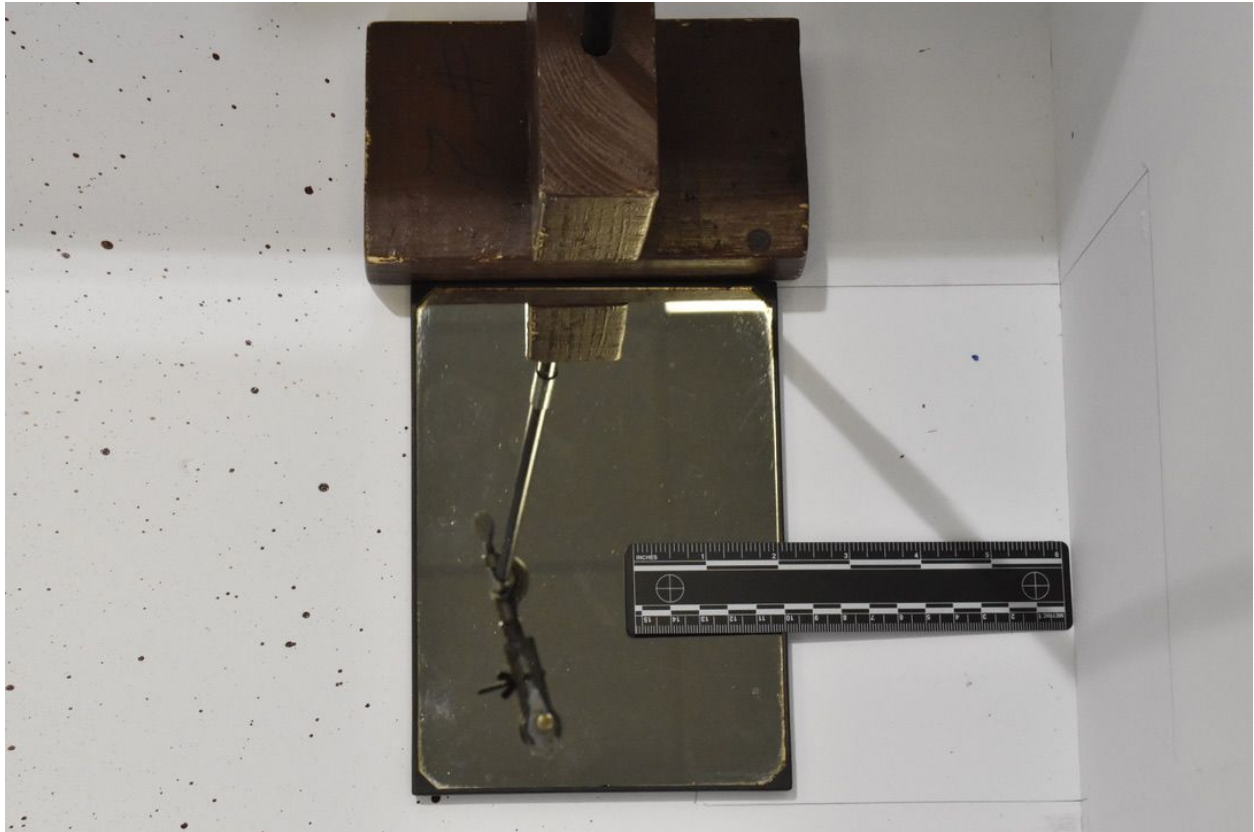
Fig. 17: Distance From Mounting Surface

Blood was warmed to approximately 34-37 degrees Celsius in the same methods used in the impact spatter simulations. Twelve drops were released from the eye dropper two to three seconds apart. Control and denim samples were placed on the wall perpendicular to the flat mirror. The secondary spatter was created on the control and denim samples as a result of the blood drops falling from the eye dropper, impacting the existing two milliliters of blood on the flat mirror, and moving into free flight onto the control and denim samples. Figure 18 shows a control sample following satellite spatter simulation:

Fig. 18: Control Sample S2 After Satellite Spatter Simulation

A total of ten satellite spatter trials were conducted, including five control poster board samples and five denim samples. Though the researcher wore gloves throughout trials, one small, transfer stain was noted before the satellite spatter trial was conducted on control sample number two (S2). The stain was photographed prior to the trial to prevent the stain from being included in subsequent analysis.

After each trial, all samples were set aside to dry and photographed with and without scale. Images were taken with a Nikon D3500 camera and a Nikon 18.0-55.0 mm f/3.5-5.6 lens in the same manner as the impact spatter simulations.

Infrared Photography

        Following simulation trials, each denim sample was photographed using a Fujifilm XT1

IR camera, Fujifilm XF 18-135 mm f/3.5-5.6 LM OIS WR lens, and B+W 39 093 IR 830 nm

filter. The camera was mounted on an aluminum Giottos MT 9360 tripod. The samples were

placed on the floor and the camera was adjusted on the tripod to be parallel with the floor. Figure

19 shows the camera set up for infrared images:

Fig. 19: Infrared Photography Set Up

The live view feature of the Fujifilm XT1 IR allowed the researcher to see the images before they were taken and adjust zoom, focus, and exposure variables as necessary. All images were taken in a well-lit room using the IR 830 nm filter. At times, the camera indicated that there was camera shake when the shutter release was depressed manually. As a result of this, a Fujifilm RR-90 remote shutter release was connected to the camera. Use of the remote shutter release minimized blur in images and the camera's prompting camera shake error message.

IR photographs were taken at ISO 100 so the researcher could zoom in on each image at a later date while maintaining the same amount of detail. After experimentation, the optimal settings for properly exposed IR images with the specific aforementioned equipment was a 60 mm zoom, ISO 100, +1 Exposure Variable (EV), f/6.4, and a 30 second shutter speed (SS). Five impact and five satellite denim samples were photographed with and without scale. images taken with the IR camera successfully rendered the denim substrate much lighter than the darker blood spatter. The contrast seen in the IR images allowed the researcher to see the blood spatter much more effectively in the IR images than in the images taken with the Nikon D3500, as seen in Appendix C.

<div align="center">**Quantitative Analysis**</div>

Preliminary Analysis - ImageJ

Part of the author's research proposal included that the IR images would not only provide a suitable contrast to view the blood spatter more effectively, but also that the IR images would allow the researcher to analyze the denim samples when Short was not able to. The problem previously encountered by Short was in the first step of preliminary quantitative analysis, which involved using ImageJ to convert each image to black and white, or binary, so the software could

measure the bloodstains. The control samples were converted to binary in ImageJ with few

issues. However, in Short's study, the denim background created "uncorrectable background

noise", when converted to binary (2016, p. 32). The author proposed that the contrast created

between the blood spatter and the denim background in IR images would allow ImageJ to

correctly distinguish between blood and denim when converted to binary. Although a sufficient

difference in contrast was observed between the IR and ambient images when viewed with the

naked eye, as seen in Appendix C, the entire denim sample was rendered black when the IR

images were uploaded into ImageJ and converted to binary, as seen in Figure 20:
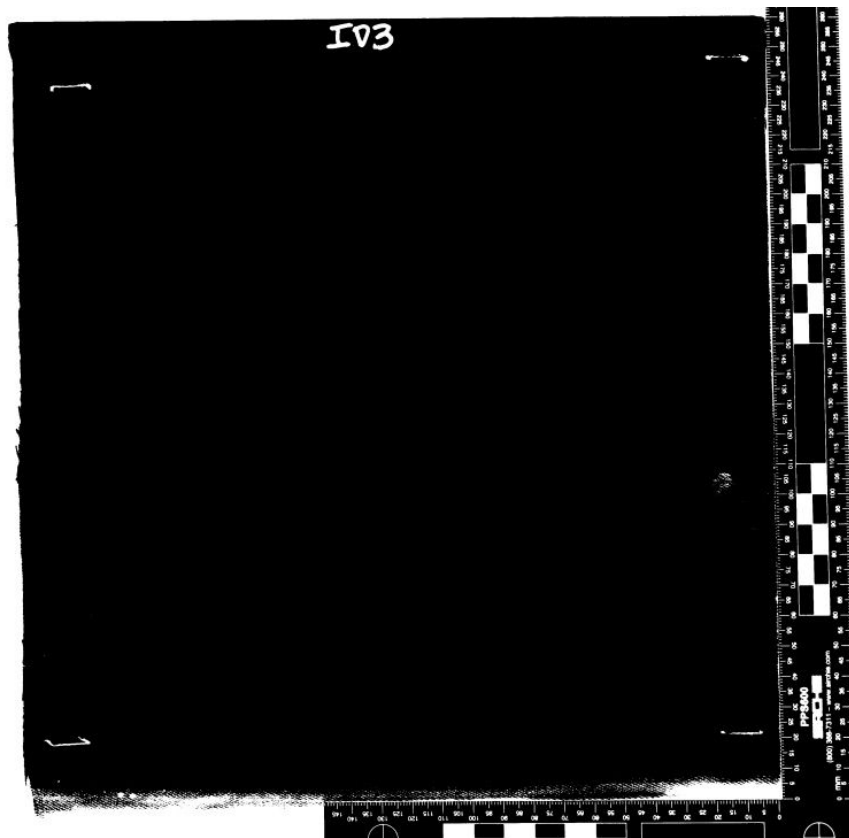
Fig. 20: IR ID3 Binary Conversion

To remedy this, the researcher adjusted the brightness and contrast by selecting "Image"

from the head toolbar, followed by "Adjust", and then "Brightness/Contrast". The author used

the "minimum", "maximum", "brightness", and "contrast" slider bars to further adjust the quality

of the image to make the spatter more prominent than the background. The image was then

converted to binary by selecting "Process" from the head toolbar, followed by "Binary", and then

"Make Binary". The resulting image is shown in Figure 21:
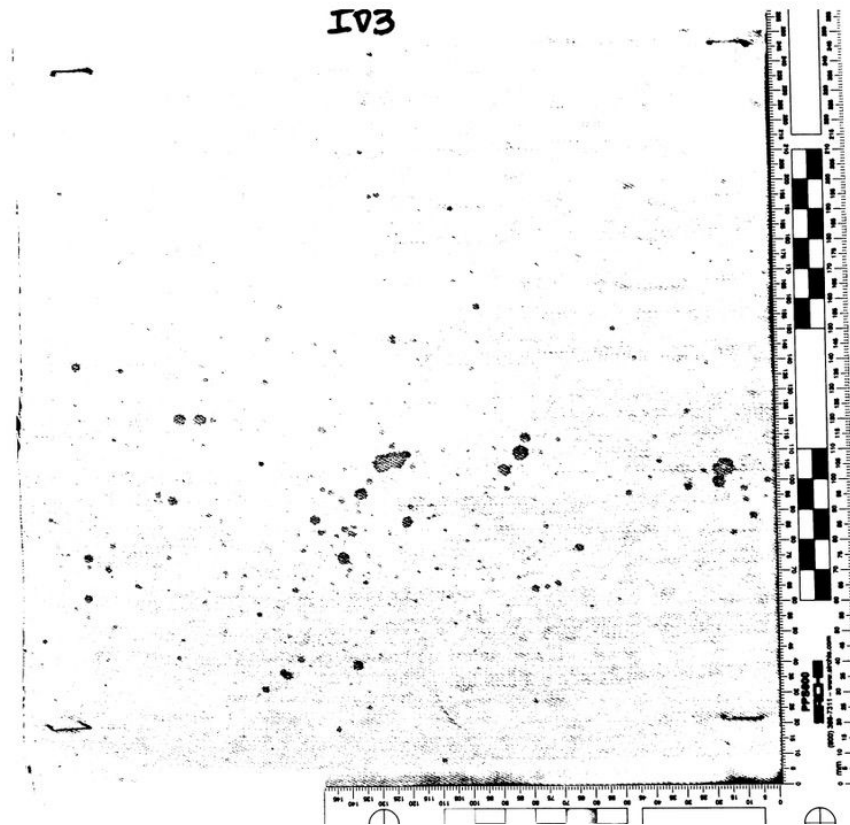
Fig. 21: IR ID3 Brightness/Contrast Enhancement and Binary Conversion

Although enhancing the brightness and contrast of the IR image in ImageJ greatly

improved the image quality after binary conversion, Figure 21 also demonstrates a speckled

background noise behind the spatter. This was created by the weave pattern in the denim fabric,

showing that ImageJ did not completely distinguish between the spatter and the substrate. In

order to determine if the background could be eliminated completely and thus provide a more

accurate analysis, the researcher uploaded both ambient and infrared images to Adobe Photoshop CC, version 19.1.5.

Preliminary Analysis - Photoshop

Initially, the researcher expected IR images to create a sufficient difference in color contrast between the fabric and the substrate. Though this was true when viewing images with the naked eye, the binary function in ImageJ did not detect the contrast. Infrared images were opened as TIF files in photoshop to determine if the program would be able to successfully erase the denim background and convert the image to binary.

One of the primary functions used by the author in photoshop was creating multiple layers. This allowed the researcher to track the steps taken throughout analysis, as well as being able to experiment with different methods and revert to previous steps. First, the image was cropped to include only the sample and the scale, renamed "original layer", and locked to prevent distortion of the original image. The layer was duplicated and the polygonal lasso tool was used to select all areas outside of the fabric, scale, and fabric identifier in the image. This eliminated unnecessary background from interfering with selections. The layer was labeled "Background Deleted". The layer was duplicated, the fabric identifier and scale was selected with the polygonal lasso tool (excluding fabric), and deleted. This left the spattered fabric by itself. The layer was labeled "Fabric Only". In order to ensure that the fabric could be traced to its correct identifier, the Background Deleted layer was duplicated again, and the fabric was deleted. This left the identifier and scale only. This layer was labeled "ID & Scale", and allowed the fabric to be viewed and selected separately from the identifier and scale. The Fabric Only layer was selected and the magic wand tool was used in an attempt to isolate blood stains from

fabric. The magic wand tool selects areas that are equal in color and tone. The magic wand tool

can be set as contiguous or not contiguous. If set to contiguous and an area of the image is

selected, the magic wand tool will select all pixels adjacent to the selected pixel which are equal

in color and tone. If the contiguous box is not checked, the magic wand tool will select pixels

throughout the entire image which are equal in color and tone. The contiguous box was

unchecked so the magic wand tool would select pixels throughout the entire layer. Additionally,

the tolerance level of the magic wand tool can be adjusted. The default tolerance value is 32. The

higher the tolerance value, the more sensitive the tool is, and the more pixels will be selected.

The lower the tolerance value, the less sensitive the tool, and fewer pixels will be selected. For

initial experimentation, the tolerance was left at the default level of 32.

When using the magic wand tool to click on a blood stain, the tool should select all other

pixels of equal color and tone. However, when the author clicked on a dark bloodstain in the

fabric only layer, the magic wand tool selected the denim weave instead, and barely selected any

bloodstains. The author hypothesized that the contrast was not prominent enough for the magic

wand tool to detect. The fabric only layer was duplicated, the brightness was raised to a value of

94, and the contrast was raised to a value of 72. The magic wand tool was used to select a

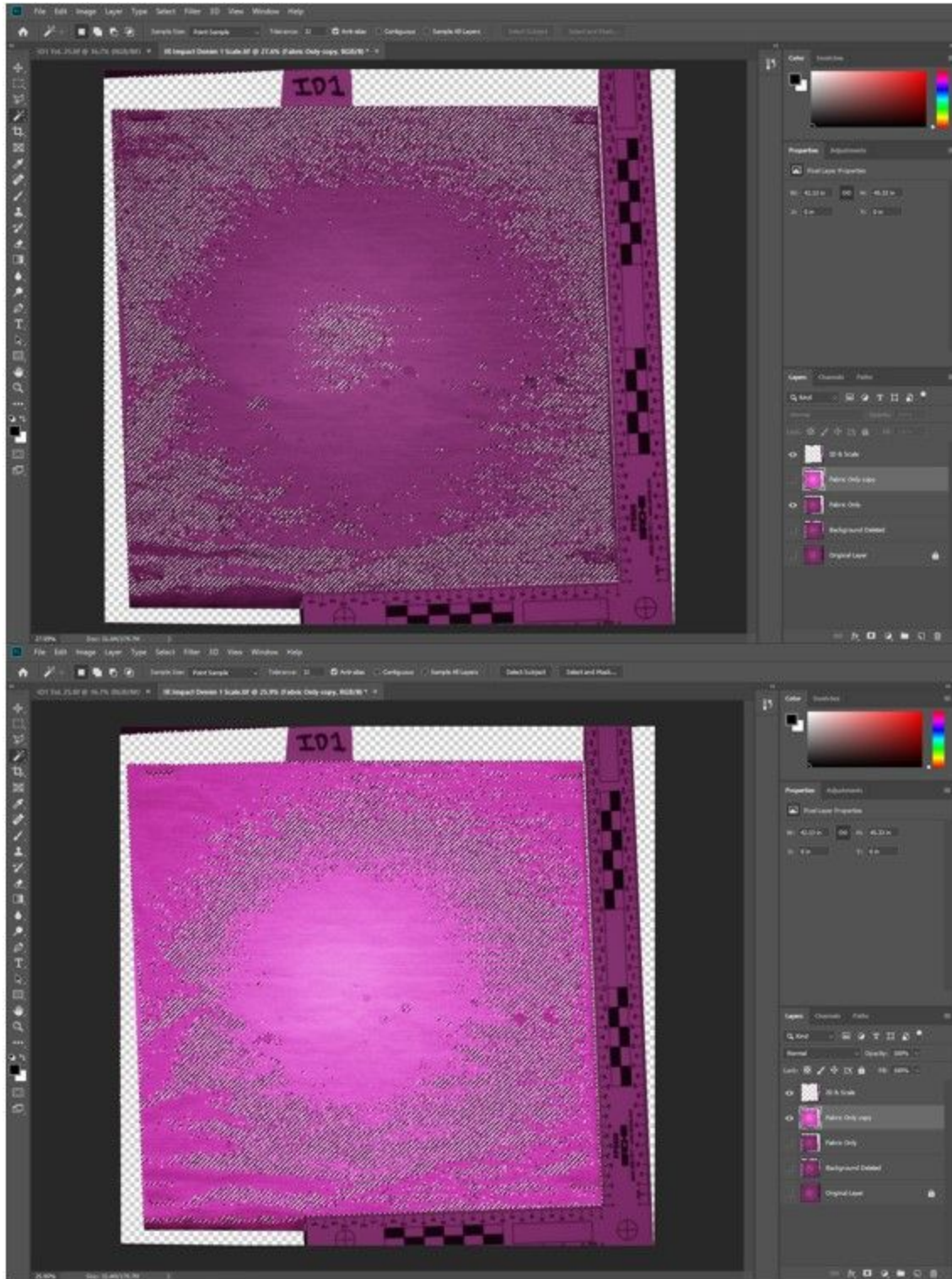bloodstain again, but the results were not improved:

Fig. 22: Magic Wand Selection (top); Magic Wand Selection with Brightness/Contrast Adjustment (bottom)

The selection of bloodstains using IR images was unsuccessful. Ambient images were uploaded into photoshop and the process was repeated with minor adjustments. The image was cropped, a layer was created with only the fabric identifier and scale, a layer was created with the fabric only, the fabric only layer was renamed B/C and the brightness level was raised to 150, and the magic wand tool was used at tolerance level 32 with the contiguous box was left unchecked. When bloodstains were selected according to this process, the magic wand tool correctly selected bloodstains independent of the denim fabric. After experimentation, the correct tolerance level to minimize tiny selections of denim was 25 for impact spatter and 20 for satellite spatter. The tool also selected areas such as staples, loose threads, seams, or dark edges that were not blood spatter, but the author was able to unselect those areas by checking the contiguous box, setting the magic wand tool to "subtract from selection", zooming in on the problem areas, and deselecting the incorrect selections by hand.

Once the bloodstains were properly selected by the magic wand tool, everything not selected by the tool, namely the denim fabric, was deleted by choosing "Select" from the head toolbar, "Inverse" from the drop down menu, followed by the backspace button. This layer was labeled "Spatter Only". The layer was duplicated, and a white background was added behind the spatter by setting the foreground color to white, selecting the paint bucket tool from the tools panel, and selecting any space that was not spatter. The layer was labeled "Spatter White". Lastly, the ID & Scale layer was viewed at the same time as the Spatter White layer. The end result isolated the blood spatter from the denim background in black and white (see Fig. 23) and A full example of all photoshop layers for ID1 is listed in Appendix D.

Fig. 23: ID1 Original imageo (top), ID1 After Photoshop (bottom)

When the files were entered into ImageJ, they were converted to binary again, which converted the scale and identifier to black and white as well. The process was repeated for all denim samples, with two adjustments for satellite denim samples. First, the magic wand tolerance was set to 20, due to the much smaller number of satellite stains in comparison to impact stains. Any resulting pixels which could possibly have been denim and not satellite spatter were tiny and below one millimeter in major or minor axis. Since ImageJ would be set to detect stains 1 square millimeter or larger, this setting would not affect results generated by ImageJ. Second, the fabric identifier was written on the satellite denim samples in silver Sharpie, while impact denim identifiers were written on the poster board above the fabric. To remedy this, the author used the polygonal lasso tool to selected around the identifier in the ID & Scale layer.

ImageJ Analysis - Denim Samples

After the denim background and other non-spatter components were subtracted from the blood stains and converted to binary in Photoshop, JPEG files of ID1-ID5 and SD1-SD5 were uploaded to ImageJ and duplicated into TIFF files. When ID1 was uploaded, the author set the scale so ImageJ could measure the stains. This was established by zooming in 600 times on the scale and using the straight line tool to draw a line from the middle of one millimeter mark to the middle of the next millimeter mark. Following this, "Analyze", then "set scale" was selected. The distance in pixels was set by ImageJ as a result of the straight line tool, the unit of length was changed to millimeters, and the scale was set to "global", as seen in Figure 24:
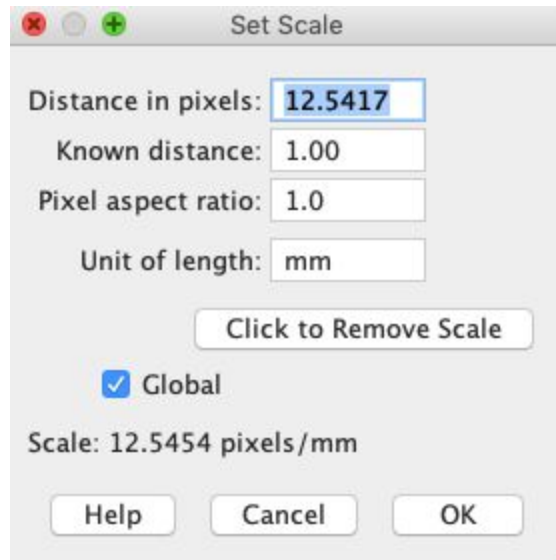
Fig. 24: Set Scale in ImageJ

This function allowed ImageJ to measure any distance selected in millimeters, in accordance

with the scale the images were taken with. The scale was set to global so the scale would be the

same for every image analyzed in ImageJ. The scale could be verified in the other samples by

drawing a line on the scale with the straight line tool in the same manner as previously discussed.

The head toolbar in ImageJ would then indicate the value of the line. If the value was

approximately 1.0 mm, the scale was correct. The global scale was established as correct and the

author proceeded with image processing.

    After the scale was set and confirmed, ID1-ID5 were converted to binary in ImageJ,

making the entire image black and white, including the fabric identifier and scale. The spatter

was outlined using the rectangular tool and saved to ensure that the stains selected by ImageJ

were contained within the selection only, the scale and fabric identifier were excluded from

generating results, and that the selection was the same when the image was closed and opened

again. Once the correct area was selected, the watershed tool was selected to separate

overlapping stains by selecting "Process", "Binary", and "Watershed". Although the watershed

command was successful in separating overlapping stains with control samples, the watershed

command incorrectly separated circular stains into cracks within the same stain within the denim

samples, as seen in Fig. 25:

Fig. 25: ID1 Watershed Command (left), ID1 Without Watershed Command (right)

Because the photoshop adjustments led to breaking up of individual stains and thus an incorrect

increase in total stain number, the watershed command was not utilized in generating denim

sample results.

ImageJ was able to generate measurements of each bloodstain from the binary image,

including the area, perimeter, circularity, major axis and minor axis. These measurements were

selected to be generated by selecting "Analyze", "Set Measurements", and checking the boxes

for "area", "shape descriptors", "perimeter", and "fit ellipse", as seen in Fig. 26:
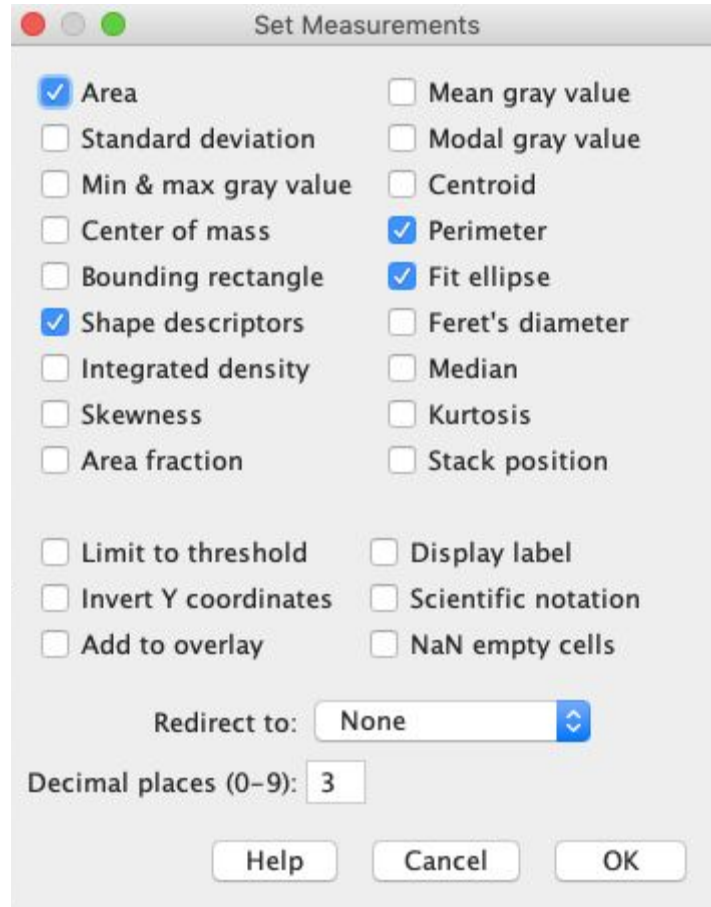
Fig. 26: Set Measurements in ImageJ

Because the scale was set previously in millimeters, the area measurement was also

generated in millimeters. The perimeter measured the outside boundary of the stains. Previous

versions of ImageJ, including the one used by Short, allowed the user to select a measurement

for "circularity". The program would generate a number from 0.0-1.0, with zero indicating an

elongated stain and a value of 1.0 indicating a perfect circle (2016, p. 35). More recent versions

of ImageJ replaced circularity with "shape descriptors" as an available measurement. The shape

descriptors function generated a measurement for circularity within the same 0.0-1.0 range, as

well as aspect ratio, solidity, and roundness. For the purpose of this study, only circularity was

considered. Lastly, "Fit Ellipse" was selected, which created a separate "drawing" of the original

selection, showing the best fit ellipse for each stain. This function generated the major and minor

axes of each best fit ellipse, which were used to calculate the impact angle.

Once the correct settings were established to generate the desired results, results were

generated by selecting "Analyze", followed by "Analyze Particles", which produced the
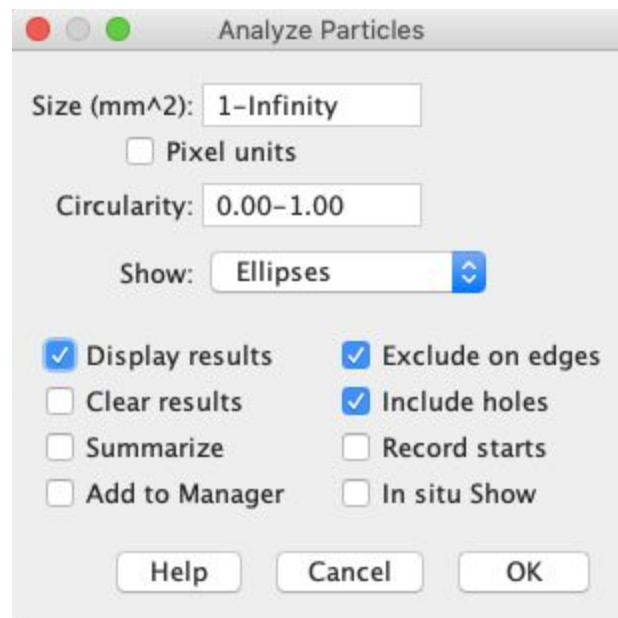
following window:

Fig. 27: Analyze Particles/Ellipses

The previously set scale measured the stains in square millimeters, and thus the "pixel units" box

was left unchecked. Typically, impact spatter is classified as medium velocity, which usually

ranges from 1-4 mm in diameter. To account for this, stain size was set from one to infinity for

impact spatter samples. Circularity was left at 0.0-1.0, as previously discussed. "Display results"

was checked to generate a table of results, "exclude on edges" was checked to exclude any stains

touching the borders of the selection, and "include holes" was checked to include any holes

(possibly resulting from bubbles) within stains. Lastly, the program was set to show ellipses.

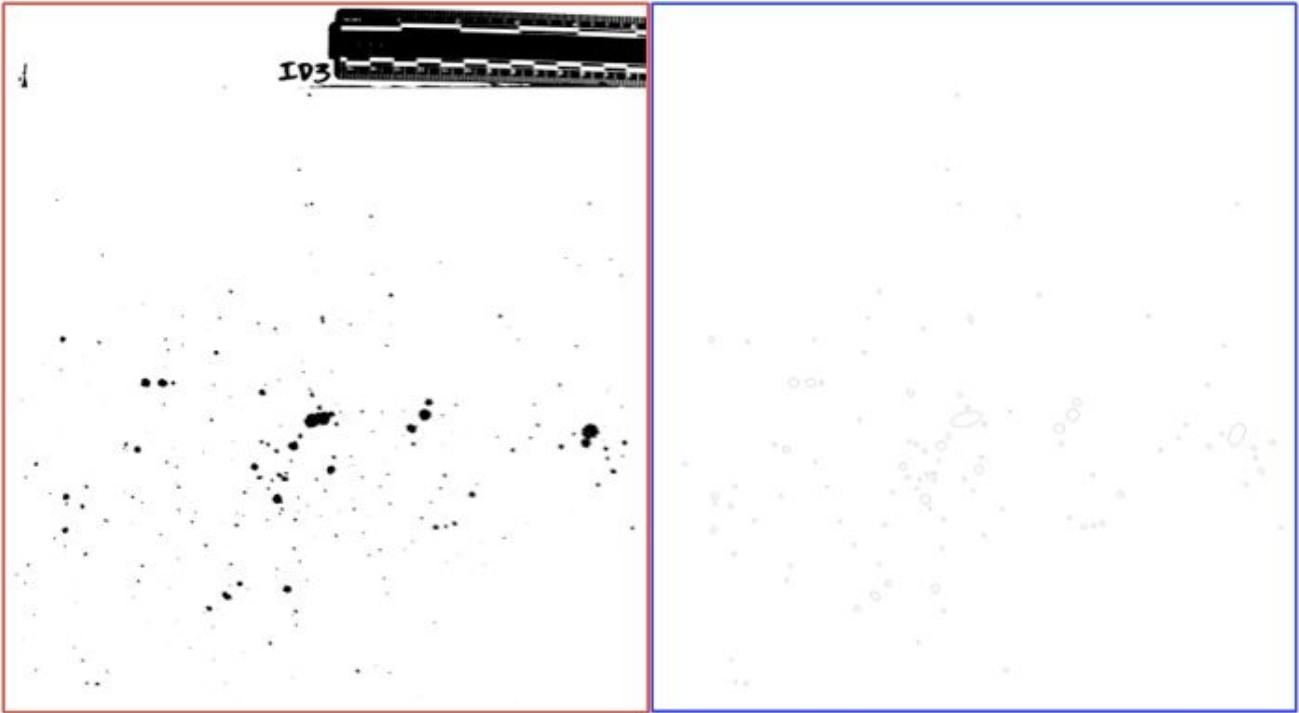This function generated the ellipse "drawing", as seen in Fig. 28:

Fig. 28: ID3 Binary (red), ID3 Ellipse Map (blue)

Also generated with the ellipse map was the results previously selected, including area,

perimeter, circularity, major and minor axes. The results table was saved as an excel file for each

sample, as shown in Fig. 29:

	Stain	Area	Perim.	Major	Minor	Angle	Circ.	AR	Round	Solidity
2	1	1.588	5.699	1.753	1.154	154.041	0.615	1.519	0.658	0.833
3	2	0.801	3.604	1.277	0.798	153.649	0.775	1.6	0.625	0.887
4	3	1.277	5.248	1.363	1.193	158.688	0.583	1.143	0.875	0.81
5	4	0.877	3.577	1.175	0.95	175.543	0.861	1.238	0.808	0.89
6	5	1.106	5.229	1.384	1.017	169.511	0.508	1.36	0.735	0.77
7	6	1.391	4.599	1.605	1.104	143.617	0.827	1.454	0.688	0.912
8	7	2.332	6.364	1.782	1.666	131.044	0.723	1.069	0.935	0.889
9	8	1.69	5.614	1.505	1.43	131.414	0.674	1.052	0.95	0.861
10	9	4.079	10.205	3.335	1.558	100.391	0.492	2.141	0.467	0.795
11	10	0.801	3.887	1.193	0.854	41.638	0.666	1.396	0.716	0.773
12	11	1.137	4.619	1.282	1.13	159.629	0.67	1.135	0.881	0.801
13	12	4.784	9.603	2.528	2.41	59.902	0.652	1.049	0.953	0.845
14	13	0.896	4.074	1.184	0.963	12.848	0.678	1.229	0.814	0.862
15	14	1.29	4.685	1.568	1.047	146.112	0.739	1.497	0.668	0.851
16	15	0.813	6.045	1.162	0.891	163.392	0.28	1.305	0.766	0.667
17	16	2.859	6.73	2.002	1.819	162.826	0.793	1.1	0.909	0.91
18	17	12.282	15.057	4.158	3.761	160.893	0.681	1.106	0.904	0.916
19	18	11.246	16.063	4.295	3.334	170.258	0.548	1.288	0.776	0.859
20	19	2.351	6.504	1.829	1.637	57.631	0.698	1.117	0.895	0.857
21	20	1.086	5.641	1.356	1.02	93.345	0.429	1.33	0.752	0.786
22	21	6.004	12.157	3.069	2.491	149.173	0.511	1.232	0.812	0.857
23	22	2.605	7.099	2.082	1.593	114.425	0.65	1.307	0.765	0.838
24	23	7.809	14.862	3.307	3.006	172.964	0.444	1.1	0.909	0.833
25	24	2.789	7.367	2.071	1.715	146.189	0.646	1.208	0.828	0.856

Fig. 29: Results Generated by ImageJ

The results were automatically generated based on the settings previously described. However,

the "angle", "AR", "round", and "solidity" were not generated by Short's older version of

ImageJ and were not used for the current study. The results were duplicated into a new excel

sheet and these columns were erased. The "angle" column was erased and replaced with "impact

angle". The impact angle was calculated for each stain in degrees by using the formula

(=DEGREES(ASIN(minor value/major value))). The process was repeated for every stain. The

final results appeared as follows:

	A	B	C	D	E	F	G
1		Area	Perim.	Major	Minor	Impact Angle	Circ.
2	I1_1	1.741	6.309	1.791	1.237	43.6836123	0.55
3	I1_2	2.961	8.405	3.364	1.121	19.465199	0.527
4	I1_3	1.69	4.778	1.479	1.455	79.6641023	0.93
5	I1_4	1.112	3.849	1.249	1.134	65.220342	0.943
6	I1_5	1.366	4.28	1.349	1.289	72.8473881	0.937
7	I1_6	3.018	6.59	2.112	1.819	59.4593593	0.873
8	I1_7	3.031	6.543	2.121	1.82	59.1023322	0.89
9	I1_8	1.607	4.599	1.469	1.394	71.6125014	0.955
10	I1_9	1.055	3.67	1.159	1.159	90	0.984
11	I1_10	1.233	4.008	1.322	1.187	63.8810468	0.964
12	I1_11	1.296	4.168	1.307	1.263	75.0908756	0.938
13	I1_12	1.118	3.915	1.25	1.139	65.6717129	0.917
14	I1_13	1.036	3.67	1.22	1.08	62.2817972	0.966
15	I1_14	1.125	3.802	1.26	1.137	64.4728194	0.978
16	I1_15	2.484	5.8	1.828	1.731	71.2511432	0.928
17	I1_16	1.029	3.643	1.151	1.138	81.3805162	0.975
18	I1_17	2.846	6.43	1.971	1.838	68.8313554	0.865
19	I1_18	3.672	7.068	2.254	2.074	66.9468458	0.924
20	I1_19	2.319	5.734	1.799	1.641	65.8074528	0.886
21	I1_20	2.04	5.276	1.645	1.579	73.714935	0.921
22	I1_21	2.954	7.126	2.05	1.835	63.5240983	0.731

Fig. 30: Final Results

In order to ensure that the researcher could view the results generated in excel and trace

each stain to its original number in the binary image, the researcher returned to the "Analyze

Particles" window and marked it to show "overlay" instead of ellipses. The resulting image

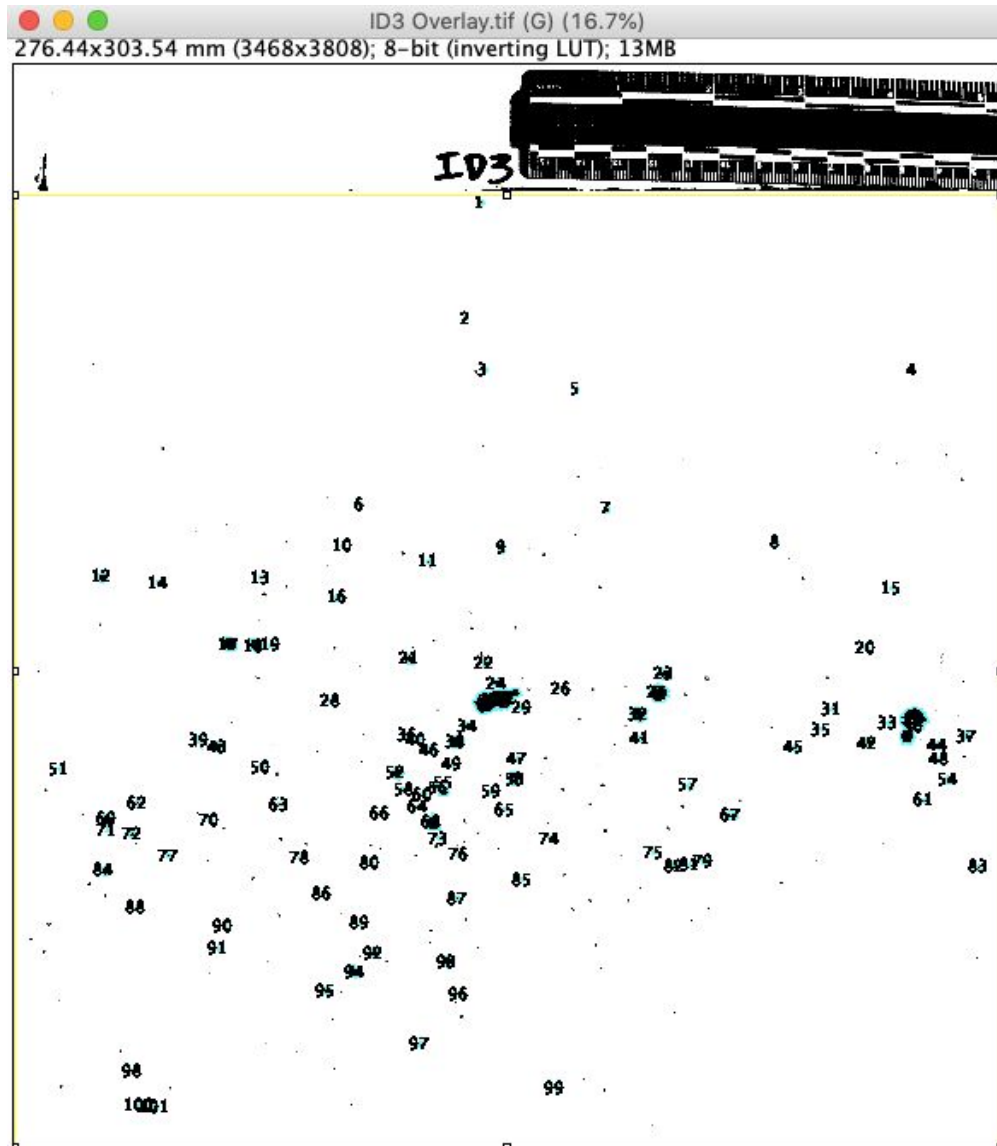outlined each stain and labeled each stain with its corresponding number, as seen in Fig. 31:

Fig. 31: ID3 labeled Overlay

After review of best fit ellipses for denim samples, the author noticed that the impact

denim samples had stains which were overlapping. This affected the best fit ellipse in the

drawing generated by ImageJ (see Fig. 28). Because the watershed command was not utilized for

denim samples, overlapping stains were counted as one stain, often a long ellipse, when they

were in fact two or three individual circles. To compensate for this, the drawing, overlay, and IR image were intercompared, the overlapping stains were identified, and subsequently excluded from results before statistical analysis.

The satellite denim samples were analyzed in the same manner as the impact samples, with minor adjustments. The fabric identifier, such as "SD1", was written in silver Sharpie on the denim itself, as opposed to the impact samples, where the identifier was written on the poster board the denim was stapled to. When converted to binary, the fabric identifier written in silver sharpie was not readily visible. To account for this, the rectangular tool was used to select the fabric identifier and adjust the brightness and contrast. This caused the identifier only to become more visible, and the image was then converted to binary. The process previously described was repeated in the same manner for the satellite samples. The global scale was confirmed, measurements were set, and results were generated with the ellipse map and a labeled overlay.

ImageJ Analysis - Control Samples

In order to compensate for a white background and white fabric, Short added a boundary to the edge of the fabric by drawing a boundary around the fabric using Paint.net and a touchscreen computer (2016, p. 32). The current researcher did not add a boundary, because the color contrast between the background and the samples was sufficient enough that it minimally affected the images when they were converted to binary. In an effort to isolate the bloodstains as much as possible, the author simply duplicated and cropped the images in ImageJ to limit the background before analysis. The images were saved as a TIF file. However, when the control images were converted to binary, the bottom corner of the scale was obscured, as seen in Figure 32:

Fig. 32: Control Sample Initial Conversion to Binary

Although the obscurement of the corner of the scale did not substantially affect the bloodstains,

the author used the polygon tool to isolate the corner of the scale, raised the brightness and

contrast using the methods previously described, and then converted the image to binary. The

scale was then rendered visible. The watershed command was then used to separate overlapping

stains. The area for analysis was selected with the polygon tool by isolating the spattered area

and omitting the scale, background, and fabric identifier. For some samples, the bottom right

corner of the poster board appeared darker due a slight bend in the stiff poster board. This bend

was made while cutting the poster board into pieces during material preparation. This area was

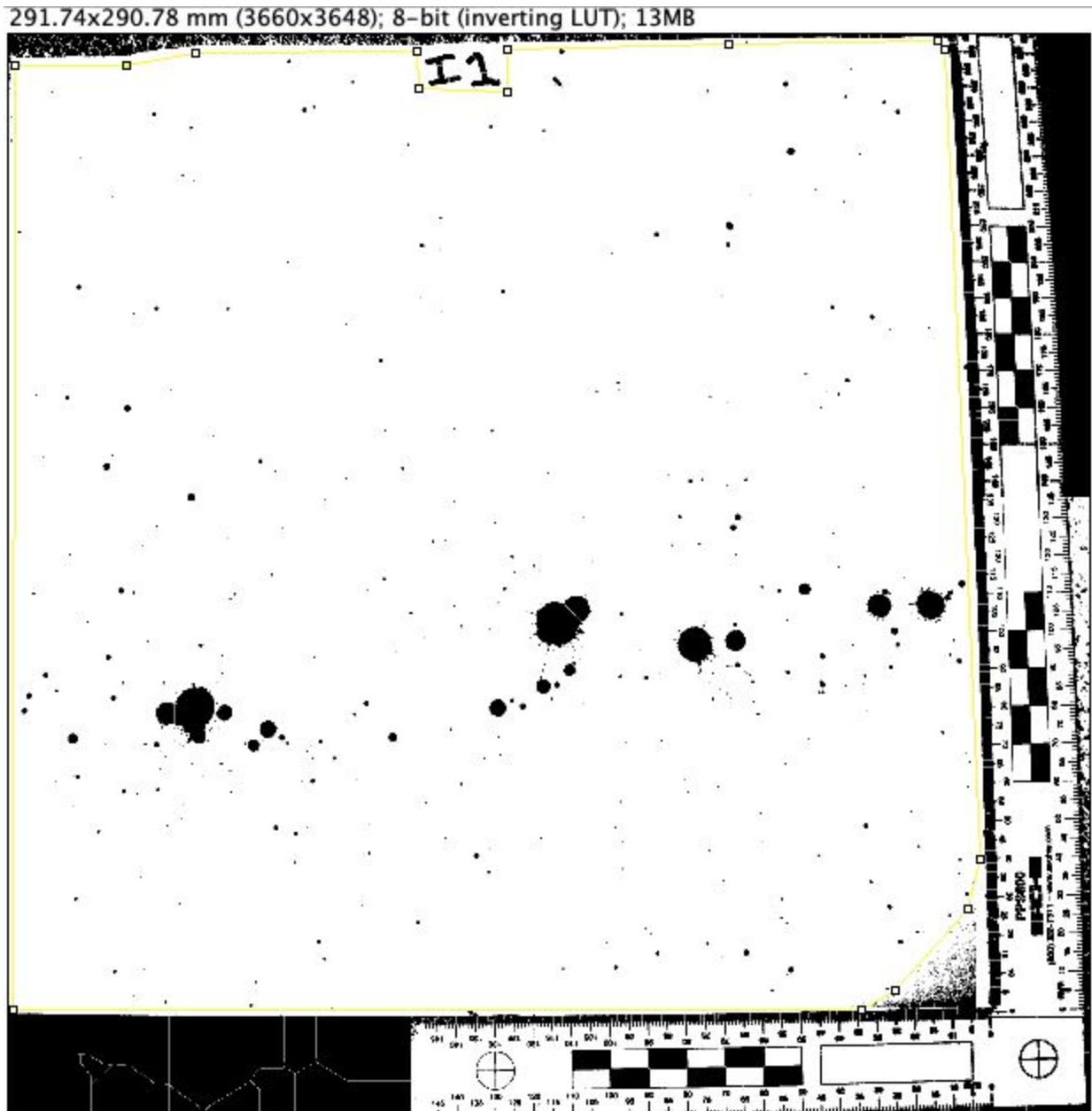excluded from analysis, as seen in Figure 33:

Fig. 33: Conversion to Binary and Area Selection Following Watershed and Scale Contrast Adjustment

If any accidental transfer stains were noted, they were also excluded from the selection using the

same method. Though this manual selection method was effective, for some samples, the corner

was prevented from inhibiting analysis simply by selecting the corner alone and then deleting it.

This cleaned up the image and prevented the corner from being accidentally included in the

results. Since the software was set to detect stains of one millimeter or greater, if any tiny specks

were accidentally included in the selection, they should not substantially affect the results.

Additionally, the overlay would be able to show if any stains were selected in that area. Before

deletion, the author zoomed in on the corner, compared it to the original image, and then

compared it to the binary image to make sure no relevant spatter was being excluded from
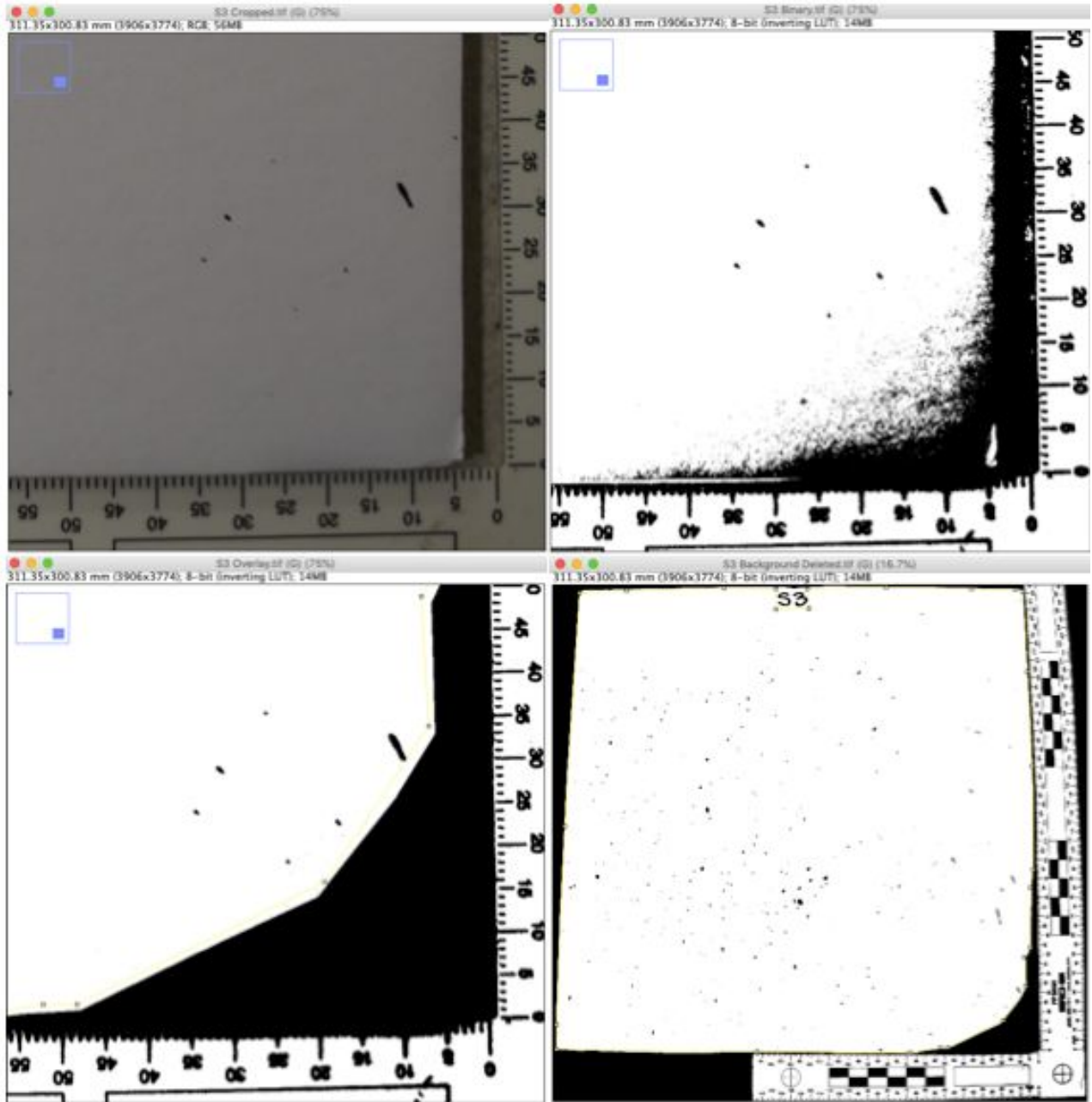
analysis, as seen in Fig. 34:

Fig. 34: S3 Original (top left); S3 binary (top right), S3 deleted corner (bottom left), S3 overall (bottom right)

Control samples were analyzed in the same manner as previously described by setting

measurements, generating an ellipse map, excel sheet with results, and labeled overlay. The

process was repeated for every impact control sample. Satellite control samples were processed

using the same methods as the impact control samples, with excluding the use of the watershed

command, due to the lack of overlapping stains.

Qualitative Analysis

Stain Selection

Bloodstains were selected via stratified random sampling in the same manner used by

Short (2016, p. 38-39). A plastic "T shirt Transformation" transparent grid overlay was acquired.

When purchased, the overlay was separated into square inches. The researcher used a yardstick

to divide each column and row in half with a permanent marker and labeled each 0.5 square inch

with a number. The resulting grid totaled 20 units on the x axis and 20 units on the y axis. Each

unit was 0.5 inches in width and length. The total overlay was 10 inches (or about 25 cm) in

width and length, in accordance with the size of the samples. The center of the overlay was

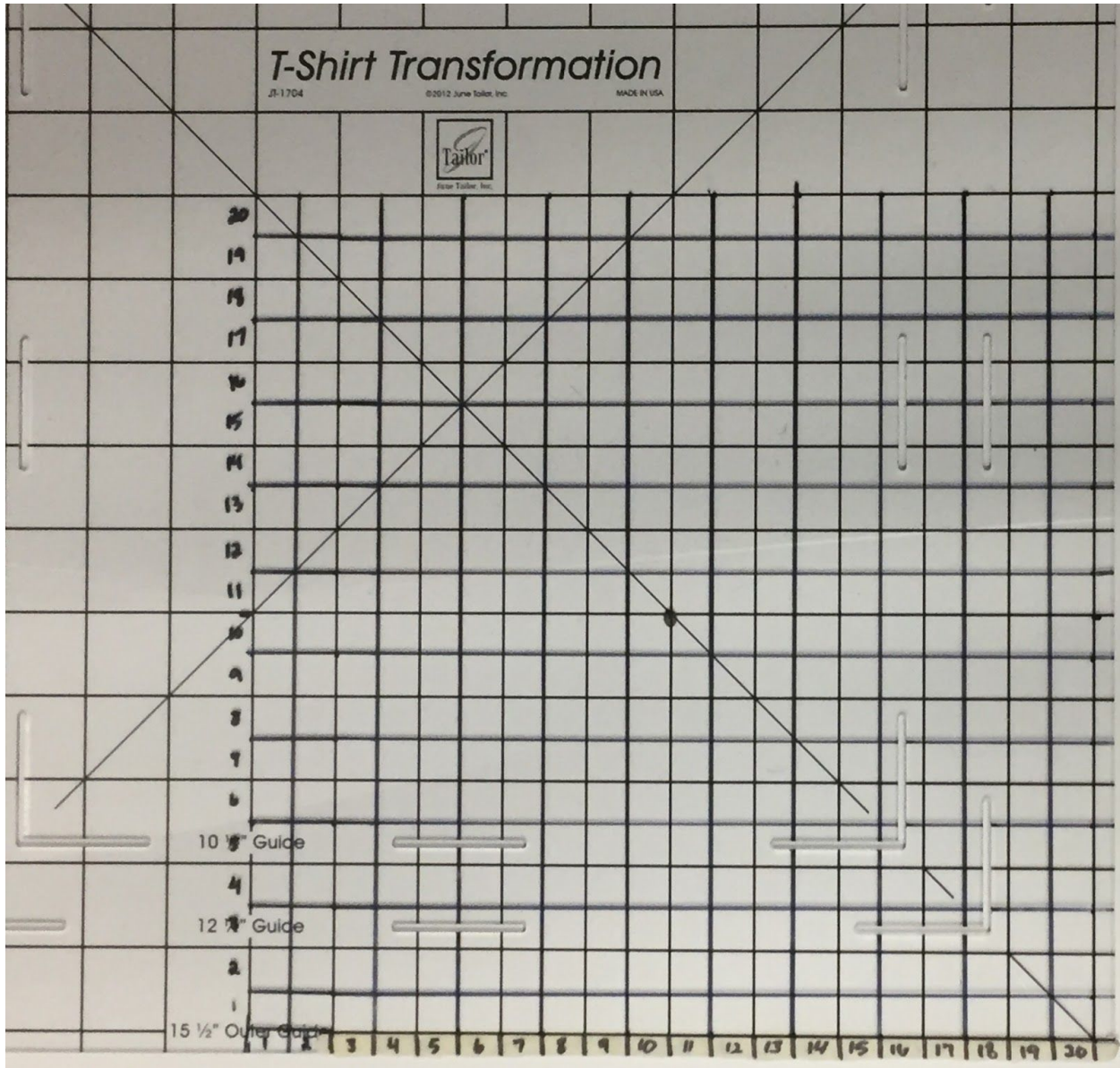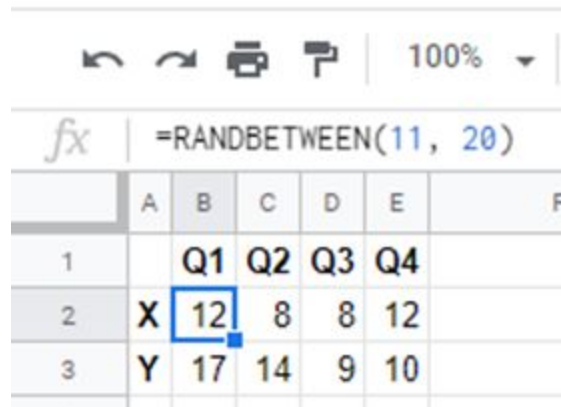marked with a dry erase marker to make the separation of each quadrant easier to find:

Fig. 35: Blank Grid Overlay

Quadrant I ranged from X coordinates 11-20 and Y coordinates 11-20. Quadrant II ranged from X coordinates 1-10 and Y coordinates 11-20. Quadrant III ranged from X coordinates 1-10 and Y coordinates 1-10. Quadrant IV ranged from X coordinates 11-20 and Y coordinates 1-10. A random number generator was created in Google Sheets using the

RANDBETWEEN formula to generate random X and Y coordinates in the correct quadrant. The

page was refreshed to generate new coordinates.

Fig. 36: Random Number Generator

A Sirchie PPS600 reversible corner scale was used to isolate each quadrant on the overlay. When

a coordinate was generated, such as (12, 17), stains would be circled with the dry erase marker

on the overlay. If there were no stains in the random coordinate, another coordinate would be

generated. The square which did not contain any stains would be marked off with a dry erase

marker. If the marked coordinate was generated again, it could be easily skipped. If a stain was

selected which was bigger than the coordinate, the entire stain was circled if it was visible in at

least half of the coordinate. If less than half of the stain was inside the coordinate, it was not

circled. The process continued until four stain-present locations were selected in each quadrant,

for a total of sixteen locations for each sample. The number of stains per quadrant was recorded

in Appendix E. After the stains were circled on the transparent overlay, they were circled on the

physical sample. After all stains had been circled, they were each labeled with a number. The

selections were then erased on the overlay and the process was repeated for both control and

denim samples.

Stain selection was completed for control samples with minimal issues, as the grid was

easily seen over the white poster board, such as in Fig. 37:
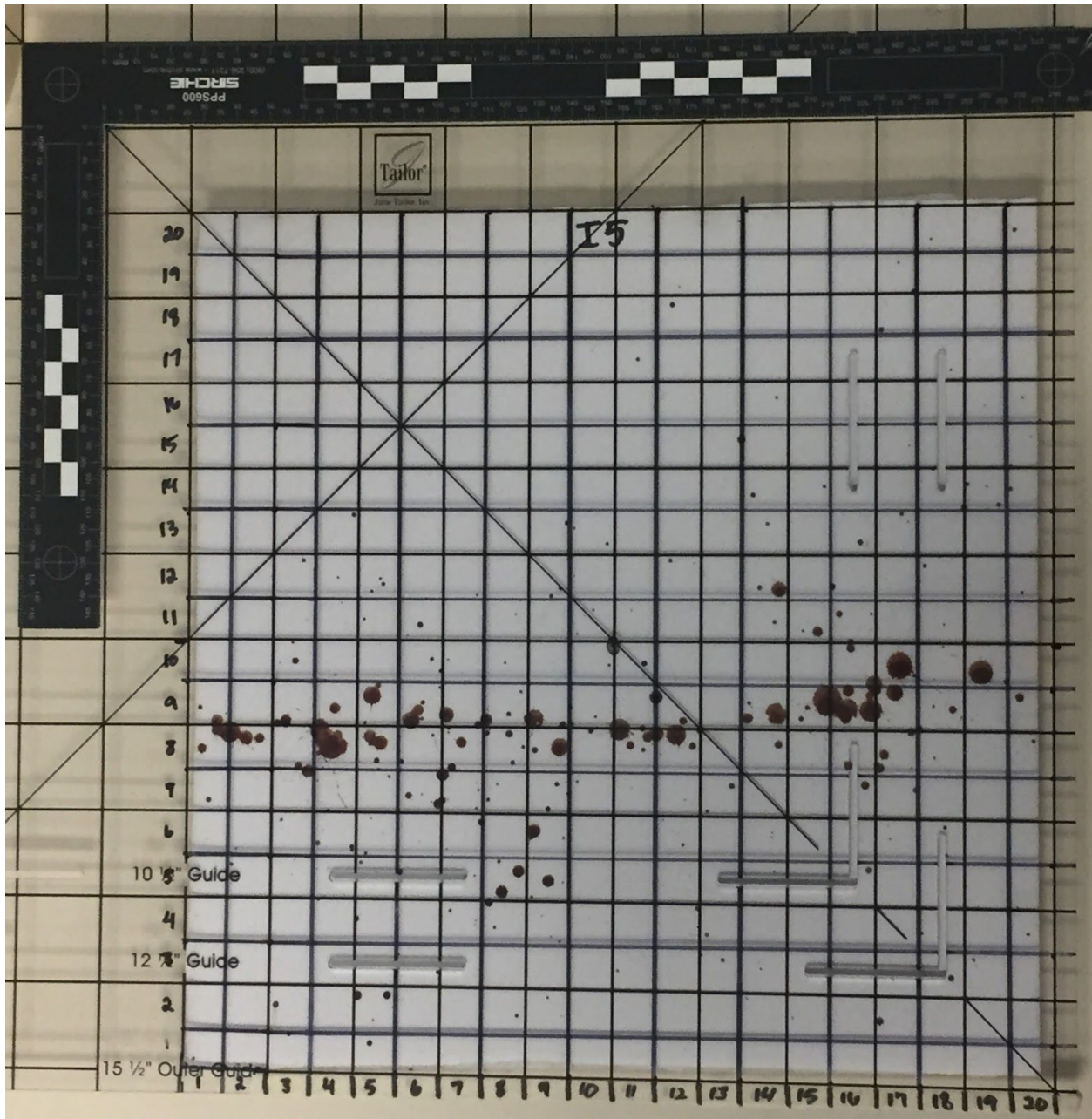

Fig. 37: Grid Overlay on Control Sample I5

The white background of the poster board made bloodstains easy to identify and select.

Conversely, the blood was difficult to visualize on the fabric due to the dark nature of the denim

and the blood. To counteract this, the Celestron Digital Handheld Microscope was used to

confirm or deny that stains were present when coordinates were randomly generated. The

microscope allowed the researcher to view stains at 4x-50x magnification. Additionally, the

stains were much more easily identified by turning on the illuminator, which emitted LED white

light from the lens. Stains within denim samples were selected in the same manner as control

samples, with the addition of using the LED illuminator within the microscope to identify stains.

Additionally, the author referred to the IR images if necessary to confirm that stains were

present. When circling stains on the fabric, the black permanent marker could not be seen on the

dark denim. An ultra fine point, white fabric paint Sharpie was tested on a separate piece of

denim, but the ink was not vibrant enough to be sufficiently visible. Ultimately, Tulip brand

matte white dimensional fabric paint was used to circle and label selected stains on denim fabric.

Coordinates were randomly selected and eliminated in the same manner as control samples.

Stain Analysis

Once the stains were selected, the number of stains per quadrant for each sample, as well

as the individual stain numbers within each quadrant, was recorded in Appendix E. Following

this, each selected stain was individually examined using the microscope at 4x and 50x

magnification. The stains were examined for four different characteristics: 1) shape, 2)

symmetry, 3) saturation, and 4) if the stain was submillimeter. An additional space was provided

to allow the researcher to take notes on each stain. These features were examined by Short and

followed the same guidelines to categorize each stain (2016, p. 40-42).

Firstly, shapes were classified as round, polygonal, or irregular. A stain was classified as

round if it was a circle or an oval and did not contain any straight edges. A stain was classified as

polygonal if it contained only straight edges, such as a square, rectangle, or parallelogram. A

stain was classified as irregular if it contained both round and straight edges. Specific shapes

were recorded in the individual notes for each stain.

Secondly, stains were recorded as symmetrical or asymmetrical. A stain was recorded as

symmetrical if it "contained mirrored characteristics about any axis", or it could be folded in half

while sharing equal characteristics. An asymmetrical stain did not contain "mirrored

characteristics about any axis" and did not share equal characteristics on both sides (Short, 2016,

p. 41).

Thirdly, stains were recorded as either saturated into the denim fabric or sitting on top of

the denim fabric. A stain was saturated if it soaked into the individual fibers. This was visible at

50x magnification. A stain counted as sitting on top of the fabric if it was especially faint due to

not soaking into the individual fibers, or appeared to be a full stain but microscopic examination

showed the stain covered the tops of the weave pattern as opposed to a continuous stain soaking

into the weave. Saturation was recorded as "top" for all stains on control samples because poster

board is a smooth, non-porous surface, preventing the blood from soaking through.

Fourthly, stains were classified as either larger than one millimeter or submillimeter by

using the microscope and a ruler. The determinations were dictated in a column labeled

"submillimeter" with the answer "yes", indicating the stain's major axis was submillimeter, or

the answer "no", indicating the stain's major axis was one millimeter or larger in diameter. If the

stain was not submillimeter, the major axis length was recorded in the individual notes.

Some bloodstains, especially larger stains, showed spines. These were more visible in

control samples. If a stain had spines, partially attached spines were not counted as additional

stains. Stains with spines were almost always counted as asymmetrical, as the majority of stains with spines prevented the stain from having equal halves. Stains which were clearly overlapping, seen mostly in impact samples, were counted as separate stains.

Narratives

Separate narratives were created for both control and denim samples. The narratives provided the opportunity to record unique notes about each sample, as well as observations regarding distribution of stains, location, directionality, shapes, overlapping stains, patterns within each sample, and any other outstanding features. IR images were referred to in conducting narratives for denim samples.

Characteristics were documented for individual selected stains on each sample in a separate Google Sheet. The total number of round, polygonal, irregular, symmetrical, asymmetrical, submillimeter (yes or no) and saturation (saturated or top) was recorded at the end of each sample. After characteristics were determined and documented for all 20 samples, the total number of impact control, impact denim, satellite control, and satellite denim stains were recorded, as well as their individual numbers and percentages for each category. A comprehensive table was created for all four sample types and the results were documented in Appendix F.

<div align="center">

Statistical Analysis

</div>

Quantitative Data

Before quantitative results could be uploaded into SPSS, it was necessary to code the fabric identifier values so individual stains could be traced back to their source. Individual stains were labeled according to their fabric identifier (S1_1, S1_2, S1_3, etc.; see Fig. 30). Once

values in the stain ID column had been coded according to their fabric identifier, the excel sheet

was uploaded into SPSS. Two columns were created and for "Board Type" and "Stain Type".

Measured stains were coded by board and spatter types. Board type was coded as "1" for denim

fabric and "2" for control/poster board. Stain type was coded as "1" for impact spatter, and "2"

for satellite spatter. These codes remained consistent across every statistical test, including those

performed on qualitative results.

A total of six two-way ANOVA tests were performed separately for each DV. The DVs

were area, perimeter, major axis, minor axis, impact angle, and circularity. The tests allowed the

researcher to compare each DV with two independent variables (IV): stain type (satellite or

impact) and board type (denim or poster board). The tests generated descriptives for each of the

four spatter and board type combinations, between-subject factors, and two-way ANOVA. This

showed if the variables were significant from one another.

Qualitative Data

Fabric identifiers, stain counts, and board type for qualitative statistics were coded in the

same manner as quantitative results. The following coding was used for the qualitative dependent

variables:

Round = 1	Symmetrical = 1	Saturated = 1	Submillimeter Yes = 1
Polygonal = 2	Asymmetrical = 2	Top = 2	Submillimeter No = 2
Irregular = 3			

A Cochran-Mantel-Haenszel (CMH) test was performed on the same two IVs (board type

and stain type) and four qualitative DVs, which included shape, symmetry, saturation (not

applicable for control samples), and submillimeter status. The test showed if there was an

association between the dependent variable and independent variable in question. The CMH test

generated a frequency count and percentages across each of the four dependent variables. CMH

was applicable to the stratified data and accounted for the confounding variable of unequal

sample sizes resulting from spatter types. After performing CMH, results would not generate for

shape because it contained three levels (round, polygonal, and irregular) instead of two. To

account for this, a chi-square test was performed on shape. Although chi-square did not account

for the confounding variable of spatter type, it allowed the researcher to compare the shape to the

board type. The Pearson Chi-Square test showed if there was a statistically significant

association between the dependent variable and the board and stain type. Phi and Cramer's V

tests were performed to test the strength of these associations.

Results and Analysis

Quantitative Data

Quantitative results generated by ImageJ produced data for stains that were 1 mm or

larger across its major axis. Total stains analyzed on the four board and spatter types are impact

control (n=968), satellite control (n=93), impact denim (n=427), and satellite denim (n=49).

There is a significant interaction of area measurement between board type and stain type

($F(1, 1533)$=5.08 p<.05). There is not a significant difference between area measurement and

denim and poster board ($F(1, 1533)$=3.42 p<.05). There is a significant difference between area

measurement and impact and satellite spatter ($F(1, 1533)$=7.36 p<.05) (See Table 1).

There is a significant interaction of perimeter measurement between board type and stain

type ($F(1, 1533)$=.62 p<.05). There is a significant difference of perimeter measurement between

impact and satellite spatter ($F(1, 1533)=6.92$ p<.05). There is a significant difference of

perimeter measurement between denim and poster board ($F(1, 1533)=4.86$ p<.05) (See Table 2).

There is a significant interaction of major axis measurement between board type and stain

type ($F(1, 1533)=5.77$ p<.05). There is not a significant difference of major axis measurement

between impact and satellite spatter ($F(1, 1533)=.23$ p<.05). There is a significant difference of

major axis measurement between denim and poster board ($F(1, 1533)=1.21$ p<.05) (See Table

3).

There is a significant interaction of minor axis measurement between board type and

stain type ($F(1, 1533)=4.98$ p<.05). There is a significant difference of minor axis measurement

between impact and satellite spatter ($F(1, 1533)=30.87$ p<.05). There is a significant difference

of minor axis measurement between denim and poster board ($F(1, 1533)=14.63$ p<.05) (See

Table 4).

There is a significant interaction of impact angle measurement between board type and

stain type ($F(1, 1533)=1.47$ p<.05). There is a significant difference of impact angle

measurement between impact and satellite spatter ($F(1, 1533)=211.06$ p<.05). There is a

significant difference of impact angle measurement between denim and poster board ($F(1,$

$1533)=219.68$ p<.05) (See Table 5).

There is a significant interaction of circularity measurement between board type and stain

type ($F(1, 1533)=375.51$ p<.05). There is a significant difference of circularity measurement

between impact and satellite spatter ($F(1, 1533)=5.94$ p<.05). There is a significant difference of

circularity measurement between denim and poster board ($F(1, 1533)=6.45$ p<.05) (See Table

6).

In summary, there is a significant interaction of area, perimeter, major axis, minor axis, impact angle, and circularity measurements between board type and stain type. There is a significant difference of area, perimeter, major axis, impact angle, and circularity measurements between impact and satellite spatter. There is not a significant difference of minor axis measurements between impact and satellite spatter. There is a significant difference of perimeter, major axis, minor axis, impact angle, and circularity measurements between denim and poster board. There is not a significant difference of area measurements between denim and poster board (See Tables 7-10).

Table 1.

Means and Standard Deviations on the Measure of Bloodstain Area

Board and Stain Type	N	Mean	Std. Deviation	95% CI	
				Lower	Upper
Denim Impact	427	3.17	3.42	2.30	4.04
Denim Satellite	49	2.78	2.26	.21	5.35
Control Impact	968	6.66	11.28	6.08	7.24
Control Satellite	93	2.44	1.84	.57	4.30
Total	1537				

Note. CI = confidence interval.

Table 2.

Means and Standard Deviations on the Measure of Bloodstain Perimeter

Board and Stain Type	N	Mean	Std. Deviation	95% CI	
				Lower	Upper
Denim Impact	427	8.14	3.79	7.58	8.70
Denim Satellite	49	7.90	3.60	6.25	9.56
Control Impact	968	8.92	6.91	8.55	9.30
Control Satellite	93	6.26	2.75	5.06	7.46
Total	1537				

Note. CI = confidence interval.

Table 3.

Means and Standard Deviations on the Measure of Bloodstain Major Axis

Board and Stain Type	N	Mean	Std. Deviation	95% CI	
				Lower	Upper
Denim Impact	427	2.11	.83	1.97	2.25
Denim Satellite	49	2.19	.81	1.79	2.60
Control Impact	968	2.58	1.68	2.49	2.67
Control Satellite	93	2.37	1.28	2.07	2.66
Total	1537				

Note. CI = confidence interval.

Table 4.

Means and Standard Deviations on the Measure of Bloodstain Minor Axis

Board and Stain Type	N	Mean	Std. Deviation	95% CI	
				Lower	Upper
Denim Impact	427	1.64	.75	1.53	1.76
Denim Satellite	49	1.44	.58	1.10	1.80
Control Impact	968	2.35	1.48	2.27	2.42
Control Satellite	93	1.26	.44	1.01	1.51
Total	1537				

Note. CI = confidence interval.

Table 5.

Means and Standard Deviations on the Measure of Bloodstain Major Axis

Board and Stain Type	N	Mean	Std. Deviation	95% CI	
				Lower	Upper
Denim Impact	427	52.47	11.14	51.45	53.50
Denim Satellite	49	52.77	19.22	49.75	55.80
Control Impact	968	68.53	9.30	67.86	69.21
Control Satellite	93	39.13	16.20	36.94	41.33
Total	1537				

Note. CI = confidence interval.

Table 6.

Means and Standard Deviations on the Measure of Bloodstain Circularity

Board and Stain Type	N	Mean	Std. Deviation	95% CI Lower	95% CI Upper
Denim Impact	427	.55	.15	.54	.57
Denim Satellite	49	.55	.15	.51	.59
Control Impact	968	.83	.13	.82	.84
Control Satellite	93	.77	.17	.74	.80
Total	1537				

Note. CI = confidence interval.

Table 7.

Means and Standard Deviations on the Measure of Area, Perimeter, Major Axis, Minor Axis, Impact Angle, and Circularity within Satellite Spatter on Denim

Variable	N	Mean	Std. Deviation
Area	49	2.78	2.26
Perimeter	49	7.90	3.60
Major Axis	49	2.19	.81
Minor Axis	49	1.44	.58
Impact Angle	49	52.77	19.22
Circularity	49	.55	.15

Table 8.

Means and Standard Deviations on the Measure of Area, Perimeter, Major Axis, Minor Axis, Impact Angle, and Circularity within Satellite Spatter on Poster Board

Variable	N	Mean	Std. Deviation
Area	93	2.44	1.84
Perimeter	93	6.26	2.75
Major Axis	93	2.37	1.28
Minor Axis	93	1.26	.44
Impact Angle	93	39.13	16.20
Circularity	93	.77	.17

Table 9.

Means and Standard Deviations on the Measure of Area, Perimeter, Major Axis, Minor Axis, Impact Angle, and Circularity within Impact Spatter on Denim

Variable	N	Mean	Std. Deviation
Area	427	3.17	3.42
Perimeter	427	8.14	3.79
Major Axis	427	2.11	.83
Minor Axis	427	1.64	.75
Impact Angle	427	52.47	11.14
Circularity	427	.55	.15

Table 10.

Means and Standard Deviations on the Measure of Area, Perimeter, Major Axis, Minor Axis, Impact Angle, and Circularity within Impact Spatter on Denim

Variable	N	Mean	Std. Deviation
Area	968	6.66	11.28
Perimeter	968	8.92	6.91
Major Axis	968	2.58	1.68
Minor Axis	968	2.35	1.48
Impact Angle	968	68.53	9.29
Circularity	427	.83	.13

Qualitative Data

Qualitative results were generated with a microscope and produced data for stains of all sizes across its major or minor axis, including submillimeter stains. Total stains selected through stratified random sampling on the four board types are impact control (n=223), satellite control (n=116), impact denim (n=170), and satellite denim (n=90). Though qualitative methods are inherently subjective, sample sizes were much more evenly distributed as opposed to the quantitative data.

There is a significant association between submillimeter measurements and saturation classifications of board type (denim and control surfaces) and stain type (impact and satellite) $x^2_{MH}(1)$=15.37, p<.05 (see Table 11). Submillimeter and ≥1 mm impact stains on denim are more likely to be saturated than on top of the fabric. Saturated impact stains on denim are more likely to be ≥1 mm. Submillimeter and ≥1 mm satellite stains on denim are more likely to be saturated

than on top of the fabric. Saturated satellite stains on denim are equally likely to be ≥1 mm. All spatter on control samples were classified as on top of the surface because a non-porous surface does not have potential to absorb blood. Both impact and satellite spatter on poster board were more likely to be ≥1 mm.

There is not a significant association between submillimeter measurements and symmetry measurements of board type (denim and control surfaces) and stain type (impact and satellite) $x^2_{MH}(1)=.576$, $p<.05$. Stains do not tend to be more symmetrical or asymmetrical based on size (see Table 12).

There is not a significant association between saturation classifications and symmetry measurements of board type (denim and control surfaces) and stain type (impact and satellite) $x^2_{MH}(1)=.391$, $p<.05$. Stains do not tend to be more symmetrical or asymmetrical based on if the blood absorbs into the surface See Table 13).

There was a significant association between board type (satellite spatter on denim, satellite spatter on poster board, impact spatter on denim, and impact spatter on poster board) and shape (x^2 (6) = 80.15, p < .05, Cramer's V = .259). Round shapes are more likely to be found with impact spatter on poster board than the other three board types. Polygonal shapes are more likely to be found with impact spatter on denim. Irregular are more likely to be found with impact spatter on denim (See Table 14).

Table 11.

Frequency Counts Between Submillimeter and Saturation Measurements

| | | Submillimeter | | |
		Yes	No	Total
Denim Impact	Saturated	34	121	155
	Top	9	6	15
Denim Satellite	Saturated	4	67	71
	Top	5	14	19
Control Impact	Saturated	0	0	0
	Top	143	80	223
Control Satellite	Saturated	92	24	116
	Top	0	0	0

Table 12.

Frequency Counts Between Submillimeter and Symmetry Measurements

| | | Submillimeter | | |
		Yes	No	Total
Denim Impact	Symmetrical	23	54	77
	Asymmetrical	20	73	93
Denim Satellite	Symmetrical	3	27	30
	Asymmetrical	6	54	60
Control Impact	Symmetrical	72	33	105
	Asymmetrical	71	47	118
Control Satellite	Symmetrical	16	9	25
	Asymmetrical	76	15	19

Table 13.

Frequency Counts Between Symmetry and Saturation Measurements

		Symmetry		
		Symmetrical	Asymmetrical	Total
Denim Impact	Saturated	71	84	155
	Top	6	9	15
Denim Satellite	Saturated	25	46	71
	Top	5	14	19
Control Impact	Saturated	105	118	223
	Top	0	0	0
Control Satellite	Saturated	25	91	116
	Top	0	0	0

Table 14.

Frequency Counts By Shape and Board Type.

	Board Type				Total
	Denim Satellite	Control Satellite	Denim Impact	Control Impact	
Round	24	32	47	142	245
Polygonal	21	30	46	39	136
Irregular	45	54	77	42	218
Total	90	116	170	223	599

Observational Data

Impact Spatter

As seen in quantitative sample sizes, impact samples generated a much larger amount of stains than satellite samples. This observation was obvious compared to satellite samples with the naked eye (see impact and satellite samples in Appendix A). Generally, impact spatter created more stains and larger stains than satellite spatter. Stains generally exhibited ninety degree or near ninety degree impact angles, and therefore showed little directionality.

Four out of five control impact and four out of five denim impact samples showed a linear pattern including larger stains (3mm in major axis or larger) throughout the bottom third of the sample. This was readily visible in both control samples and IR images of denim samples. Outside of this linear pattern, impact spatter was more evenly dispersed throughout the sample in comparison to satellite spatter, though impact spatter was usually concentrated within the bottom half of the sample. Scallops and spines were readily visible on control samples, especially for the largest stains. The largest stains on denim samples did not exhibit spines, and possibly exhibited scallops, but this could have been influenced by the weave pattern of the fabric instead of the blood impacting the target.

Overall, impact spatter tended to have more stains and larger stains than satellite spatter, showed little to no directionality resulting from ninety degree or near ninety degree stains, linear patterns with centralized dispersion of spatter, and the presence of spines and scallops.

Satellite Spatter

Satellite samples generated as little as two stains larger than one millimeter, and as many as 46 stains larger than one millimeter. Although the same methods were used to create satellite

spatter, the overall stain counts at times differed substantially between samples, as shown in S3

and S4:
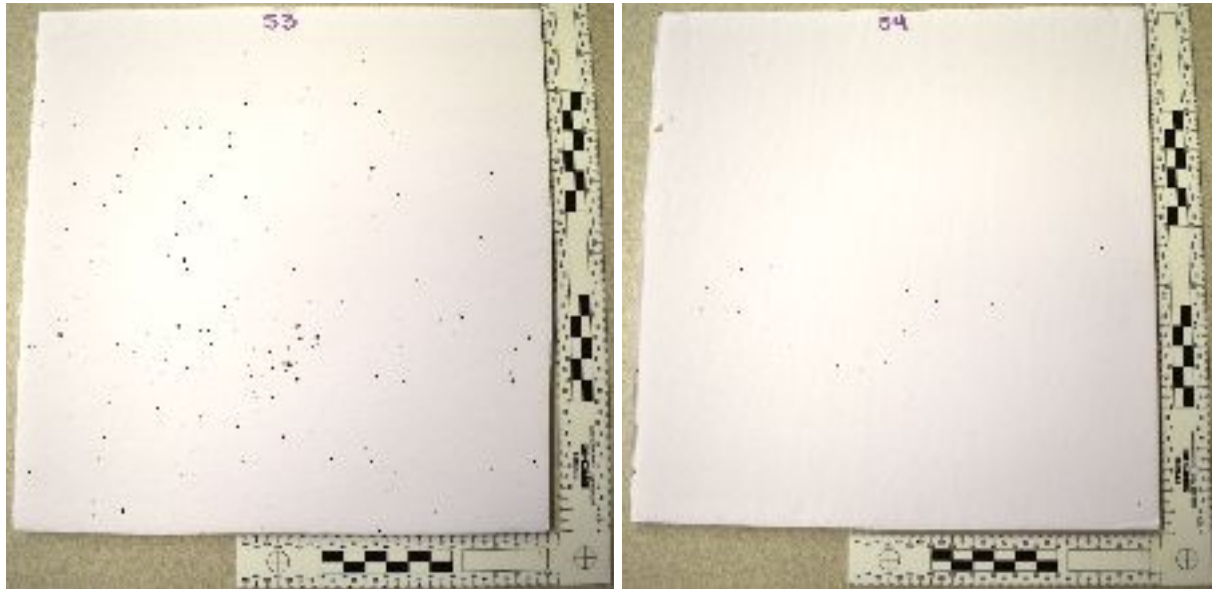
Fig. 38: S3 (left) and S4 (right)

One unique characteristic of satellite spatter is when stains form a tadpole shape with the

tail pointing back towards the parent stain. Several tadpole stains can be seen in the bottom right

section of S3. At least three tadpole stains were present in all control samples, generally in the

third and fourth quadrant (in the bottom half of the sample). Elliptical stains were fairly easily

detected through the IR images on satellite denim samples. Tadpole stains were much more

scarce throughout denim satellite samples as opposed to control satellite samples. Tadpole stains

were clearly more present and visible in control samples.

A second characteristic of satellite spatter is the random directionality of spatter. In other

words, the spatter points in several directions, as opposed to one direction consistently. Stains of

varying impact angles and random directionality was were noted on all satellite samples. Overall,

this was more clearly demonstrated on control samples than denim samples. For some denim

samples, the stains which exhibited random directionality were submillimeter and the margin of

difference in directionality was more slight when compared to control samples.

Lastly, the Short found a "v-shape dispersion pattern" within satellite control samples

(2016, p. 56). This pattern could possibly contrast with the linear pattern seen in impact spatter.

The current control and denim samples did not demonstrate the v-shape pattern.

Overall, blood into blood satellite spatter demonstrated characteristics including smaller

and less stains than impact spatter, the presence of tadpole stains, random directionality, and a

wider range of impact angles than impact spatter.

Discussion

Quantitative Data

There is a significant interaction between board type and stain type on area, perimeter,

major axis, minor axis, impact angle, and circularity measurements. The ANOVA tests were able

to separate board type from stain type, confirming that when considering each dependent

variable to classify stains as either satellite or impact spatter, the analyst would be better able to

make a determination when both board type and stain type are considered. Because there was a

significant interaction between board type and stain type for all six DVs, future research could

use all six variables to build a model on which stains within certain ranges can be classified as

either impact or satellite spatter specifically on a smooth, non porous surface or denim.

Additionally, a regression model could be built measuring these six DVs, in an attempt to

determine if we can predict the measurements we would expect to see between impact and

satellite spatter on denim and a smooth, non-porous surface.

There is a significant difference between impact and satellite spatter on area, perimeter, major axis, impact angle, and circularity measurements. Generally, these measurements differ between impact and satellite spatter. Future research could include generating a range for each of these measurements for each type of spatter separately. If stains fit the ranges of satellite spatter variable or impact spatter variables, this could indicate if groups of stains are satellite or impact spatter.

There is not a significant difference of minor axis measurements between impact and satellite spatter. Generally, minor axis measurements do not differ between impact and satellite spatter. This is not a surprising result, considering that as a stain's impact angle decreases, the stain becomes less round and more elliptical. An increase in length, or major axis, significantly changes the impact angle calculation, whereas the minor axis, or width, will vary less considerably than the major axis. A not significant finding in difference of minor axis measurements between impact and satellite spatter grants supporting statistical evidence to what is already known.

There is a significant difference of perimeter, major axis, minor axis, impact angle, and circularity measurements between denim and poster board. Generally, these measurements differ between denim and poster board. This finding confirms that the surface will influence these measurements, which shows that further research is needed to understand how blood behaves on denim, specifically in relation to the DVs in question. The current study examined 100% cotton denim, but further studies could include different weave patterns and denim of various components, such as 95% cotton and 5% elastane.

There is not a significant difference of area measurements between denim and poster board. Generally, area measurements do not differ between denim and poster board. The size of the stains were not significantly affected by the qualities of denim fabric when compared to a smooth, non-porous surface. In other words, stains generally show the same area on a control surface than they would on the type of denim in question.

As previously discussed, one major criticism of BPA is the subjectivity of pattern classifications, suggesting that classifying a group of bloodstains as one pattern type or another pattern type is open to interpretation. These statistics provide methods which promote a more objective basis for differentiating between impact and satellite spatter while considering differences in surface types, either by confirming what is already known or providing a statistical basis for future research.

Qualitative Data

Both satellite and impact spatter on denim were more likely to be greater than 1 mm. In looking at the samples overall, one would expect satellite samples to have more submillimeter stains than impact samples, but CMH results showed that both spatter types tended to have stains larger than one millimeter on denim.

Symmetry, in conjunction with either saturation or size of stains, does not provide an indication in classifying impact or satellite bloodstain patterns. This variable does not provide useful statistical data for future research.

Round stains are most commonly found in impact spatter on smooth non porous surfaces. This frequency likely has to do with the fact that impact spatter had more stains overall than

other types of spatter, and they were most easily seen on control samples as opposed to denim samples.

Polygonal and irregular stains are more likely to be found on impact denim samples. This likely results from the weave pattern in the denim. Shape was more likely to be distorted into an irregular or polygonal shape because the blood would follow the path of least resistance across straight edges of the weave pattern. This resulted in stains that were rectangular, diamond, square, or other shapes which exhibited straight edges, when they would normally create regular shapes like circles or ellipses, as seen with the high frequency of round stains in impact control samples (see Table 14).

Observational Discussion

Impact Spatter

The principal characteristics noted in impact spatter observations included the tendency have more stains and larger stains than satellite spatter, little to no directionality resulting from ninety degree or near ninety degree stains, linear patterns with centralized dispersion of spatter, and the presence of spines and scallops.

As previously discussed, one of the main differences between impact and satellite spatter is that impact spatter usually occurs at medium or high velocity because it requires the application of force, while the type of satellite spatter in question is a low velocity event caused by blood dripping into blood. The application of force likely contributed to the larger amount of stains on impact samples in comparison to satellite samples, even though the mousetrap was closed by gravity and not snapped shut. Further studies should explore the differences between impact spatter involving these two velocities. The lack of directionality resulted from the stains

being deposited on a vertical surface. Spines and scallops can sometimes indicate directionality, but they were rarely visible in denim samples. This might be because the spines were very small, but spines noted on denim samples in microscopic examination were listed as "possible spines" because they were unclear. The possible spines could also have been noted as possible scallops, however, the scallops could also have been a slight distortion on the edges of the stains due to the weave pattern of the fabric.

Satellite Spatter

The principal characteristics noted in satellite spatter observations included smaller and less stains than impact spatter, the presence of tadpole stains, random directionality, and a wider range of impact angles than impact spatter.

The smaller stains and less frequent stains likely resulted from the lack of force applied to satellite spatter, being that it is a low velocity event. In a case scenario where a piece of evidence was submitted with an unknown pattern classification, the frequency of stains and general size of stains should not be considered alone in pattern classification, especially if the amount of stains on the sample is limited.

The clearest tadpole stain on all satellite denim samples was located on the bottom edge of SD1. The stain exhibited a tail which appeared to skid across the denim weave, making it appear disconnected from the parent stain. The tail was picked up by the binary image after photoshop processing, but not by the ellipse function in ImageJ, due to the disconnection from the parent satellite. Several elliptical stains could possibly be classified as tadpole stains on denim satellite samples, but the denim weave made the tail difficult to identify. The only clear tadpole stain on all satellite denim samples was noted on SD1 in Fig. 39.
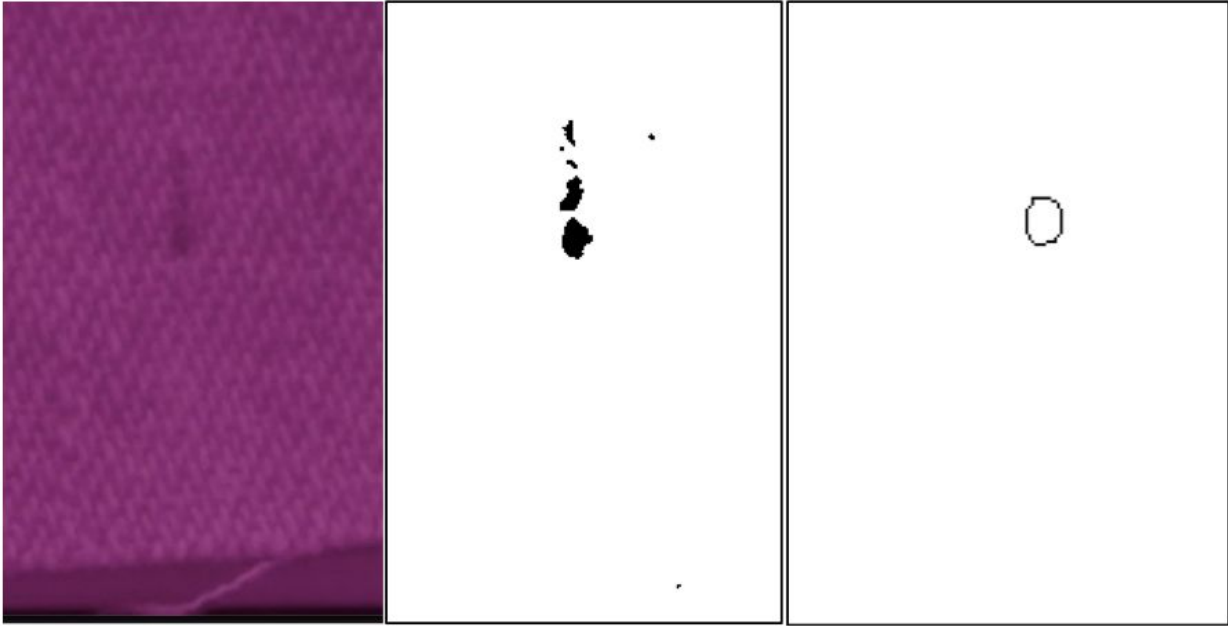
Fig. 39: Tadpole Stain on IR image of SD1 (left), Binary Image (middle), Ellipse (right)

The tail was likely not included in the ellipse because it was submillimeter and detached from the parent stain.

Random directionality was present in control samples more than in denim samples. The unclear tails and lack of tadpole stains on denim samples could possibly be a factor in this. If the tails were more clear on denim samples, they would indicate directionality more effectively. Additionally, twice as many stains ≥1 mm were detected on denim satellite samples (n=46) versus control samples (n=93). This left less stains to analyze for directionality on denim samples.

Lastly, by looking at the stains from the outside, impact spatter showed more circular stains, indicating impact angles closer to ninety degrees, and satellite spatter had more elliptical stains, indicating impact angles lower than ninety degrees. However, as seen in Table 5, the mean impact angle for denim impact spatter and control impact spatter was 52 and 68, respectively, and the mean impact angle for denim satellite spatter and denim control spatter was

52 and 39, respectively. One would expect to see a difference in mean impact angle between denim impact spatter and denim satellite spatter, but instead they are both 52. This mean is possibly skewed by the unequal sample size, with denim satellite collecting only 49 stains ≥ 1 mm, and denim impact collecting 427 stains ≥ 1 mm.

<u>Conclusion</u>

Statistics performed on quantitative data showed that there is a significant interaction between board type and stain type on area, perimeter, major axis, minor axis, impact angle, and circularity measurements. These dependent variables can be used to build a predictive regression model on which stains within a certain ranges can be classified as either impact or satellite spatter specifically on a smooth, non-porous surface or denim. When attempting to classify bloodstain patterns as either impact or satellite spatter, all dependent variables discussed should be considered in conjunction with one another, as opposed to one or two features at a time.

Statistics performed on qualitative data provided expected results, suggesting that the tests were accurately presenting the data. The most notable results showed that the shape was likely distorted by the weave pattern in the denim. Where stains would normally be round on a smooth non-porous surface, they may appear to show some straight edges on denim due to blood following the straight edges of the weave pattern.

IR photography was a successful tool in this study, expanding on the visualization research needs specified by SWGSTAIN. Although the Fujifilm XT1 IR camera, like all cameras, can be expensive, the equipment used in this study was efficient and provided minimal difficulties for the author. The most substantial findings related to IR photography in this study are the efficiency of the live view function prior to taking images, the ability to take comparison

quality images with 100 ISO (allowing the researcher to zoom in on very small stains later), and the determination that the best filter to view blood in this circumstance was at 830 nm.

Current methods for differentiating between impact and satellite spatter rely on classification criteria including unique characteristics within the patterns, which were largely present in the current study, though sometimes less frequent or clear in denim samples. Impact spatter on a vertical surface, as simulated in this study, tended to have centralized dispersion of spatter including linear patterns, overall larger stains, little to no directionality resulting from ninety degree or near ninety degree stains, and the presence of spines. In comparison, blood into blood satellite spatter demonstrated characteristics including uneven spatter dispersion, overall smaller stains, random directionality seen with varying impact angles, and the presence of tadpole shaped stains. That being said, the statistical analyses performed in this study provide the basis for a potential model which could give scientific backing to impact or satellite pattern classification in addition to the presence of these unique features. These findings may serve as a foundation on which future researchers can build upon, allowing analysts to make determinations in case work. Should this occur, analysts should follow established methodology and take into account the context of the entire scene, including witness statements. The hypothesis was supported by the results in this study.

References

Adair, T. W., & Shaw, R. L. (2005). Enhancement of bloodstains on washed clothing using

     luminol and LCV reagents. IABPA News, 21(4), 4-10.

AAFS American Standards Board. (2017). Terms and Definitions in Bloodstain Pattern Analysis.

     Retrieved from https://asb.aafs.org/wp-content/uploads/2017/11/033_TR_e1_2017.pdf

Basu, N., & Bandyopadhyay, S. K. (2017). Bloodstain pattern analysis–A less explored

     domain. IJAR, 3(1), 200-211.

Bevel, T., & Gardner, R. M. (2008). Bloodstain pattern analysis with an introduction to crime

     scene reconstruction. CRC press.

de Castro, T., Nickson, T., Carr, D., & Knock, C. (2013). Interpreting the formation of

     bloodstains on selected apparel fabrics. International Journal of Legal Medicine, 127(1),

     251-8. doi:http://dx.doi.org.vortex3.uco.edu/10.1007/s00414-012-0717-3

DiRienzi, Joseph. (2009). Blood spatter analysis. In A. Embar-Seddon and A. Pass (Ed.),

     Forensic Science. Hackensack: Salem. Retrieved from

     https://online-salempress-com.vortex3.uco.edu

Duncan, C. D. (2015). Advanced Crime Scene Photography. CRC Press.

Farrar, A., Porter, G., & Renshaw, A. (2012). Detection of Latent Bloodstains Beneath Painted

     Surfaces Using Reflected Infrared Photography. Journal of Forensic Sciences., 57(5),

     1190-1198.

Gardner, R. M. (2006). Defining a methodology for bloodstain pattern analysis. Journal of

     Forensic Identification, 56(4), 549-557. Retrieved from

http://vortex3.uco.edu/login?url=https://search.proquest.com/docview/194792896?accoun

tid=14516

Gore, S. E., Laing, R. M., Wilson, C. A., Carr, D. J., & Niven, B. E. (2006). Standardizing a

pre-treatment cleaning procedure and effects of application on apparel fabrics. *Textile*

research journal, *76*(6), 455-464.

Hill, T. (2011). Visualizing Bloodstain Patterns on Dark or Multi-colored, Multi-designed

Clothing using Luminol and Adobe Photoshop Layers. IABPA Journal of Bloodstain

Pattern Analysis.

Holdren, J. P., Lander, E. S., Press, W., Savitz, M., Austin, W. M., & Chyba, C. (2016). Report

To the President Forensic Science in Criminal Courts: Ensuring Scientific Validity of

Feature-Comparison Methods. *Subcommittee on the Social and Behavioral Sciences*

Team: United States Government.

Keenan, H. K. (2012). A Comparison of Bloodstains on Fabric: Characteristics of Impact

Spatter.

Lin, A. C. Y., Hsieh, H. M., Tsai, L. C., Linacre, A., & Lee, J. C. I. (2007). Forensic applications

of infrared imaging for the detection and recording of latent evidence. Journal of Forensic

Sciences, 52(5), 1148-1150.

Miles, H. F., Morgan, R. M., & Millington, J. E. (2014). The influence of fabric surface

characteristics on satellite bloodstain morphology. Science & Justice, (54)(4), 262-266.

National Research Council. (2009). Strengthening forensic science in the United States: a path

forward. National Academies Press.

Organization of Scientific Area Committees, Bloodstain Pattern Analysis Subcommittee

(OSAC). (2019). Research and Development Needs. Retrieved 13 July 2019, from

https://www.nist.gov/topics/organization-scientific-area-committees-forensic-science/osa

c-research-and-development-needs#Bloodstain

Raymond, T. (1997). Crime scene reconstruction from bloodstains. Australian Journal of

Forensic Sciences, 29(2), 69-78.

Robinson, James L. (2009). Blood residue and bloodstains. In A. Embar-Seddon and A. Pass

(Ed.), Forensic Science. Hackensack: Salem. Retrieved from

https://online-salempress-com.vortex3.uco.edu

Schuler, R. L., Kish, P. E., & Plese, C. A. (2012). Preliminary observations on the ability of

hyperspectral imaging to provide detection and visualization of bloodstain patterns on

black fabrics. Journal of Forensic Sciences, 57(6), 1562-1569.

Short, J. (2016). *A Comparative Analysis of Impact Spatter and Satellite Spatter on Fabric.*

University of Central Oklahoma.

Slemko, J. A. (2003). Bloodstains on fabric: The effects of droplet velocity on fabric

composition. *IABPA News,* 3-11.

Stanley, C. B. (2018). Bloodstain Pattern Analysis Subcommittee. Retrieved April 15, 2018 from

https://www.nist.gov/topics/forensic-science/bloodstain-pattern-analysis-subcommittee

Sterzik, V., Panzer, S., Apfelbacher, M., & Bohnert, M. (2016). Searching for biological traces

on different materials using a forensic light source and infrared photography.

International journal of legal medicine, 130(3), 599-605.

Scientific Working Group on Bloodstain Pattern Analysis (SWGSTAIN). (2009). Recommended

     Terminology. Retrieved from http://www.swgstain.org/resources

Scientific Working Group on Bloodstain Pattern Analysis (SWGSTAIN). (2009). Response to

     the NAS Report. Retrieved from http://www.swgstain.org/resources

Scientific Working Group on Bloodstain Pattern Analysis (SWGSTAIN). (2011). Current

     Research Needs for Bloodstain Pattern Analysis. Retrieved from

     www.swgstain.org/resources

Taylor, M., Laber, T., Kish, P., Owens, G., & Osborne, N. (2016). The Reliability of Pattern

     Classification in Bloodstain Pattern Analysis—PART 2: Bloodstain Patterns on Fabric

     Surfaces. Journal of Forensic Sciences., 61(6), 1461-1466.

Tobe, S. S; Watson, N., & Daeid, N. N. (2007). Evaluation of six presumptive tests for blood,

     their specificity, sensitivity, and effect on high molecular-weight DNA. *Journal of

     forensic sciences, 52*(1)-102, 109.

Webb, S. K. (2004). Luminol vs BlueStar: A comparison study of latent blood reagents.

     Technical Note from the Saint Louis Metropolitan Police.

Xiao, R., Zhao, X., Zhuh, X., & Zhang, L. (2010). Distinguishing bloodstains from botanic

     stains using digital infrared photography. *Journal of forensic identification., 60*(5), 524.
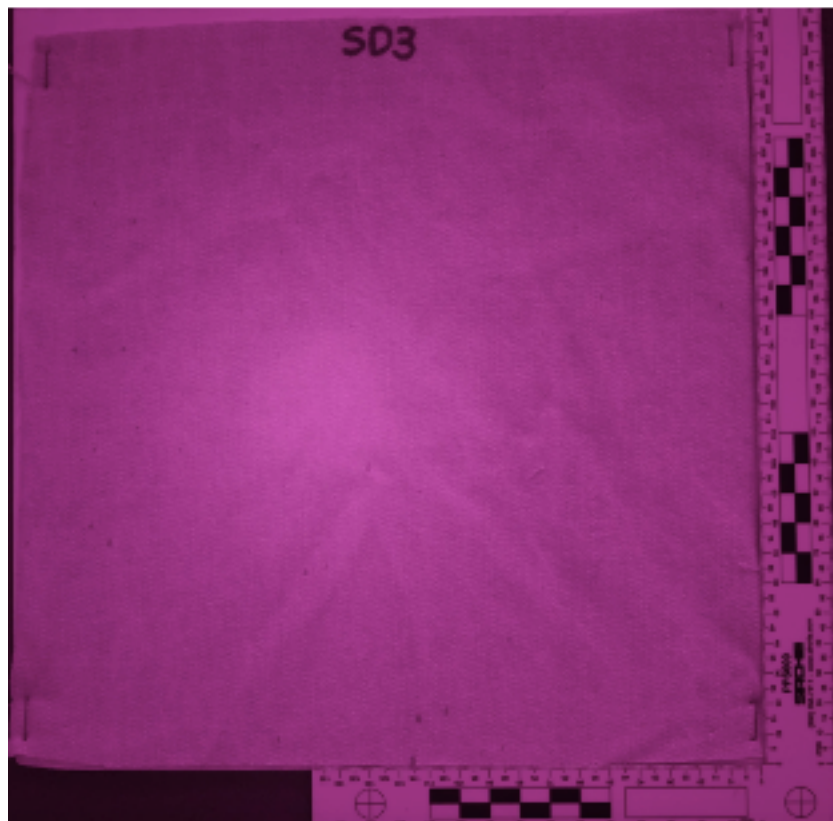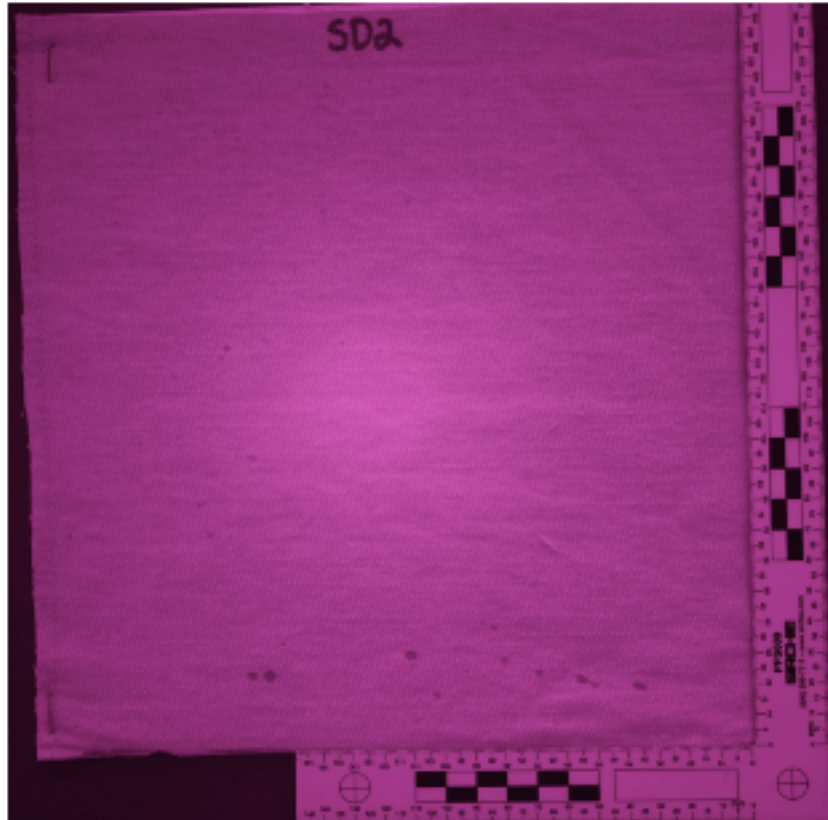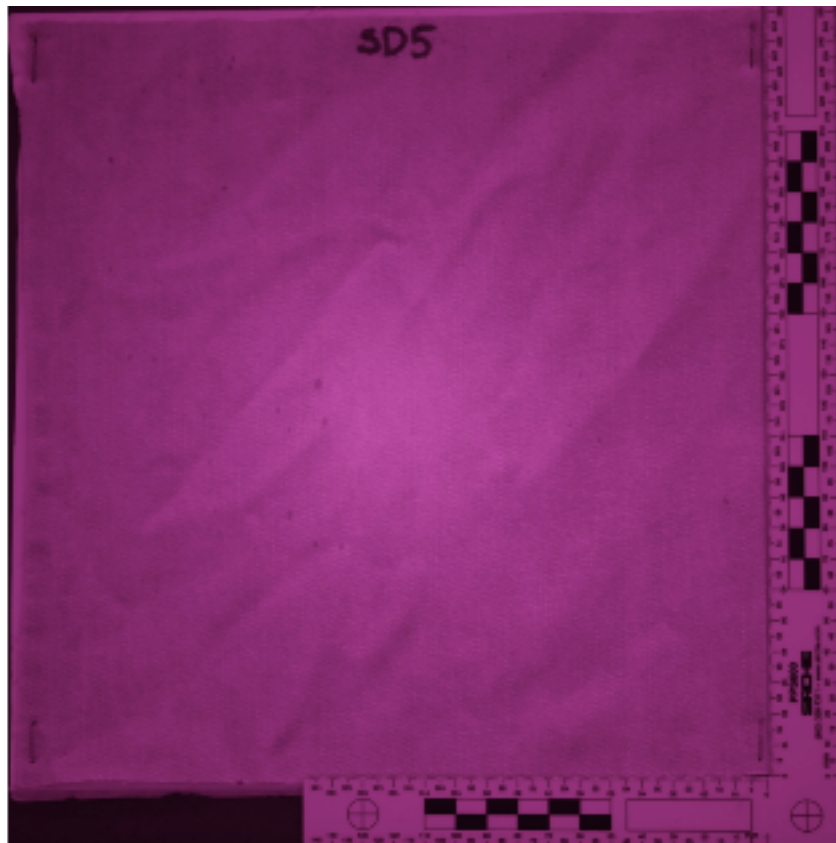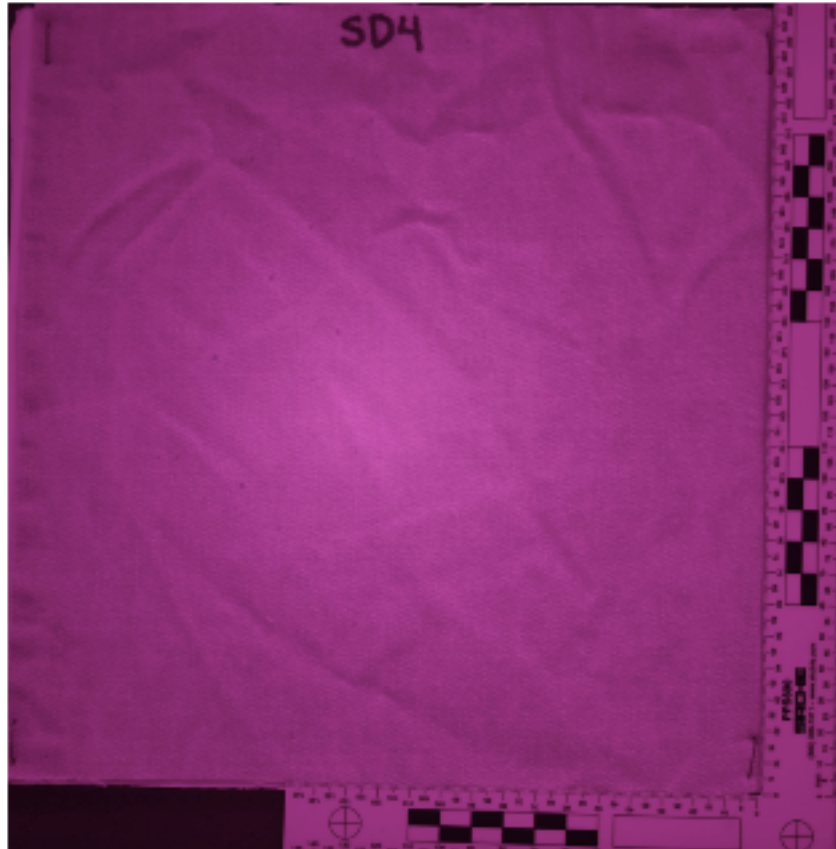
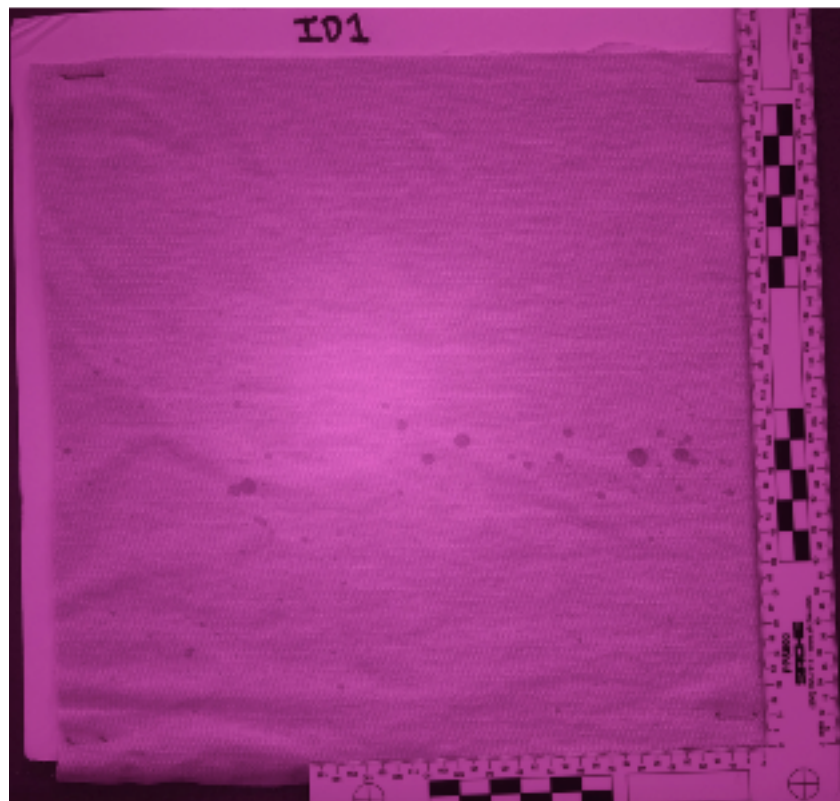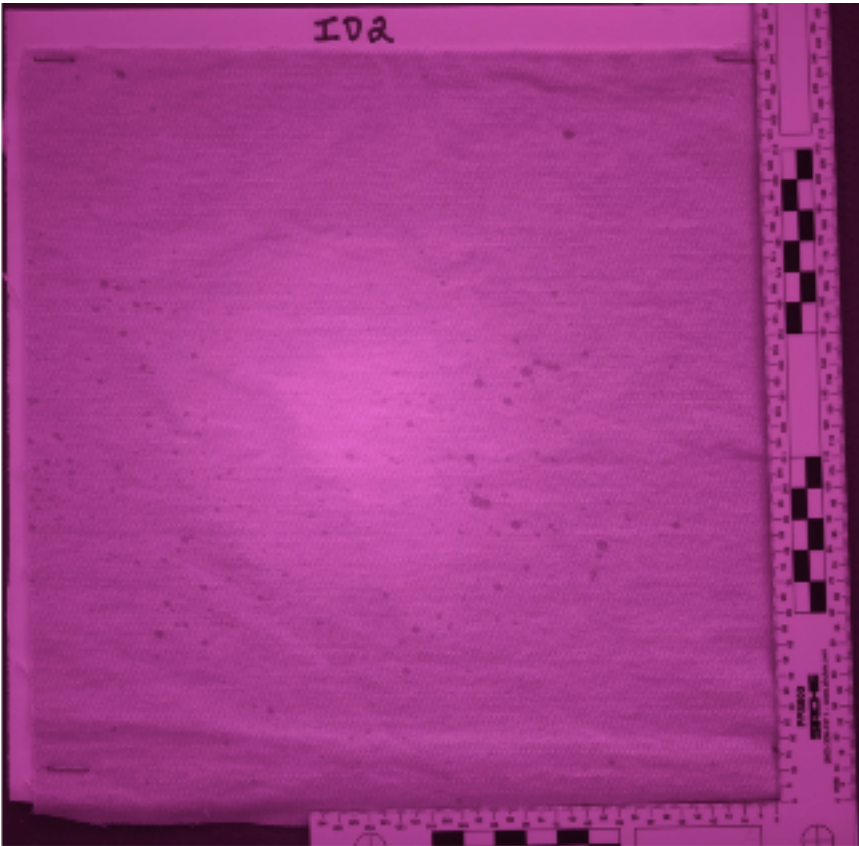**Appendix A - Spattered Control and Denim Samples**
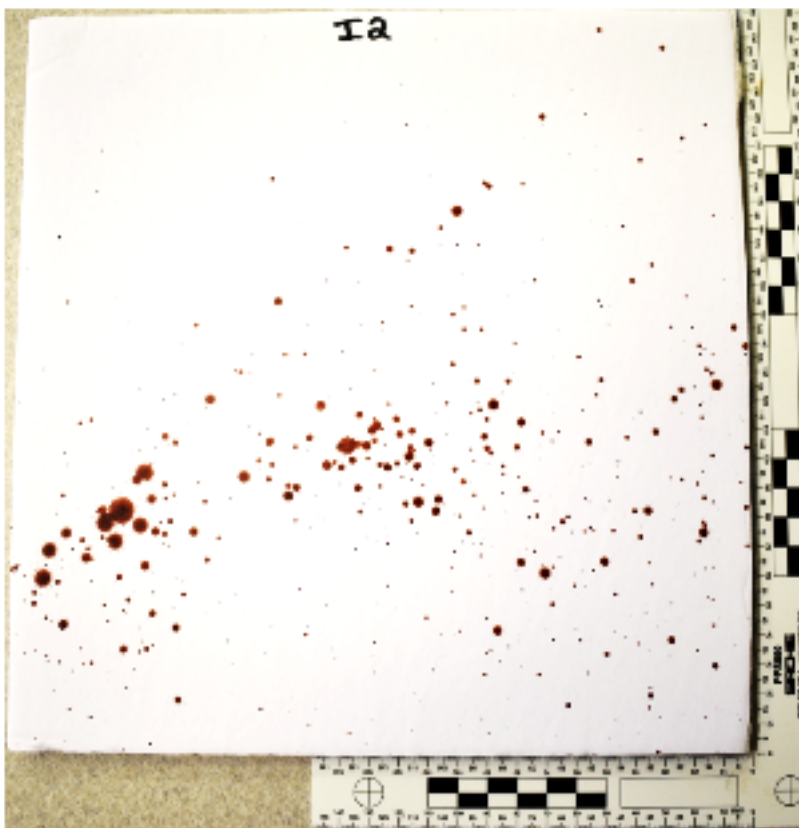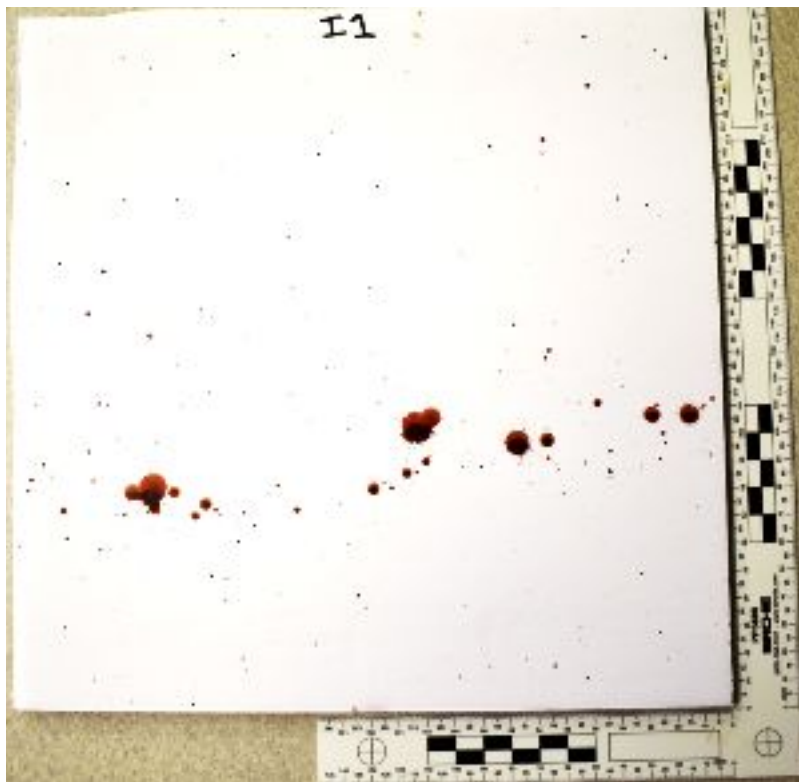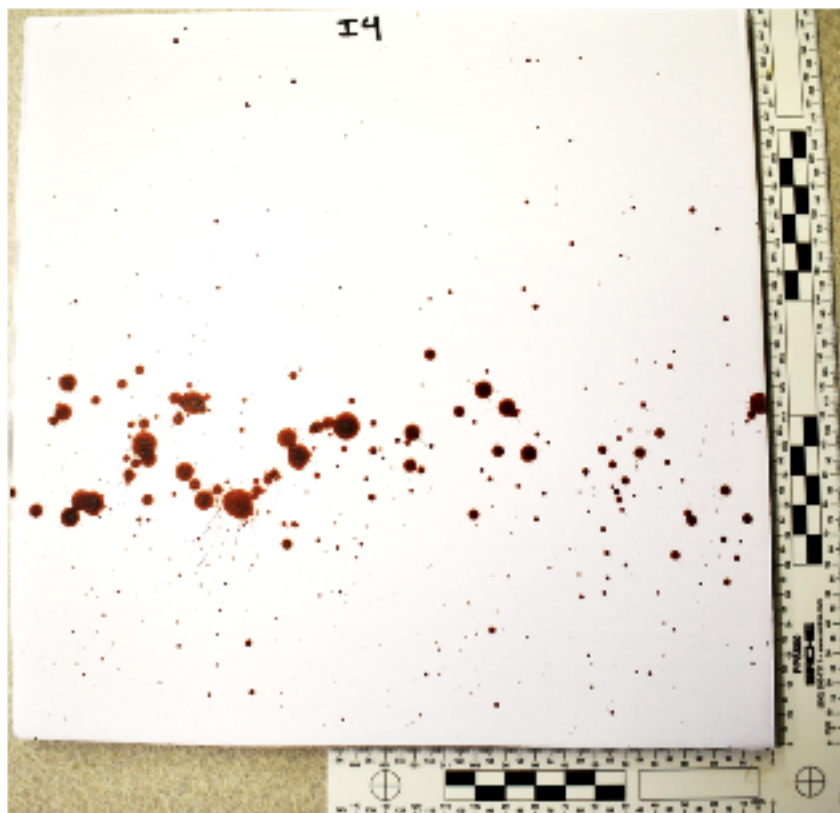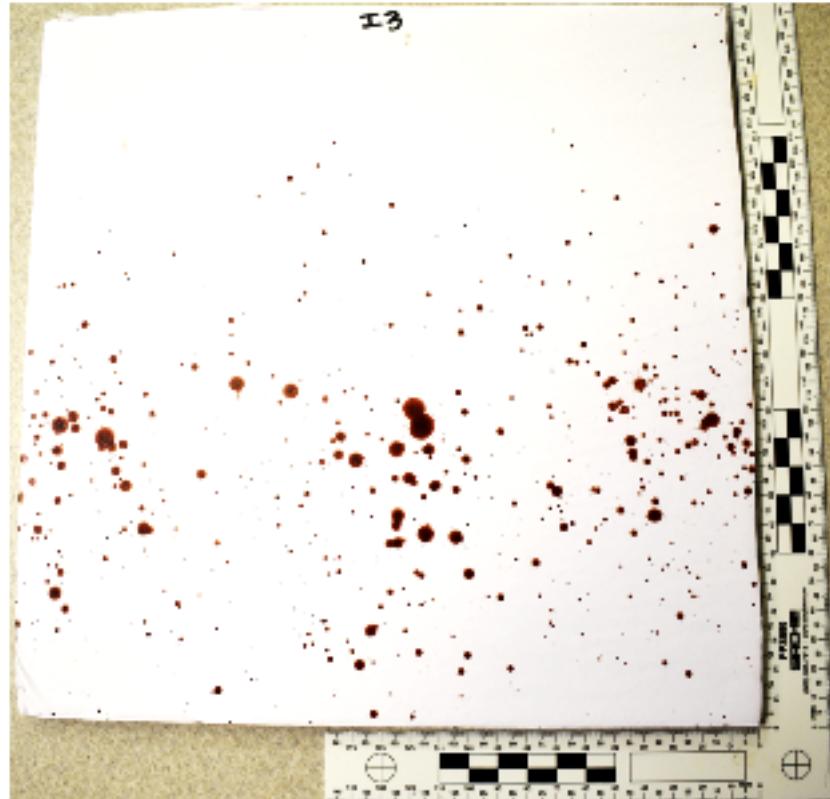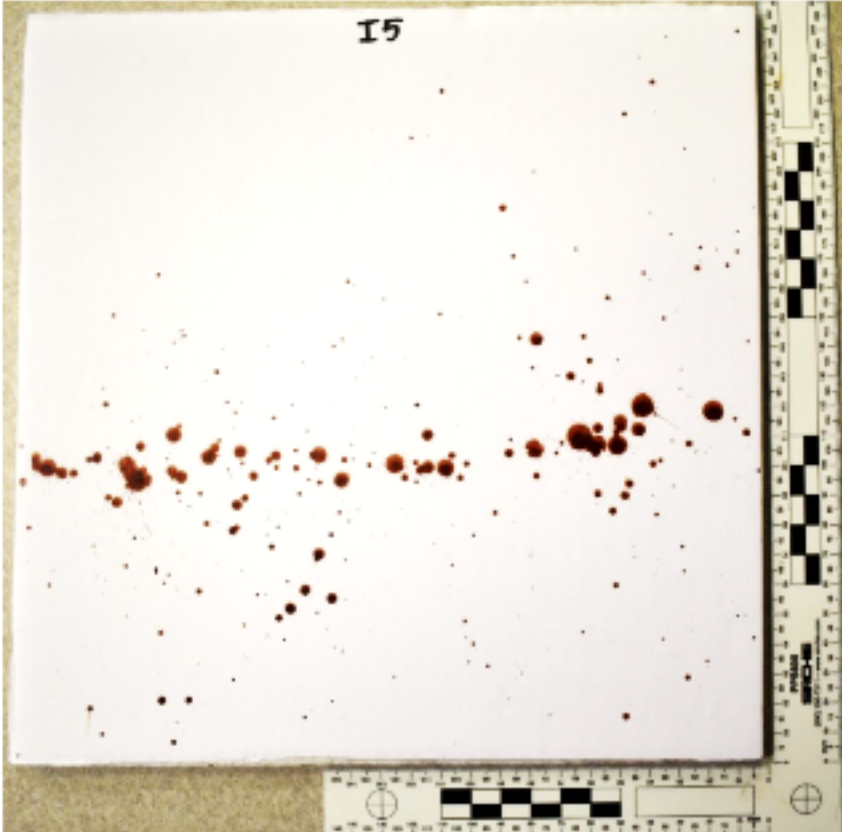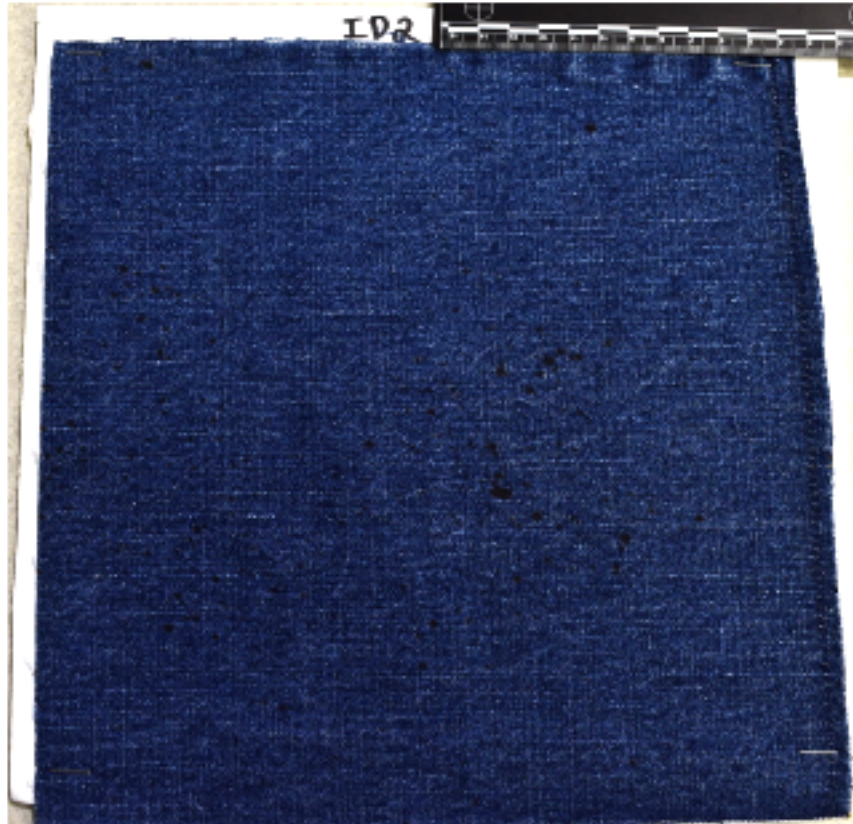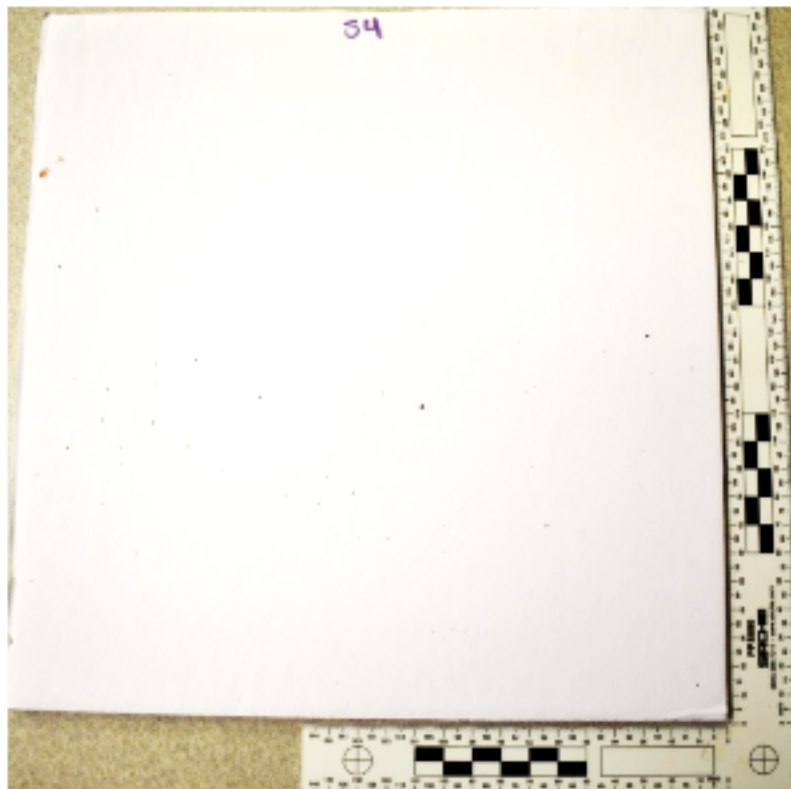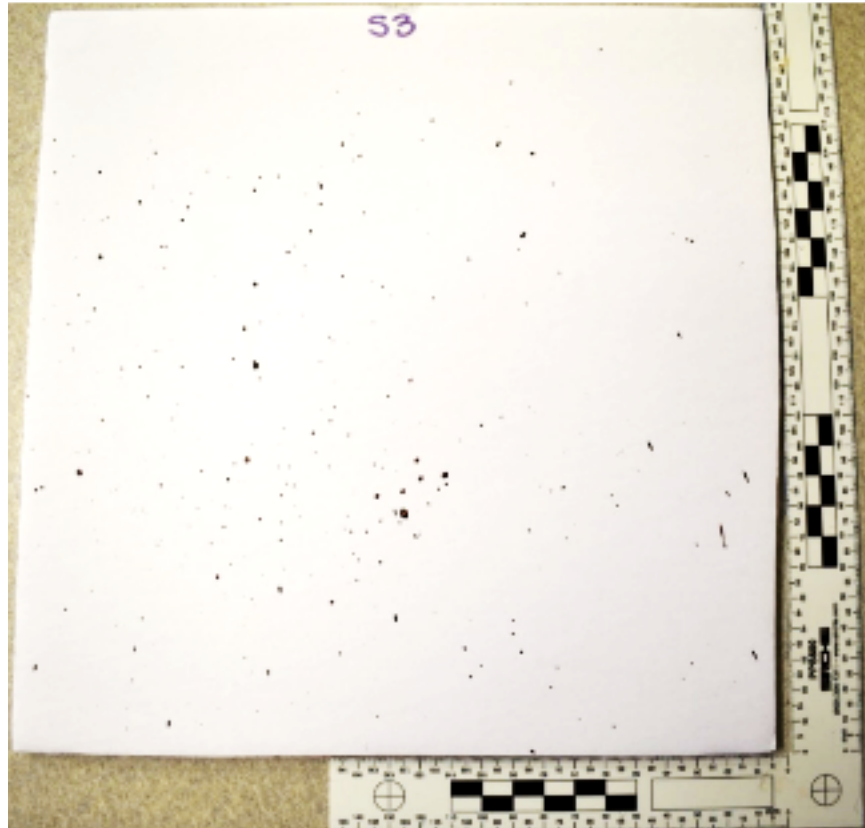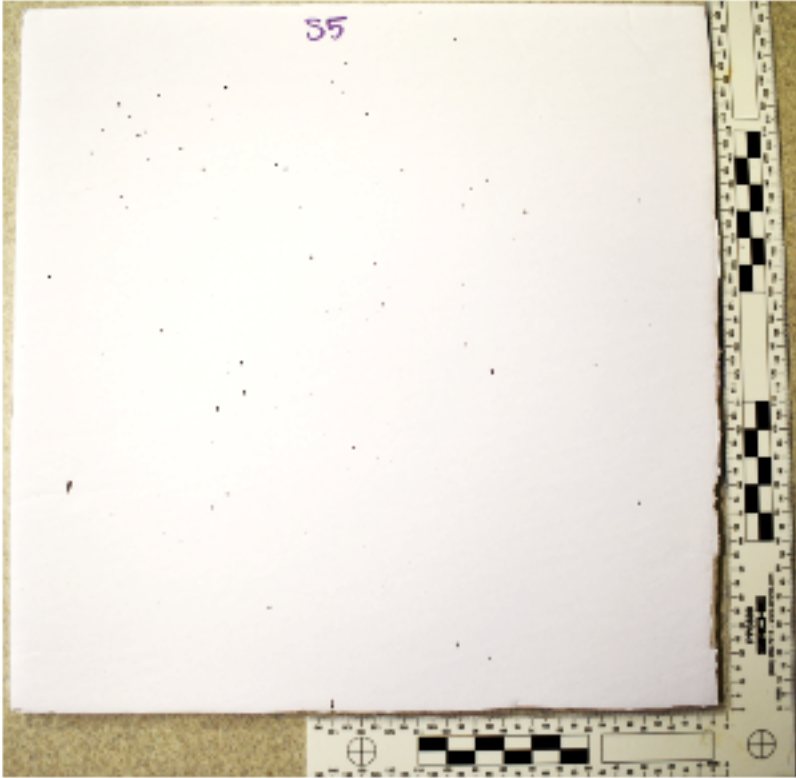
Appendix B - Infrared Images of Denim Samples
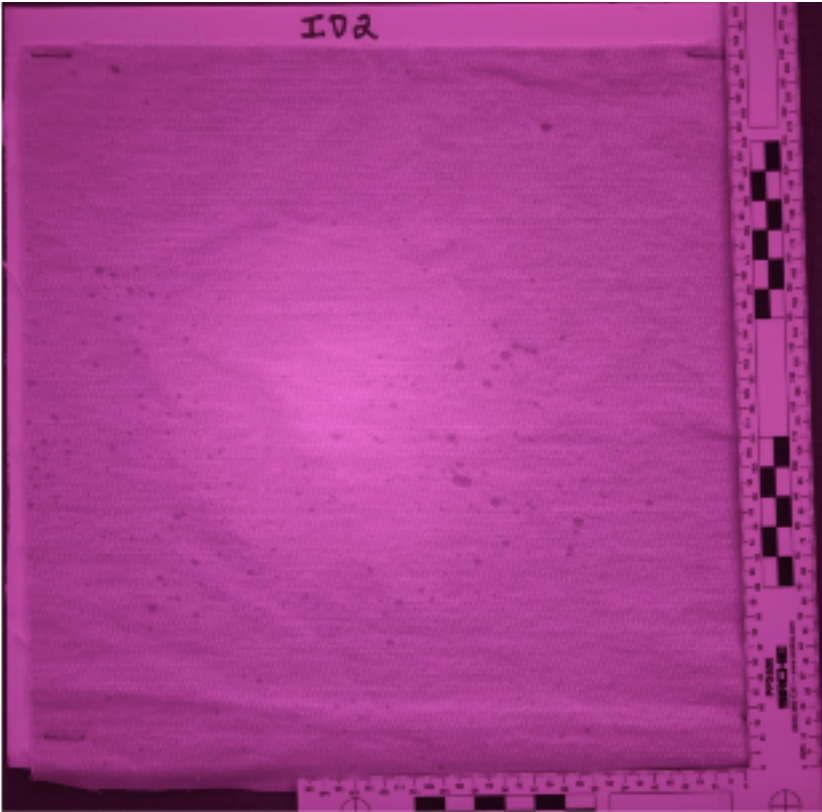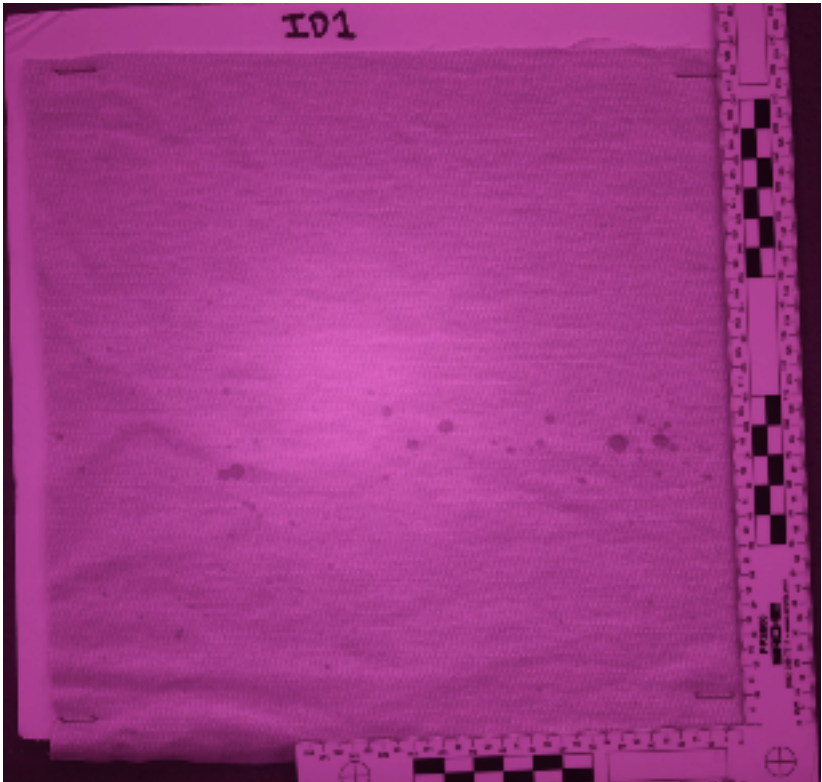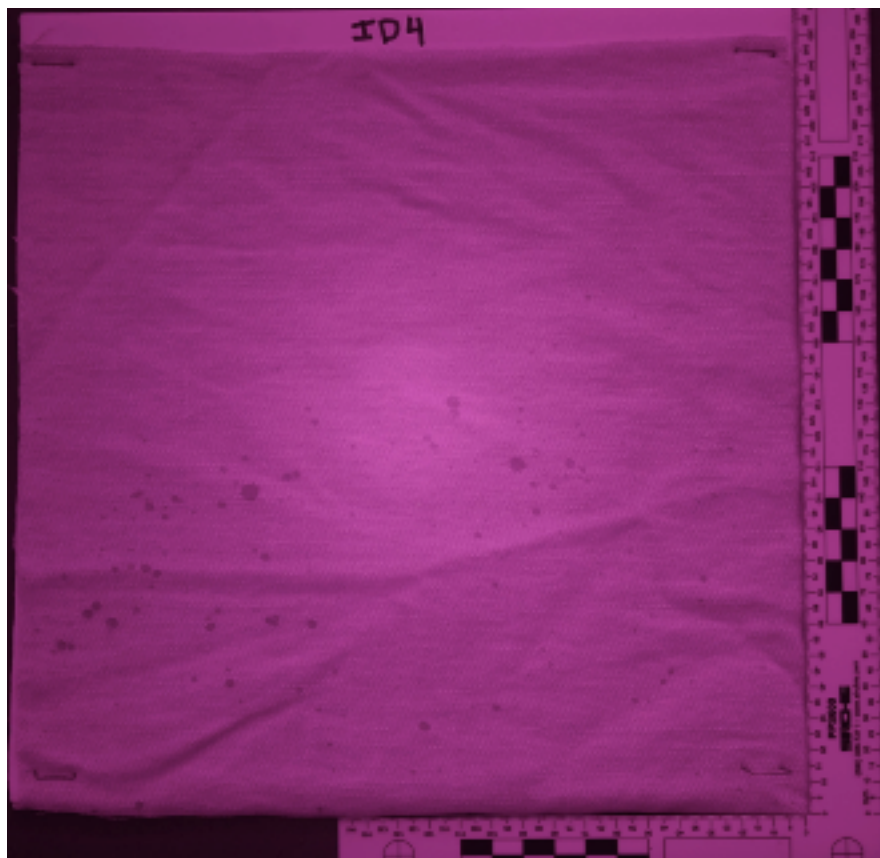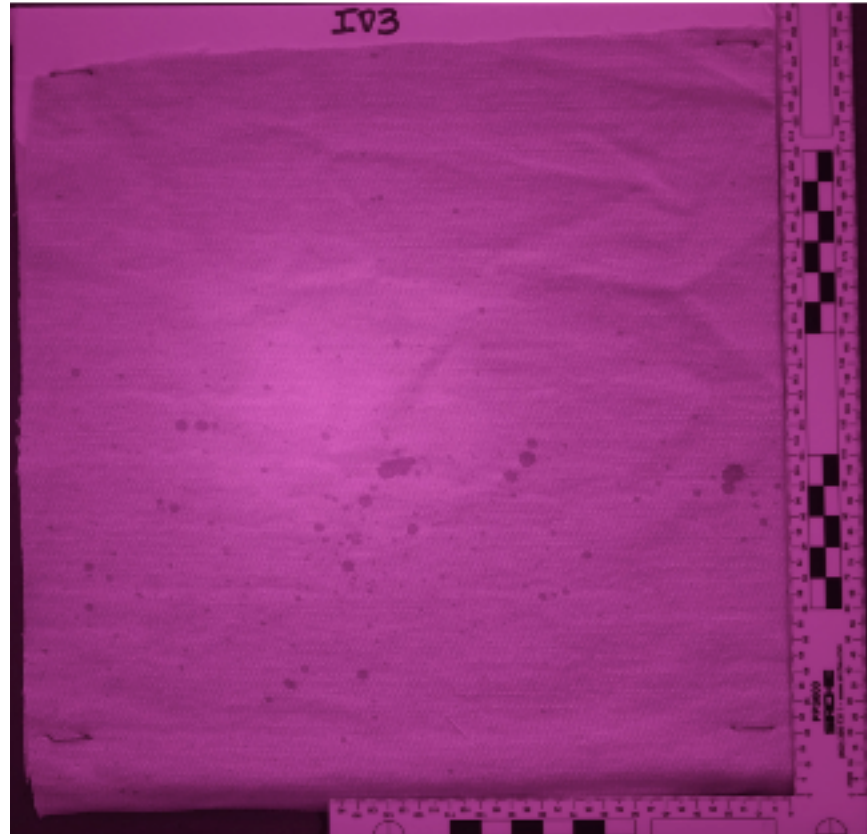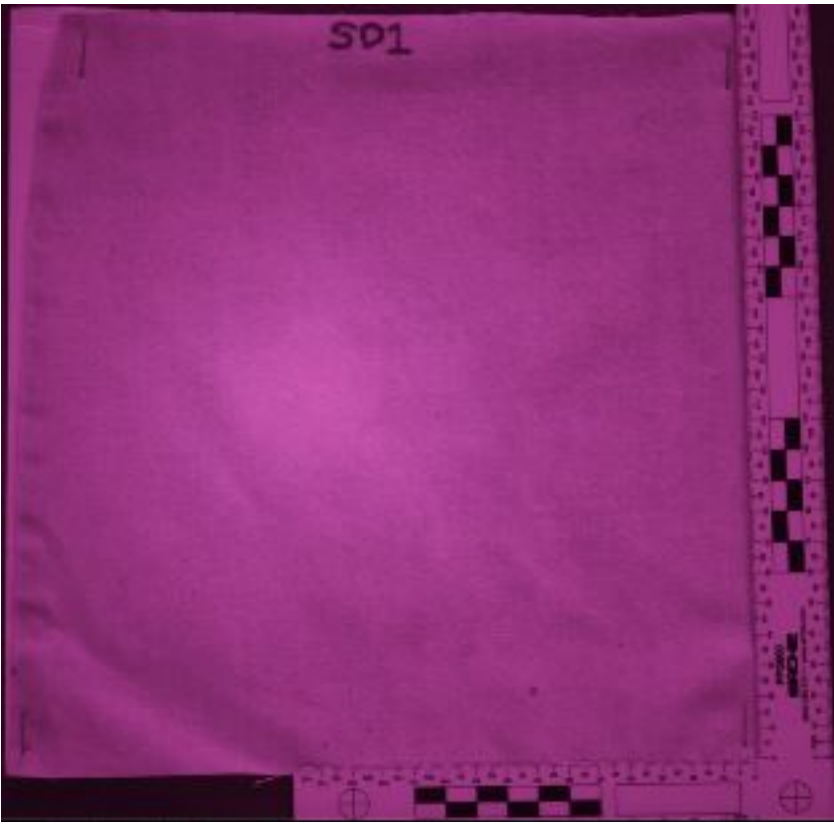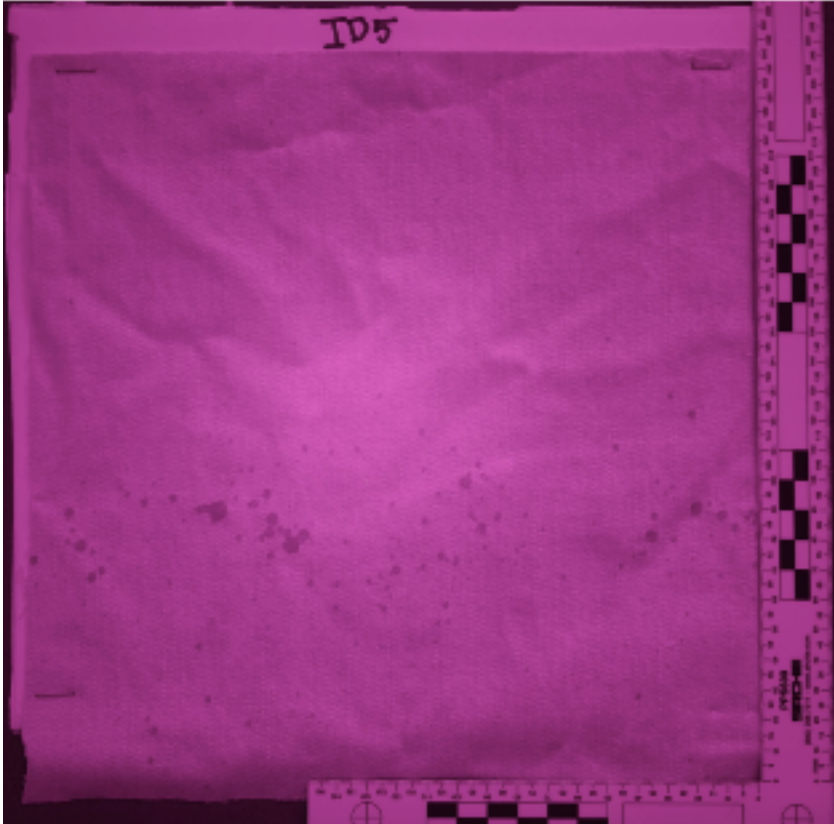
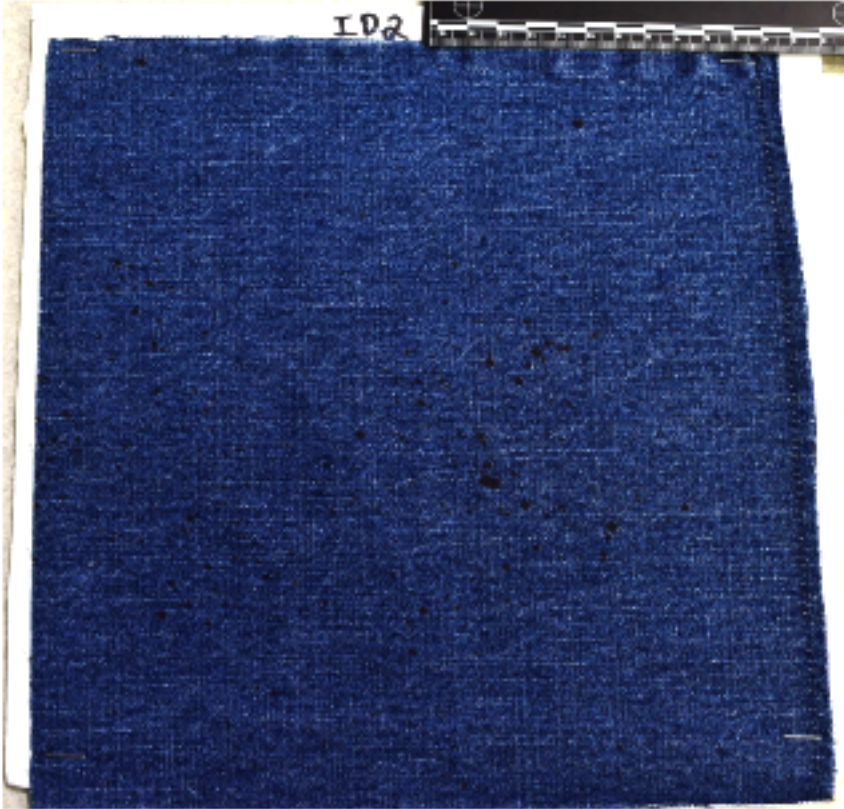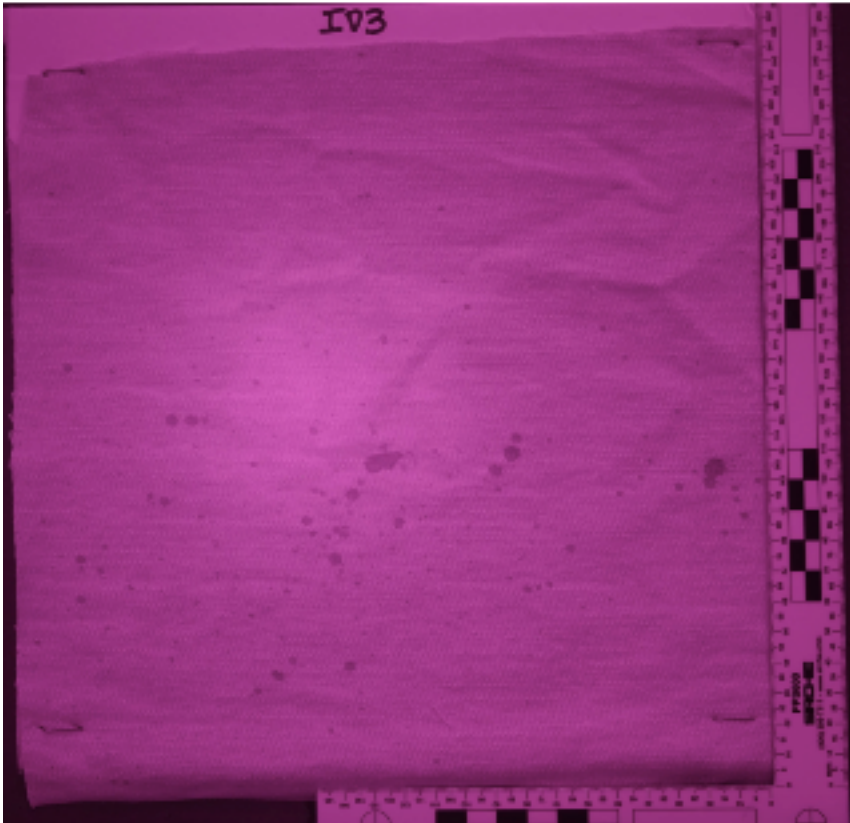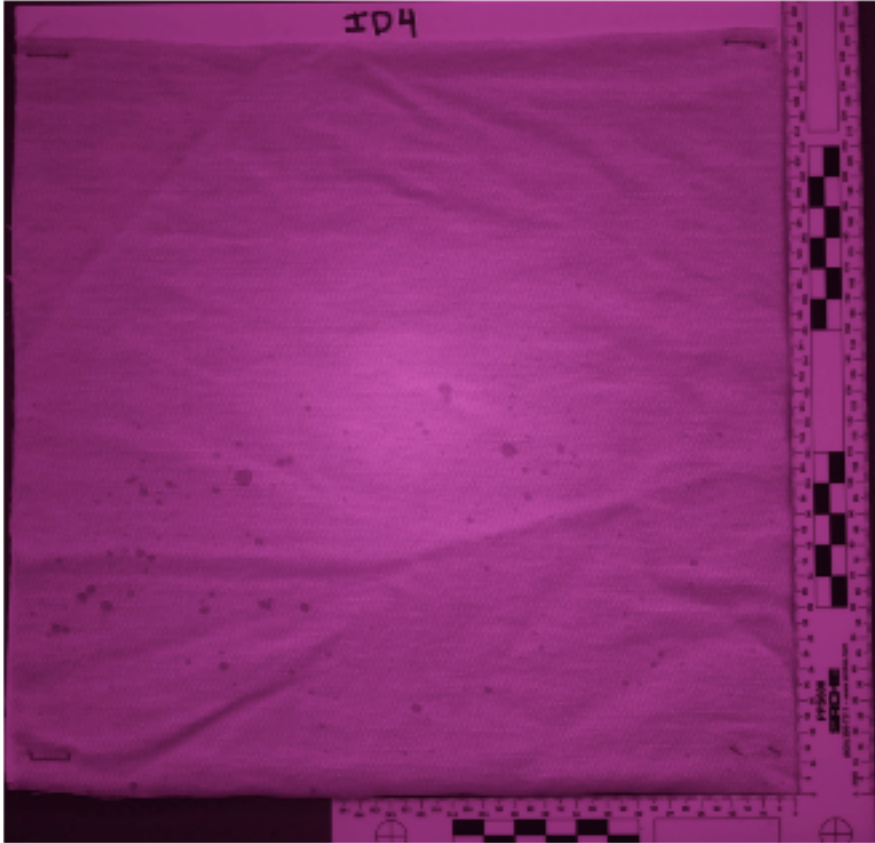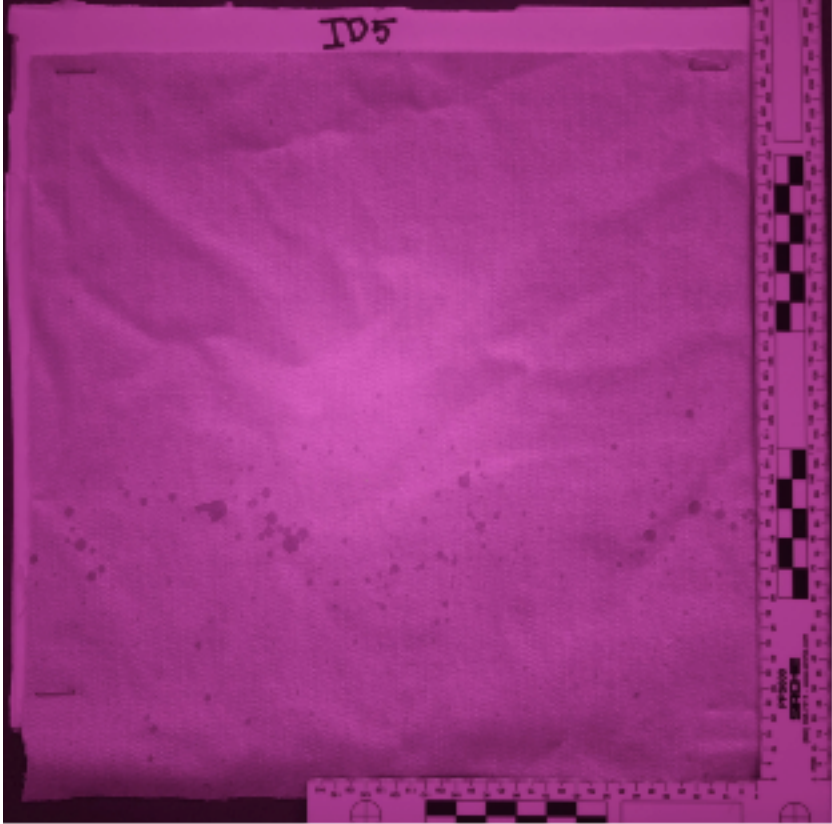**Appendix C - Ambient and Infrared Spattered Denim Samples**

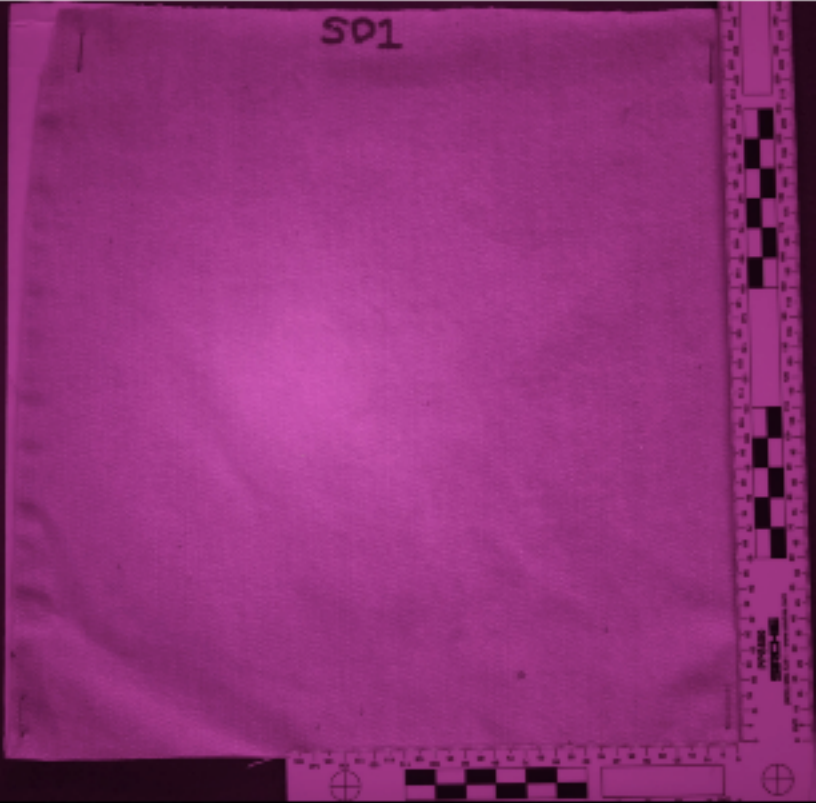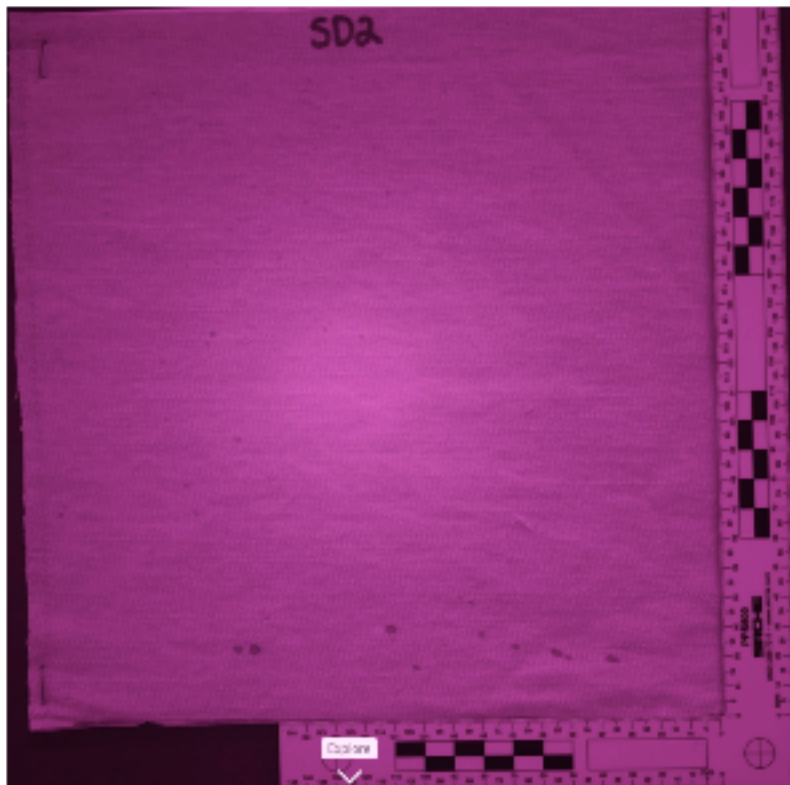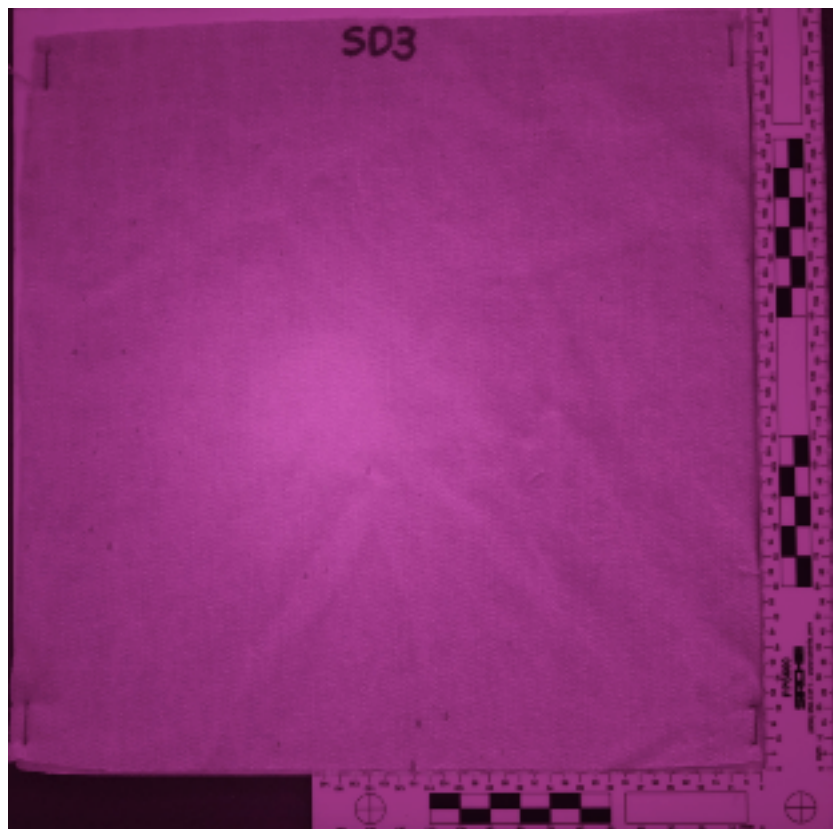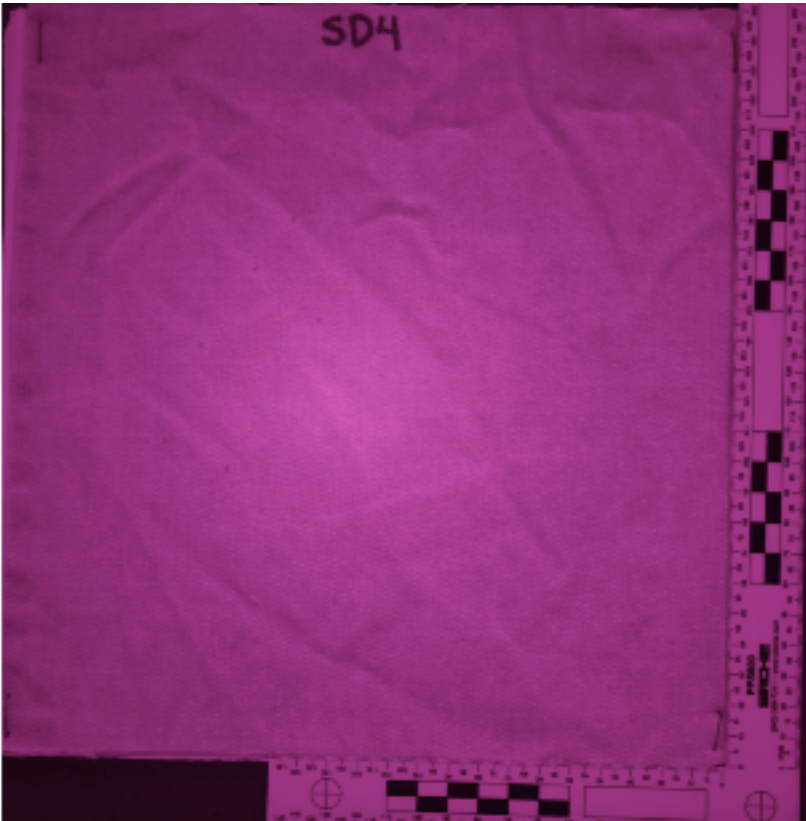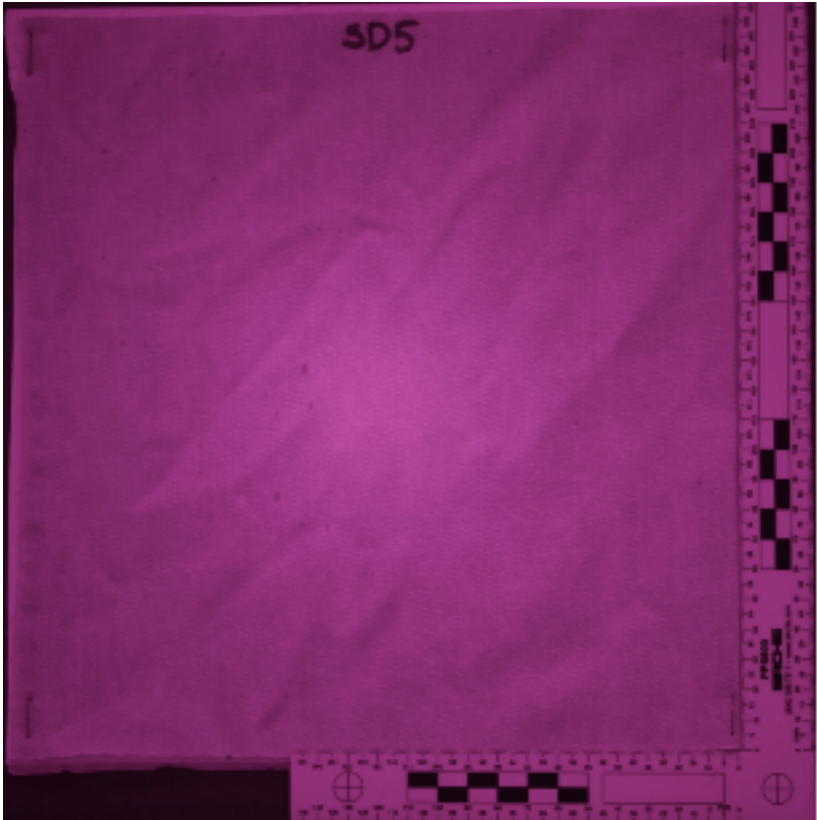**Appendix D - Photoshop Layers for Denim Samples**

Original Layer

Background Deleted

Brightness/Contrast Adjusted

Spatter Only

Spatter White + ID & Scale Layer

Appendix E - Qualitative Stain Counts by Quadrant

ID	QUAD 1	Stain #s	QUAD 2	Stain #s	QUAD 3	Stain #s	QUAD 4	Stain #s	TOTAL	
I1	5	1-5	5	6-10	5	11-15	18	16-33	33	
I2	6	1-6	8	7-14	10	15-24	22	25-46	46	
I3	8	1-8	5	9-13	14	14-27	9	28-36	36	
I4	7	1-7	4	8-11	21	12-32	19	33-51	51	
I5	7	1-7	12	8-19	23	20-42	15	43-57	57	223
S1	5	1-5	6	6-11	5	12-16	4	17-20	20	
S2	7	1-7	4	8-11	5	12-16	6	17-22	22	
S3	6	1-6	9	7-15	10	16-25	7	26-32	32	
S4	4	1-4	5	5-9	7	10-16	4	17-20	20	
S5	7	1-7	4	8-11	6	12-17	5	18-22	22	116
ID1	4	1-4	5	5-9	4	10-13	6	14-19	19	
ID2	8	1-8	6	9-14	20	15-34	16	35-50	50	
ID3	5	1-5	6	6-11	21	12-32	5	33-37	37	
ID4	5	1-5	8	6-13	8	14-21	9	22-30	30	
ID5	5	1-5	5	6-10	17	11-27	7	28-34	34	170
SD1	5	1-5	5	6-10	5	11-15	4	16-19	19	
SD2	4	1-4	5	5-9	5	10-14	5	15-19	19	
SD3	4	1-4	5	5-9	7	10-16	4	17-20	20	
SD4	4	1-4	4	5-8	5	9-13	1	14	14	
SD5	4	1-4	7	5-11	4	12-15	3	16-18	18	90

Appendix F - Comprehensive Qualitative Results

Impact Control (N=223)

Shape	#	%	Symmetry	#	%
Round	142	64%	Symmetrical	105	47%
Polygonal	39	17%	Asymmetrical	118	53%
Irregular	42	19%			

Weave	#	%	Submillimeter	#	%
Top	N/A	N/A	Yes	143	63%
Saturated	N/A	N/A	No	80	36%

Satellite Control (N=116)

Shape	#	%	Symmetry	#	%
Round	32	27%	Symmetrical	43	37%
Polygonal	30	26%	Asymmetrical	73	63%
Irregular	54	47%			

Weave	#	%	Submillimeter	#	%
Top	N/A	N/A	Yes	92	79%
Saturated	N/A	N/A	No	24	21%

Impact Denim (N=170)

Shape	#	%	Symmetry	#	%
Round	47	28%	Symmetrical	77	45%
Polygonal	46	27%	Asymmetrical	93	55%
Irregular	77	45%			

Weave	#	%	Submillimeter	#	%
Top	15	9%	Yes	43	25%
Saturated	155	91%	No	127	75%

Satellite Denim (N=90)

Shape	#	%	Symmetry	#	%
Round	24	27%	Symmetrical	31	34%
Polygonal	21	23%	Asymmetrical	59	66%
Irregular	45	50%			

Weave	#	%	Submillimeter	#	%
Top	19	21%	Yes	9	10%
Saturated	71	79%	No	81	90%